LEGIBILITY NOTICE

A major purpose of the Technical Information Center is to provide the broadest dissemination possible of information contained in DOE's Research and Development Reports to business, industry, the academic community, and federal, state and local governments.

Although a small portion of this report is not reproducible, it is being made available to expedite the availability of information on the research discussed herein.

Distribution Category: Atomic, Molecular, and Chemical Physics (UC-411)

ARGONNE NATIONAL LABORATORY
9700 South Cass Avenue
Argonne, Illinois 60439

ANL/APS/TM--7

DE90 018002

ANL/APS/TM-7

SYNCHROTRON X-RAY SOURCES AND NEW OPPORTUNITIES IN THE SOIL AND ENVIRONMENTAL SCIENCES: WORKSHOP REPORT

Proceedings of a workshop held at

Argonne National Laboratory
January 8-10, 1990

Workshop Co-Chairs:

Darrell G. Schulze, Purdue University

Joseph V. Smith, The University of Chicago

July 1990

work sponsored by

U.S. DEPARTMENT OF ENERGY
Office of Energy Research

NOTICE

This document was prepared by Darrell Schulze (Purdue University), Sharon Anderson (Michigan State University), and Shas Mattigod (Battelle, Pacific Northwest Laboratories) as an account of a workshop sponsored by the Advanced Photon Source User Organization; by Argonne National Laboratory, Division of Educational Programs; and by The University of Chicago. The document is reproduced here as received.

Executive Summary

When the Advanced Photon Source (APS) becomes operational at Argonne National Laboratory in the mid-1990's, it will be the most intense source of x-rays for scientific research in the U.S. The APS will make significant advances possible in many areas; among these are the soil and environmental sciences. This report is the result of a workshop entitled *Synchrotron X-Ray Sources and New Opportunities in the Agricultural and Related Sciences,* held at Argonne National Laboratory on January 8-10, 1990. Most of the workshop participants were soil chemists and mineralogists, and the report reflects the perspectives of this group.

The APS will provide state-of-the-art research capabilities for various x-ray based techniques. These are considered under three broad headings: (1) x-ray absorption spectroscopy, (2) x-ray diffraction and scattering techniques, and (3) x-ray fluorescence microprobe and microtomography.

X-ray absorption spectroscopy (XAS) provides information on the nearest-neighbor and next-nearest-neighbor interactions of almost all elements of the periodic table. XAS will provide new information on the cation environment and oxidation state in crystalline and poorly crystallized solids such as soil clay minerals, on the coordination environment of soluble and surface sorbed species, and on the solid state physics of soil minerals. XAS studies of cation distribution within layer silicate minerals will provide information on the shrink-swell properties of soil clays as a function of ion substitution within the crystal structure. This will provide new insights in how to manage the shrink-swell properties of soils for agricultural, industrial, and municipal uses. XAS studies of poorly crystallized, high surface area iron and aluminum hydroxides will provide new insights into how these materials react with phosphate and heavy metals, and will provide a better understanding of the role of these materials in soils and sediments. Information from XAS will be critical for the verification and refinement of contaminant sorption models currently used to predict the fate of environmental pollutants.

Synchrotron-based x-ray diffraction and scattering experiments are extensions and improvements over existing laboratory-based techniques. The ability to obtain complete x-ray diffraction patterns within seconds will make it possible to study the dynamics of some processes for the first time. For example, it will be possible to monitor the swelling behavior of smectite clay during the wetting process, or to monitor swelling differences which occur as structural iron is oxidized. Small angle x-ray scattering experiments will make it possible to follow the dynamics of the interactions of clays with organic molecules or with aluminum hydroxy polymers.

The extremely brilliant x-ray beams will decrease the detection limit for various reactive trace and poorly-crystallized minerals in soils. They will make it possible to easily study the detailed spatial distribution of minerals within soils for the first time, and make it possible to obtain accurate structural information for many of the minerals which occur as extremely fine particles in soils. The result will be a better understanding of the properties of the bulk soil system.

The x-ray fluorescence microprobe will make it possible to obtain elemental analysis at the parts per million level at spatial resolutions of only a few square micrometers. This will provide new information on the trace element distribution within soils and at the soil-root interface. Studies on the trace element distributions within fossil fuel combustion by-products will provide information needed to dispose of these materials in an environmentally sound manner. Microtomograpy will make it possible to study certain processes without physically sectioning the object. Studies of the soil-root interface are one potential application.

The soil and environmental scientists represented at this workshop are a new user group for synchrotron radiation. Many more new applications are likely to emerge as the group becomes more experienced with synchrotron-based techniques.

Authors

Calvin C. Ainsworth
Earth & Environmental Sciences
Battelle, Pacific Northwest Labs.
Battelle Blvd.
Richland, WA 99352

Ercan E. Alp
Advanced Photon Source
Argonne National Laboratory
Argonne, IL 60439

James E. Amonette
Earth & Environmental Sciences
Battelle, Pacific Northwest Labs.
Battelle Blvd.
Richland, WA 99352

Sharon J. Anderson
Department of Crop and Soil Sciences
Michigan State University
East Lansing, MI 48824

Paul M. Bertsch
Savannah River Ecology Lab.
University of Georgia
P.O. Drawer E
Aiken, SC 29801

Jerry M. Bigham
Department of Agronomy
Ohio State University
2021 Coffey Road
Columbus, OH 43026

William F. Bleam
Department of Soil Science
University of Wisconsin-Madison
1525 Observatory Drive
Madison, WI 53707

Paul R. Bloom
Department of Soil Science
University of Minnesota
St. Paul, MN 55108

Joe B. Dixon
Soil & Crop Sciences Department
Texas A&M University
College Station, TX 77843-2474

James B. Harsh
Department of Agronomy and Soils
Washington State University
Pullman, WA 99164-6420

Clifford T. Johnston
Department of Soil Science
University of Florida
2169 McCarty Hall
Gainsville, FL 32611

Shas V. Mattigod
Earth and Environmental Sciences
Battelle, Pacific Northwest Labs.
Battelle Blvd.
Richland, WA 99352

S. M. Mini
Advanced Photon Source
Argonne National Laboratory
Argonne, IL 60439

M. Ramanathan
Advanced Photon Source
Argonne National Laboratory
Argonne, IL 60439

Mark L. Rivers
Department of Applied Sciences
Brookhaven National Laboratory
Upton, NY 11973

Darrell G. Schulze
Department of Agronomy
Purdue University
West Lafayette, IN 47907

Joseph W. Stucki
Department of Agronomy
University of Illinois
1102 South Goodwin Avenue
Urbana, IL 61801

Steven R. Sutton
Department of Applied Sciences
Brookhaven National Laboratory
Upton, NY 11973

Michael L. Thompson
Department of Agronomy
Iowa State University
Ames, Iowa 50011

Samuel J. Traina
Department of Agronomy
Ohio State University
2021 Coffey Road
Columbus, OH 43210

Contents

Acknowledgments

We would like to thank the Advanced Photon Source Users Organization, Argonne National Laboratory, and the Consortium for Advanced Radiation Sources, for sponsoring the workshop. In particular we would like to thank David Moncton, Gopal Shenoy, and Ercan Alp of Argonne National Laboratory, and Mark Rivers and Steve Sutton of the University of Chicago and the National Synchrotron Light Source for sharing their expertise and experience during the workshop and during the preparation of the report. A special thanks to Elizabeth Stefanski, User Program Administrator for the APS, for handling the workshop arrangements and to Susan Picologlou for editing the manuscripts. Finally we would like to thank Sandy DeVault, Jolynn Pritchard, and Thomas Mueller of Purdue for help in preparation of the report, and Bonnie Meyer of the APS for help in its distribution.

Chapter 1

Introduction

The discovery of x-rays in the late 19th century had a profound impact on many areas of the physical and biological sciences. Soil science was no exception. Modern concepts of soil clay mineralogy began to develop in the 1930's when x-ray diffraction showed soil clays to be crystalline. Commercially available x-ray diffractometers became common in soil science departments in the 1950's. X-ray diffraction analysis and other x-ray techniques, such as x-ray fluorescence spectroscopy, continue to be major analytical techniques of soil mineralogists and chemists. The increasing availability of extremely high intensity x-rays from synchrotron sources provide exciting new techniques for the study of soil and geologic materials.

The purpose of this report is twofold: (1) to introduce the soil and environmental science communities to synchrotron-based techniques, and (2) to describe areas of research in the soil and environmental sciences which are likely to benefit from the application of these techniques. This report is the result of a workshop entitled *Synchrotron X-ray Sources and New Applications in the Agricultural and Related Sciences* which was held at Argonne National Laboratory on January 8-10, 1990. The major group represented at the workshop consisted primarily of soil and environmental scientists. The report is therefore entitled, *Synchrotron X-ray Sources and New Applications in the Soil and Environmental Sciences*, in order to best represent the final contents of the document.

The report is divided into 6 chapters. Chapter 1 consists of this introduction and includes a very brief description of synchrotron radiation sources. Chapter 2 describes the technical details of the synchrotron radiation sources which will be available at the Advanced Photon Source. Chapter 3 is tutorial in nature and briefly describes x-ray absorption spectroscopy, a technique which is not yet widely familiar to the soil and environmental sciences communities. Chapters 4, 5, and 6 then describe potential applications of synchrotron-based x-ray absorption spectroscopy, x-ray scattering and diffraction, and x-ray fluorescent microprobe techniques to problems in the soil and environmental sciences.

1.1 Synchrotron Radiation

A very brief description of synchrotron radiation and its generation is given below to introduce terminology which may be new to some readers. A more comprehensive introduction is given by Winick (1987).

Synchrotrons and *storage rings* are machines in which electrons or positrons are forced into a near-circular path within an evacuated ring-shaped chamber by means of powerful magnets. A *synchrotron* is designed to bring low-energy particles to some high energy in order that the high energy particles can be made to strike a target. A *storage ring*, on the other hand, is designed to keep a high energy particle beam circulating for hours. Instead of being perfect circles, both synchrotrons and storage rings consist of a series of circular arcs connected by straight segments. *Bending magnets* at each of the circular sections serve to redirect the beam down the next straight section. Charged particles give off electromagnet radiation whenever they are accelerated or decelerated. A change in direction of motion is an acceleration, therefore the particles in a synchrotron or storage ring emit radiation when they pass through the bending magnets. When the particles are travelling at speeds well below the speed of light, very weak low-frequency radiation is emitted in almost all directions. If, however, the electrons are travelling at or near the speed of light (relativistic speeds), they emit large amounts of radiation and almost all of this radiation is emitted in the forward direction, that is, tangential to the trajectory of the particles.

The radiation emitted by a bending magnet is at least 3 to 4 orders of magnitude more intense than the radiation emitted by conventional laboratory x-ray generators. Even greater intensity increases can be obtained by using *insertion devices*, magnetic devices mounted on the straight sections of the storage ring. Insertion devices cause the particle beam to "wiggle" or "undulate" as it passes through the device, thus they are either *wigglers* or *undulators*. The acceleration imparted to the particles as they pass through a wiggler or undulator results in the emission of radiation several orders of magnitude greater than that emitted by a bending magnet. Wigglers produce "white radiation," with the intensity distributed approximately equally over all energies. Undulators, in contrast, produce radiation only over discrete energy ranges, but the intensity within these ranges is several orders of magnitude greater than that produced by a wiggler.

1.2 Properties of Synchrotron Radiation

Synchrotron x-ray sources have unique properties which make them of interest to soil and environmental scientists.

1. The radiation is extremely intense. The high intensity makes it possible to study single crystals as small as a few μm on edge (some clay minerals for example), to do x-ray absorption spectroscopy at spatial resolutions of only a few μm^2, and to study dilute natural systems.

2. The radiation is emitted over a wide range of energies. The wavelength of interest can be easily selected using an appropriate monochromator. This makes it possible to do x-ray absorption spectroscopy and to take advantage of various anomalous scattering techniques which allow one to study specific elements in a complex matrix.

3. The radiation is highly collimated. The almost parallel beam of radiation minimizes certain problems caused by the divergent beams of laboratory x-ray sources. The optics of the experimental system can often, therefore, be quite simple.

4. The radiation has a pulsed time structure. The pulsed time structure, along with the high intensity, makes it possible to study chemical reactions on time scales as small as nanoseconds.

5. The radiation is highly polarized.

1.3 Synchrotron Radiation Sources

Current synchrotron facilities in the U.S. include the Stanford Synchrotron Radiation Laboratory (SSRL) on the Stanford Positron-Electron Accelerating Ring (SPEAR), the Cornell High-Energy Synchrotron Source (CHESS), and the National Synchrotron Light Source (NSLS) at Brookhaven National Laboratory.

SPEAR and CHESS were originally built to serve the needs of the high-energy physics community. It soon became apparent, however, that the x-rays emitted by the bending magnets could be used by a variety of other disciplines. "Parasitic" experiments were soon set up. As demand increased, second generation facilities dedicated solely to the production of synchrotron radiation were built. The NSLS is such a second generation facility. The Advanced Photon Source, to be completed at Argonne National Laboratory in the mid-1990s, is a third-generation facility designed to produce extremely high x-ray intensities by taking full advantage of undulator and wiggler technology.

Synchrotron x-ray sources have many applications in the soil and environmental sciences. The soil and environmental sciences community represents a new users-

group for synchrotron x-ray sources. Many potential areas of research are identified in this report, but many more are likely to develop as this group becomes more experienced with synchrotron-based techniques.

1.4 References

Winick, H. 1987. Synchrotron Radiation. Scientific Amer. 257(5):88-99.

Chapter 2

Characteristics of the Advanced Photon Source and Comparison with Existing Synchrotron Facilities

Mark L. Rivers

2.1 Introduction

The Advanced Photon Source will provide significant increases in photon intensity over existing synchrotron sources. Undulators will increase the flux in the 3-40 keV range by several orders of magnitude with relatively narrow energy bandwidths. Wigglers and bending magnets will provide much higher flux in the energy range above 40 keV with a smooth energy spectrum. In this section we will discuss the details of the spectral characteristics of the APS sources, and compare these with those of existing U.S. hard x-ray synchrotron storage rings.

There are several figures of merit which can be used to compare the photon output from synchrotron radiation sources, and which one is appropriate depends upon the nature of the beam line and the experiment. (The nomenclature for these parameters is not standard. We use the APS conventions here.) The *flux* is the number of photons/second/horizontal angle (θ)/bandwidth, integrated over the entire vertical opening angle (ψ). It is the appropriate figure of merit for an experiment which can use all of the photons in a particular energy interval from a synchrotron port. Examples are EXAFS or fluorescence experiments on large samples. The *brightness* is the flux/vertical angle (ψ). The brightness is thus the number of photons per solid angle, and is the appropriate figure of merit for an experiment which uses a collimator to define a small beam. Examples include x-ray diffraction in a diamond cell, the x-ray fluorescence microprobe, and high spatial resolution spectroscopic studies (EXAFS) of interfaces.

The flux and the brightness can depend both upon the intrinsic opening angle of the radiation and upon the electron beam divergence, but they are nearly independent of the size of the electron beam. This is because the intrinsic opening angle for all of

the sources is large enough that at the end of a typical beam line the fan of radiation is much larger than the electron beam. The *brilliance* is the brightness/source area. The brilliance is the appropriate figure of merit when a beam line contains focusing optics, because the source dimensions then limit the minimum focused spot size which can be produced.

The conventional figures of merit are appropriate if the experiment is using a restricted energy bandwidth. Some experiments, for instance energy dispersive x-ray diffraction and the white light fluorescence microprobe, can use a broad energy band, and for these the flux, brightness, or brilliance *integrated* over energy would be more appropriate. Using this criterion, the continuum sources, (bending magnets and wigglers) are more competitive with the undulators.

Since most existing geoscience synchrotron experiments use pinholes rather than focusing optics, and we imagine that the first generation experiments on the APS probably will as well, in the following discussion we compare the brightness rather than the brilliance of the various sources. Note that because the APS is designed to be a very low emittance storage ring, it will compare even more favorably with existing synchrotron facilities when considering focusing beam lines which can exploit the high brilliance. Note in the following discussion that the phrase *electron beam* should be interpreted as electron beam or positron beam, depending upon the storage ring. The APS will use a positron beam.

2.2 Bending Magnets

The brightness (in units of photons/sec/mrad^2/0.1%BW) of a bending magnet (Winick, 1980) is

$$B_{BM} = 1.33 \times 10^{13} E^2 I H_2(\varepsilon/\varepsilon_c) \qquad (2.1)$$

where E is the storage ring energy in GeV, I is the ring current in A, ε is the x-ray energy, ε_c is the critical energy of the storage ring, and $H_2(\varepsilon/\varepsilon_c)$ is a function plotted in Figure 2.1. The critical energy of a storage ring is equal to

$$\varepsilon_c = 2.218\, E^3/\rho = .6651\, B\, E^2 \qquad (2.2)$$

where ρ is the bending radius in meters and B is the magnetic field in Tesla. Since most synchrotron storage rings have bending magnet fields of 0.9 ± 0.3 T, the critical energy depends upon the square of the electron or positron energy. Table 2.1 shows the storage ring parameters for the bending magnets at the Advanced Photon Source (APS), the National Synchrotron Light Source (NSLS) at Brookhaven National

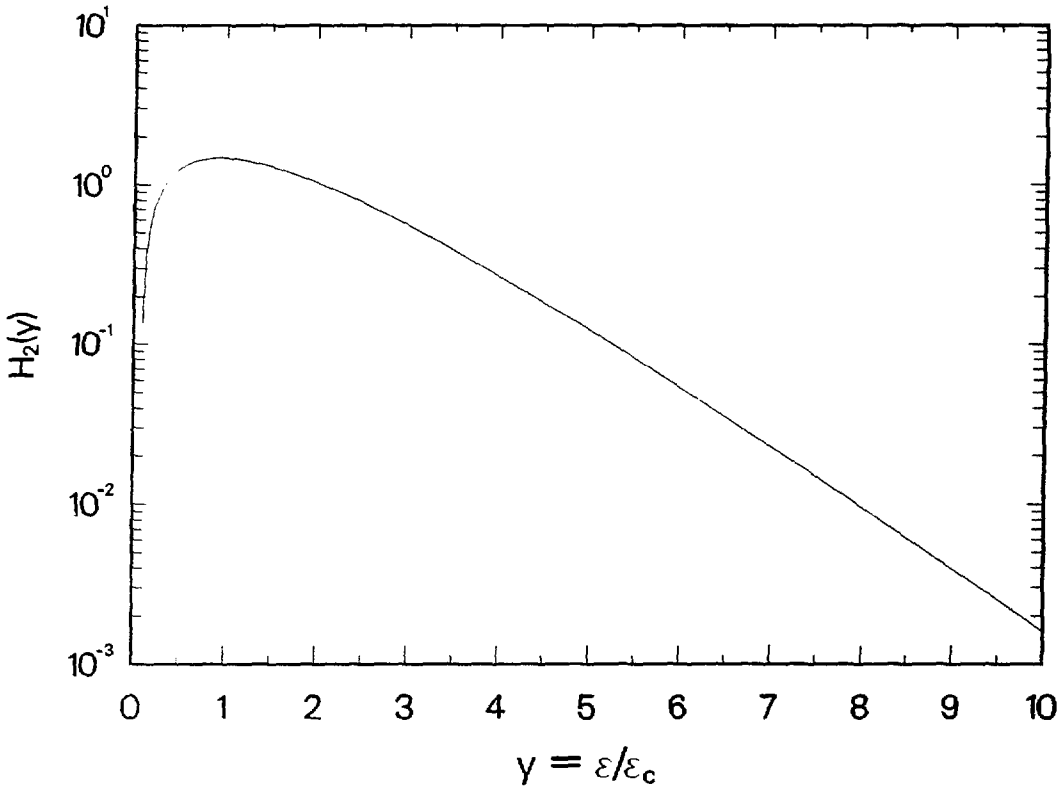

Figure 2.1. Function $H_2(\varepsilon/\varepsilon_c)$.

Table 2.1. Parameters for bending magnet sources.

Source	Energy (GeV)	Current (mA)	Peak field (T)	Bending radius (m)	ε_c (keV)
APS	7.0	100	0.6	39.0	19.6
NSLS	2.5	250	1.2	6.87	5.0
CHESS	5.5	75	0.57	32.0	11.5
SSRL	3.0	100	0.79	12.6	4.7

Laboratory, the Cornell High Energy Synchrotron Source (CHESS), and the Stanford Synchrotron Radiation Laboratory (SSRL).

The intrinsic vertical opening angle of the radiation at the critical energy is about $1/\gamma$, where γ is $1.957 \times 10^3 E$. For storage ring energies in the range of 2.5 - 7 GeV the opening angles are 70 - 200 μrad. The actual vertical opening angles are somewhat larger because of the vertical divergence of the electron or positron beam, but this is generally a small effect. For an experimental station located 20 m from the source at the NSLS, the beam height is about 4 mm. Since this is much larger than the 0.5 mm vertical size of the electron beam, the flux through an aperture is independent of the electron beam emittance.

The in-plane radiation from a bending magnet is linearly polarized, with the electric vector in the horizontal plane. Above and below the plane of the electron orbit the radiation is elliptically polarized. For a finite emittance source the in-plane radiation is less than 100% linearly polarized. For the APS bending magnets the calculated in-plane polarization is 99-99.5% (Figure 2.2).

The calculated brightnesses (Equation 2.1) of the four bending magnet sources are plotted in Figure 2.3. Note that above 3 keV the brightness decreases nearly exponentially with energy. The slope of the curves is a function of the critical energy, while the brightness at the critical energy varies linearly with the ring current and with the square of the ring energy. The advantage of the APS for bending magnet radiation is clearly the greater brightness at high energies. The brightness of the APS bending magnets is 10 times greater than the NSLS bending magnets at 15 keV, but because the APS beam lines must be twice as long, the actual gain in throughput is only a factor of 2.5. At 60 keV, however, the actual gain is more than a factor of 1000. There are several geoscience experiments which can make use of this high brightness at high energy. High pressure x-ray diffraction requires high energy x-rays

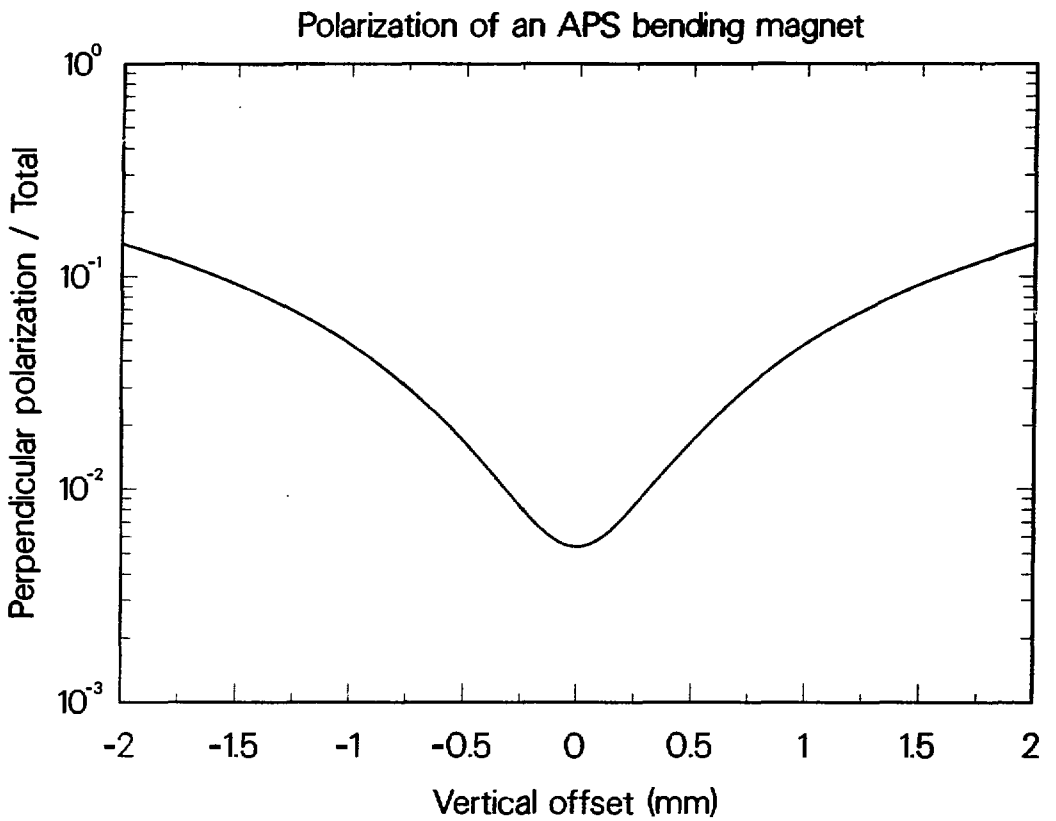

Figure 2.2. Polarization of the radiation from an APS bending magnet including beam emittance effects. The curve shows the fraction of vertically polarized radiation at 19.5 keV as a function of vertical position at 50m from the source. It assumes a vertical beam emittance of 0.7 nm rad, and a vertical β value of 17m.

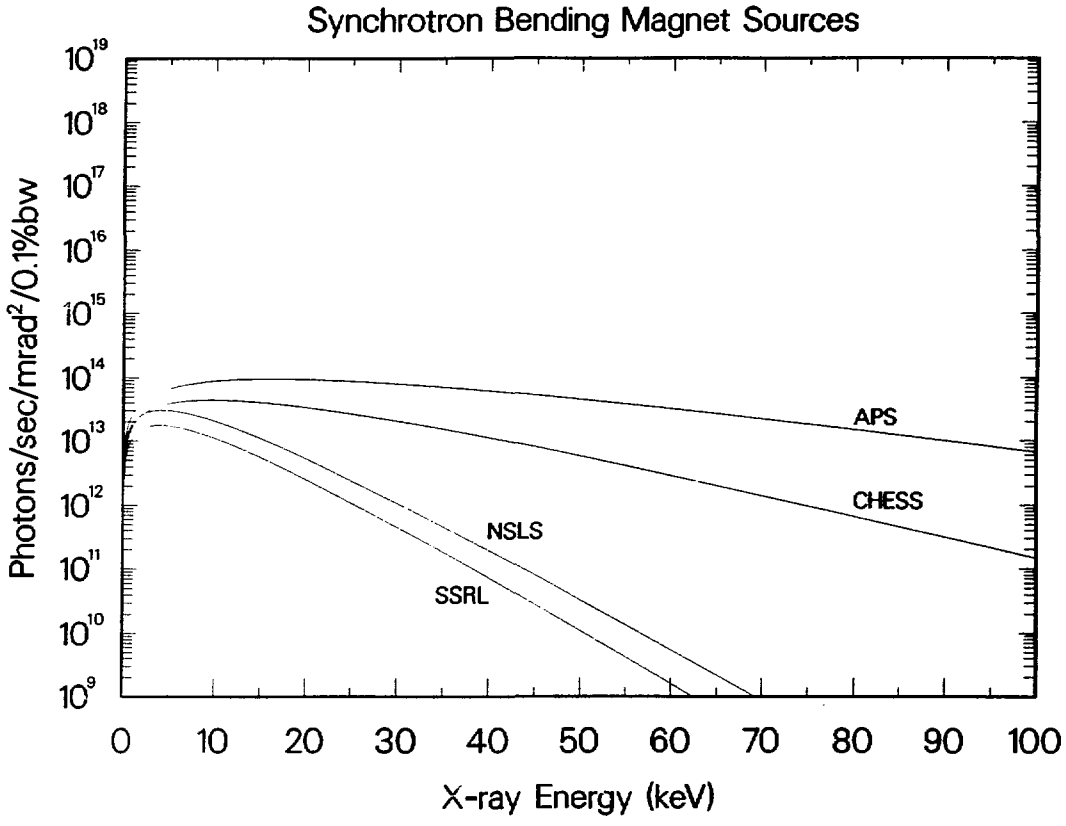

Figure 2.3. Brightness of selected synchrotron x-ray bending magnet sources.

both to pass through the pressure cell and to sample a large volume of reciprocal space when using the energy dispersive technique. The fluorescence microprobe requires high energy photons to excite the K-lines of the rare-earth and other high-Z elements. Since the brightness of the APS at 60 keV is comparable to that of the NSLS at 15 keV, it should be possible to detect 1 ppm of the rare-earth elements in a 20-30 micron spot, the sensitivity which has been demonstrated with the NSLS X-26 microprobe for Sr.

The brightness of an APS bending magnet is within a factor of 2 of that of the NSLS superconducting wiggler, X-17, over the range from 0-100 keV. The geoscience community began work on X-17 in 1990, both with a dedicated high pressure diffraction beam line and with high energy x-ray fluorescence analyses on the materials science beam line. It is anticipated that the demand for time on X-17 will make it difficult to get much running time for any single experiment each year. The availability of many similar beam lines at the APS will be a tremendous asset.

2.3 Wigglers

The spectrum from a wiggler is, to a good approximation, equal to that from a bending magnet with the same field, scaled by the number of poles in the wiggler. The wiggler field can be chosen to be greater or less than the field of the bending magnets. The APS has proposed two types of wigglers, the high energy wiggler "A" which has a 1.0 T field and a critical energy of 32.6 keV, and a low energy wiggler "B" which has a 0.3 T field and a critical energy of 9.8 keV. Table 2.2 gives the parameters of these wigglers, as well as those for some wigglers on existing storage rings. The predicted brightness of these wigglers is plotted in Figure 2.4.

Table 2.2. Parameters for wiggler sources.

Source	Energy (GeV)	Current (mA)	Peak field (T)	ε_c (keV)	Poles
APS "A"	7.0	100	1.0	32.6	20
APS "B"	7.0	100	0.3	9.8	40
NSLS X-17	2.5	250	5.0	20.8	5
NSLS X-25	2.5	250	1.2	5.0	22
CHESS	5.5	75	1.5	30.2	6
SSRL 54-pole	3.0	100	1.0	6.0	54

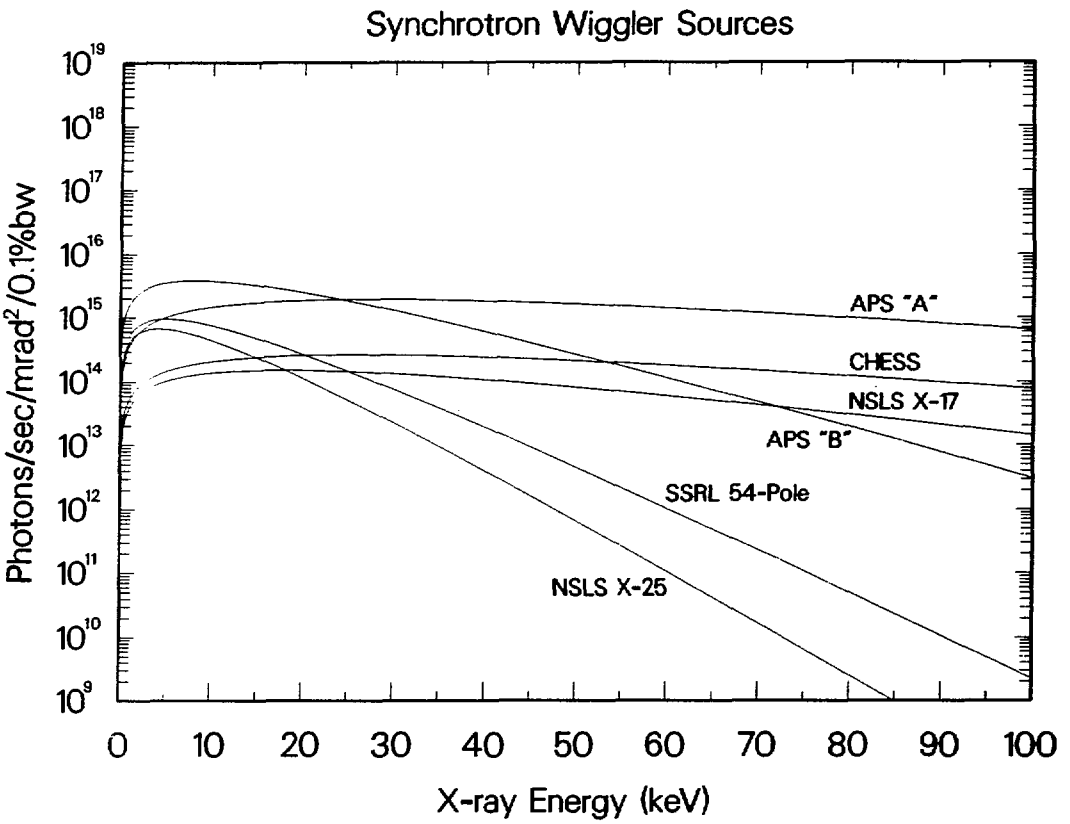

Figure 2.4. Brightness of selected synchrotron x-ray wiggler sources.

The brightness of the "A" wiggler is nearly 100 times greater than the APS bending magnets at high energy. Such a device would permit ppb level fluorescence analyses of rare earth elements (REE) in 10 μm spots. It could be used for high energy x-ray diffraction, reducing data collection times dramatically. The "B" wiggler brightness is 100 times that of an NSLS bending magnet at 10 keV. This device is ideal for spectroscopy at low energies, and for single crystal and powder x-ray diffraction.

The radiation from a wiggler is linearly polarized, with the electric vector in the horizontal plane. Unlike that from a bending magnet, the radiation from a wiggler is linearly polarized not only in the orbital plane, but above and below it as well. This high degree of linear polarization can be very useful for XRF microprobe and fluorescence EXAFS experiments, where scattered backgrounds can be minimized by taking advantage of the polarization. There are some experiments which would benefit from the increased flux of a wiggler but which require elliptically or circularly polarized radiation. For these experiments helical wigglers can be used, since the radiation from a helical wiggler is circularly polarized.

2.4 Undulators

By far the most compelling reason to build the APS is to be able to use hard x-ray undulators. Undulators are periodic, low magnetic field devices whose output is very different from bending magnets and wigglers. The output has peaks in its energy spectrum, and is highly collimated in both the vertical *and* horizontal directions. In the following discussion we will consider first the theory of an undulator on an ideal, zero-emittance storage ring, and then see how the results differ for real rings. We will consider the predicted performance of two proposed undulators on the APS (Argonne National Laboratory, 1987). The parameters of these undulators and an existing undulator at the PEP storage ring at SSRL are given in Table 2.3.

For an undulator on a zero-emittance source, the energy of the nth harmonic in keV is

$$\varepsilon_n = \frac{0.950nE^2}{(1 + K^2/2)\lambda_u} \tag{2.3}$$

where λ_u is the undulator period in cm. K, the deflection parameter, is

$$K = 0.934\lambda_u B_0 \tag{2.4}$$

and B_0 is the peak magnetic field (Kim, 1985). As the undulator gap is decreased, the magnetic field and K increase, and the energy of each of the harmonics

Table 2.3. Parameters for undulator sources.

Source	Energy (GeV)	Current (mA)	σ_x (μrad)	σ_y (μrad)	λ_u (cm)	Periods	K	Fundamental (keV)
APS "A"	7.0	100	25	10	3.3	158	0.4-2.5	3.5-13.0
APS "B"	7.0	100	25	10	2.3	226	0.3-1.1	13.0-19.5
PEP	8.0	20	33	27	7.7	25	0.3-1.83	3.0-7.6

decreases. The contribution of the higher harmonics increases, and at $K > 10$ the device is a wiggler. APS undulator "A" has a K range of 0.4 - 2.5, corresponding to fundamental energies of 3.5 - 13.0 keV.

The brightness of the nth harmonic is

$$B_n = 1.74 \times 10^{14} N^2 E^2 I F_n(K) \tag{2.5}$$

where N is the number of periods in the undulator and $F_n(K)$ is a function plotted in Figure 2.5. For the APS undulator "A" the brightness at 10 keV is about 6.4×10^{18} photons/sec/mrad^2/0.1% BW, or more than 5 orders of magnitude greater than an NSLS bending magnet.

The characteristic opening angle in both the horizontal and vertical directions of the nth harmonic is

$$\sigma_r = \sqrt{\frac{\lambda_n}{L}} \tag{2.6}$$

where λ_n is the photon wavelength and L is the length of the undulator. For APS undulator "A" with the fundamental at 1 Å (12.4 keV), $\sigma_r = 4.5$ μrad. Note that this is 15 times less than the intrinsic vertical opening angle of the bending magnet radiation.

The bandwidth of the nth harmonic is

$$\frac{\Delta\lambda}{\lambda} = \frac{1}{nN} . \tag{2.7}$$

For the APS "A" device the bandwidth of the fundamental is 0.63%.

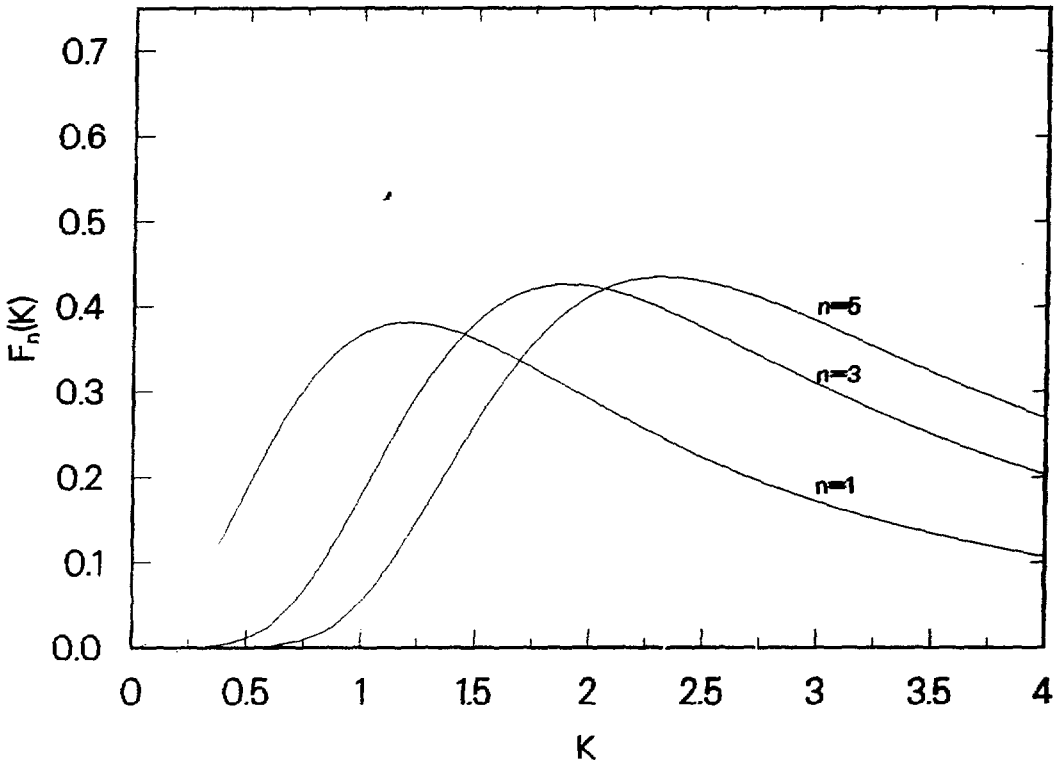

Figure 2.5. Function $F_n(K)$.

In the ideal case, only the odd harmonics are present in the on-axis radiation. Even harmonics, however, are present in the off-axis radiation.

If we now consider an undulator on a real storage ring with non-zero emittance the theory must be modified. Qualitatively, the effect of the angular divergence of the electron beam ($\sigma_{x'}, \sigma_{y'}$) is to "smear out" the photon beam, such that the on-axis radiation has the characteristics of the radiation from an ideal source averaged over an opening angle equal to the divergence angle of the electron beam. Thus, the peak brightness is reduced, the even harmonics are now present in the on-axis beam, and the energy of each harmonic is "red-shifted" slightly. The most significant effect of the non-zero electron beam divergence is the reduction in the peak brightness of each harmonic. The ratio of the finite emittance brightness to the zero emittance brightness is about

$$\frac{B_{EE}}{B_{ZE}} = \frac{\sigma_r^2}{\sqrt{(\sigma_r^2+\sigma_{x'}^2)\,(\sigma_r^2+\sigma_{y'}^2)}} \,. \tag{2.8}$$

If the electron beam divergence is large, ($\sigma_{x'} >> \sigma_r$ and $\sigma_{y'} >> \sigma_r$), then

$$\frac{B_{EE}}{B_{ZE}} = \frac{\sigma_r^2}{\sigma_{x'}^2\,\sigma_{y'}^2} \,. \tag{2.9}$$

For the APS undulators $\sigma_{x'} \approx 25\ \mu$rad, $\sigma_{y'} \approx 10\ \mu$rad. For undulator "A" at 12.4 keV, $\sigma_r \approx 4.5\ \mu$rad, and the reduction in peak brightness (Equation 2.8) is thus about a factor of 14. The envelopes of the peak brightness of the first and third harmonics of the APS undulators, over their respective K ranges, are plotted in Figure 2.6. Also plotted is the brightness of an undulator which has been installed on the PEP storage ring at SSRL. These curves were predicted using Equations 2.5, 2.6, and 2.8.

To quantitatively predict the entire spectrum from an undulator on a real storage ring requires sophisticated computer models. We have used the program **SMUT** (Sensible Modeling of Undulator Throughput) written by Chris Jacobsen of SUNY Stony Brook (Rarback *et al.*, 1987), to predict the spectra of the APS "A" and "B" undulators at their minimum and maximum K values. These spectra are plotted in Figures 2.7 - 2.10. **SMUT** includes the effect of the non-zero beam emittance, but it does not yet include the effects of any magnetic field errors in the undulator itself. These errors tend to reduce the amplitudes of the higher order harmonics, so that

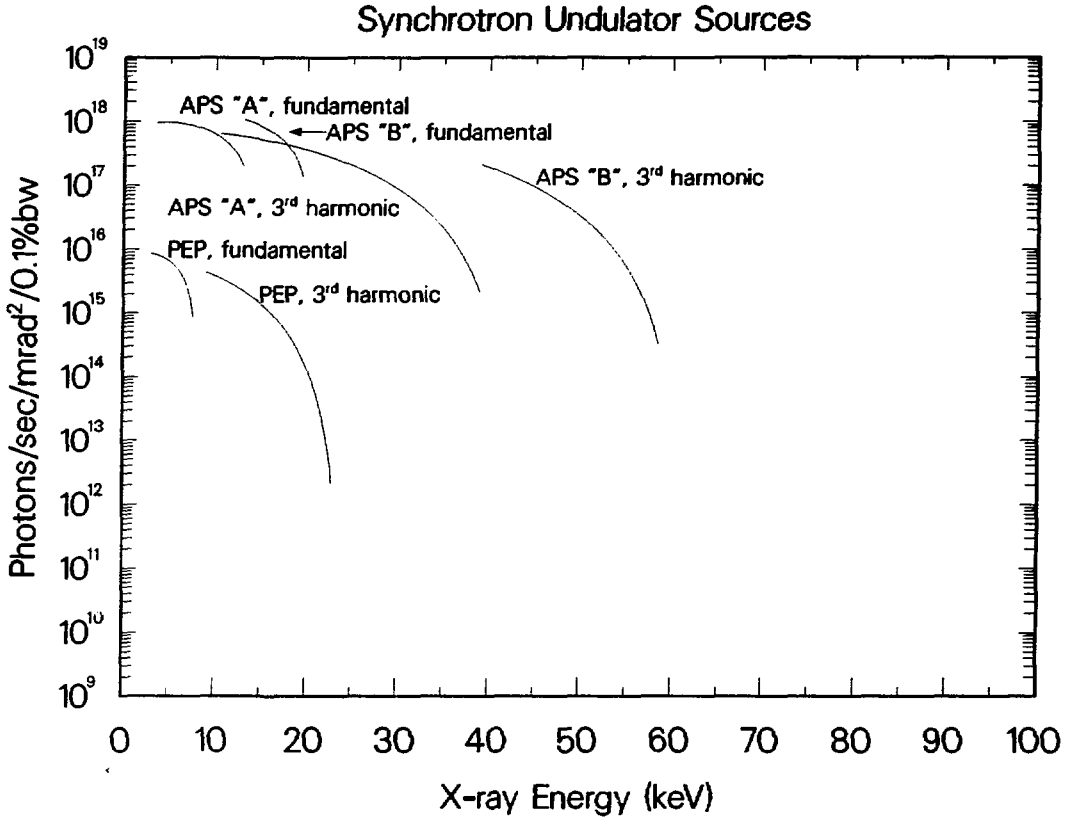

Figure 2.6. Peak brightness of selected synchrotron x-ray undulator sources.

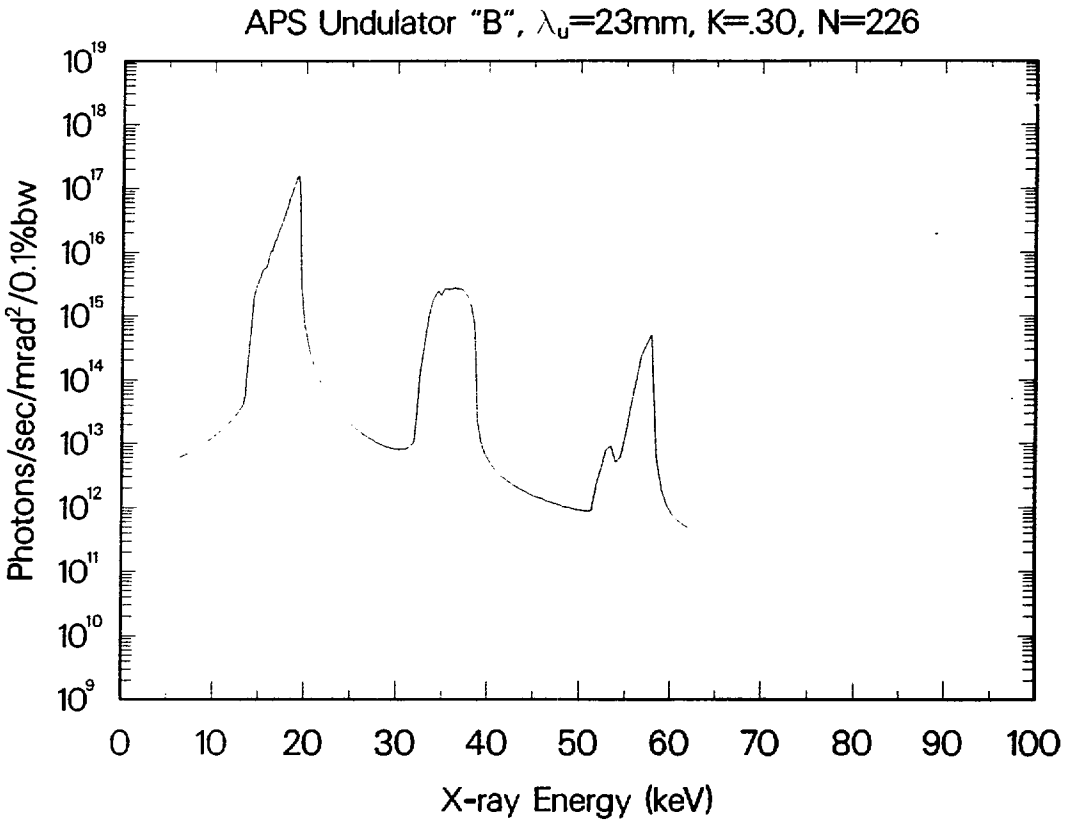

Figure 2.7. Brightness of the APS undulator "B" with K=0.30.

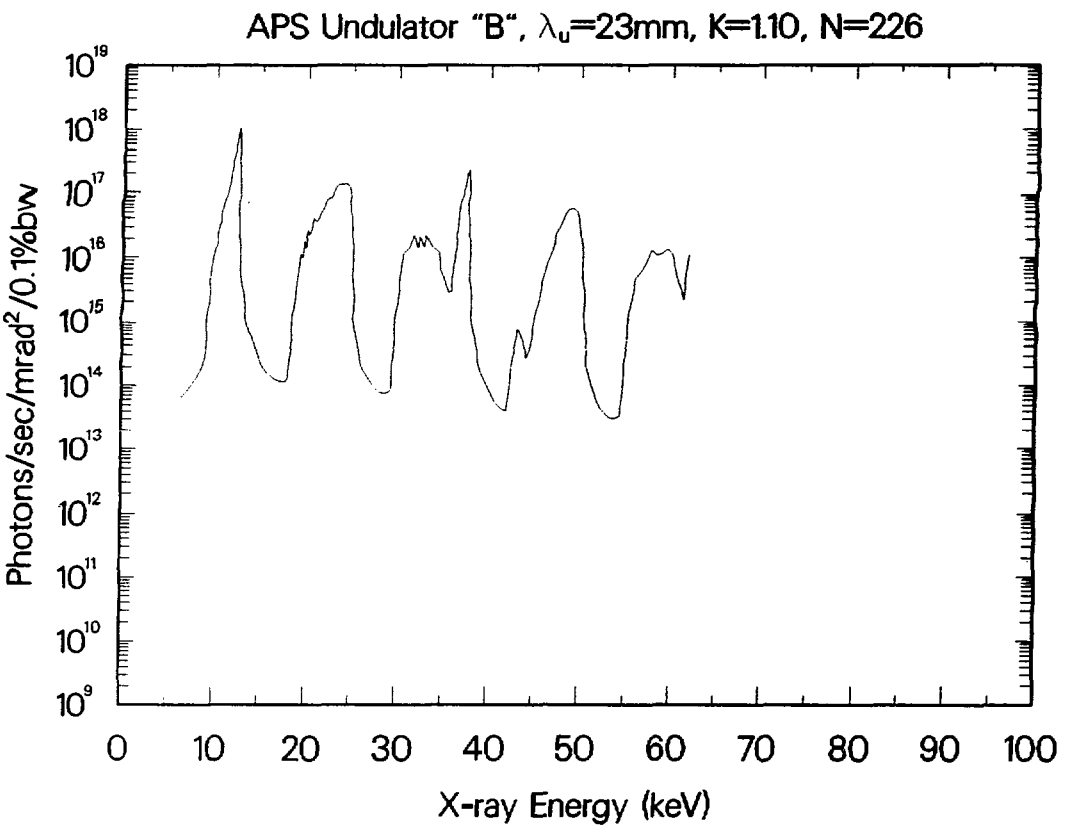

Figure 2.8. Brightness of the APS undulator "B" with K=1.10.

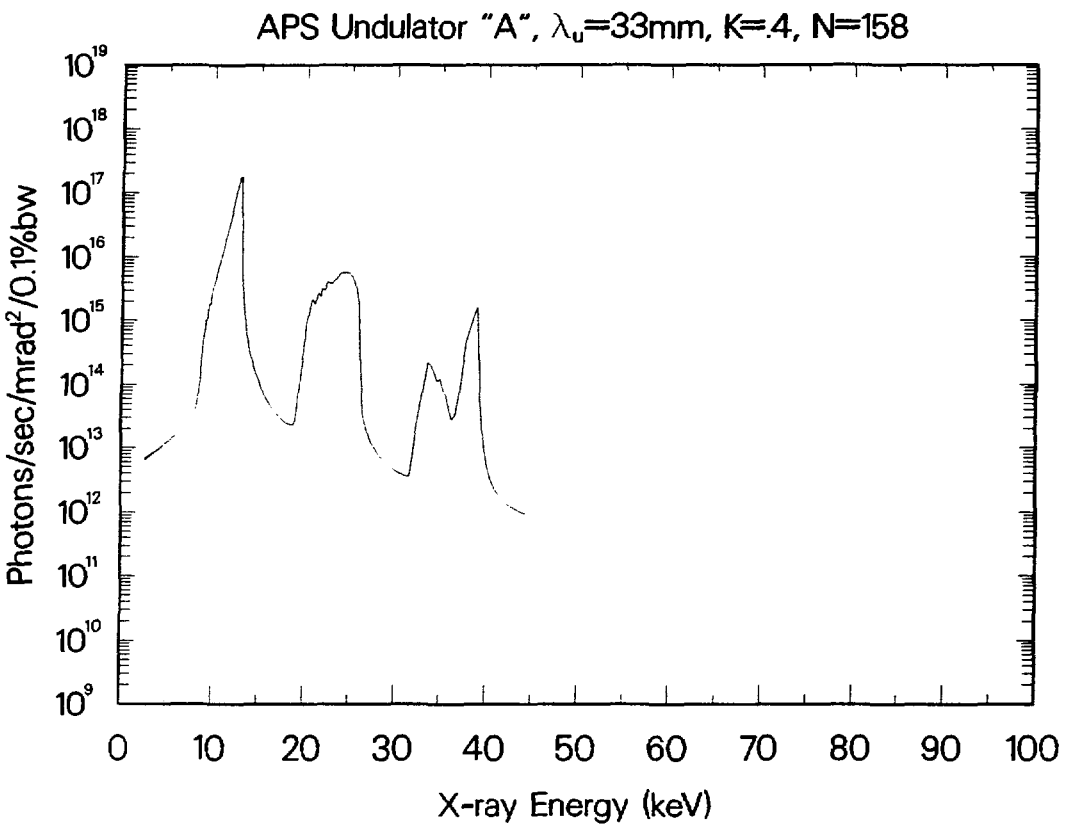

Figure 2.9. Brightness of the APS undulator "A" with K=0.40.

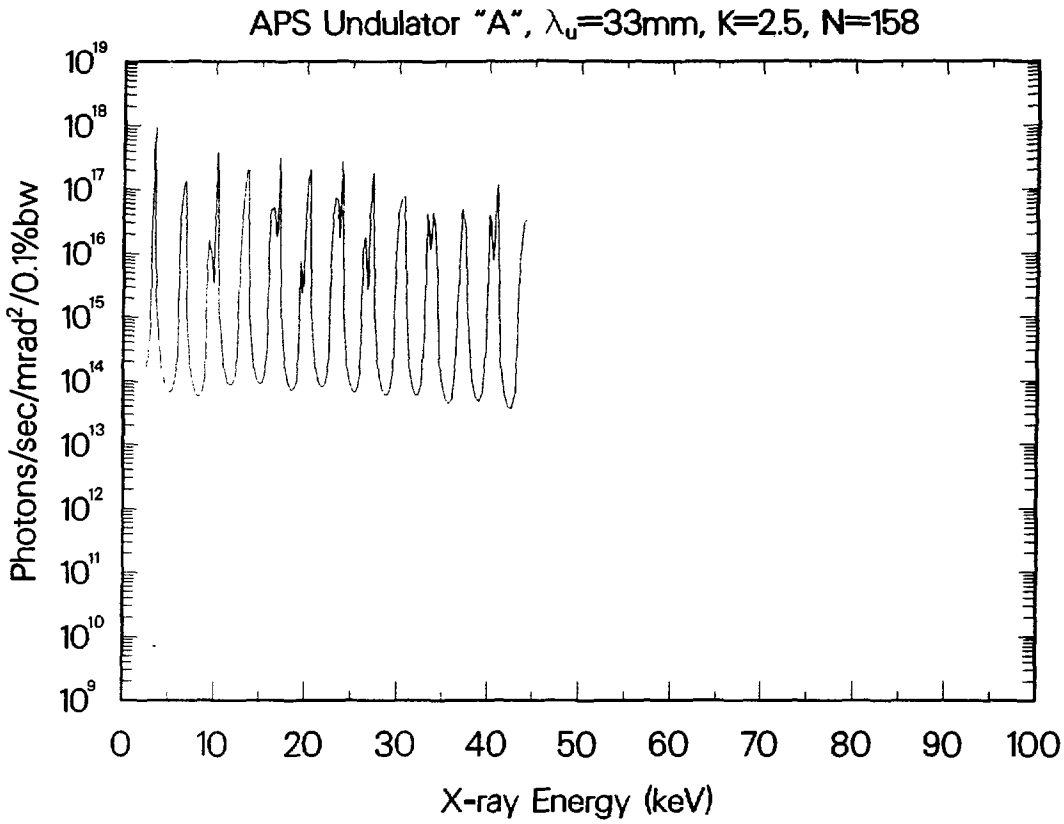

Figure 2.10. Brightness of the APS undulator "A" with K=2.50.

the harmonics beyond the third in Figures 2.8 and 2.10 are probably not realistic. There are several other features worth noting in these predicted spectra.

The brightness of the second harmonic is considerable, being larger than the third harmonic in many cases. The second harmonic, although it is not shown in Figure 2.6, increases the energy coverage of both undulators. The second harmonics tend to be quite flat-topped, which makes them suitable for spectroscopy without the need to adjust the undulator gap.

The non-zero emittance gives rise to low energy shoulders on the first and third harmonics, but the peak-to-valley ratios are still superb, more than four orders of magnitude. This is excellent for x-ray fluorescence, since one can adjust the undulator to produce large numbers of photons just above the absorption edge, but have very few scattered photons at the fluorescent energy below the edge.

The on-axis radiation from an undulator is linearly polarized, with the electric vector in the horizontal plane. Off-axis the radiation contains both vertical and horizontal polarization components. The pattern of the off-axis polarization is quite complex, with the characteristic shape being different for each harmonic.

Comparing the predicted intensities of the undulators with the bending magnets, one sees that the APS "A" undulator has a brightness at 10 keV which is 14,000 times greater than an NSLS bending magnet. This is a most remarkable increase. For XRF this implies, for instance, that one could reduce the spot size by a factor of 100, to well below 1 μm, with the same sensitivity demonstrated at NSLS X-26. Alternatively, one could use less efficient detectors with much better resolution and lower backgrounds to dramatically improve sensitivities and reduce interferences. The undulator source *brilliance* means that one can use focusing optics to achieve even higher intensity on the sample. It should be quite possible to achieve sub-micron beams with $>10^{10}$ photons/sec. This will permit fundamentally new experiments in x-ray diffraction, spectroscopy, and trace element analyses.

Recent analyses (P. J. Viccaro, personal communication) have shown that it is possible to "taper" an undulator, e.g. set the gap larger at one end than the other. This can be done even with an undulator which is designed to be used untapered most of the time. The tapered undulator produces a spectrum with much flatter tops on the harmonic peaks, e.g. greater bandwidth in each harmonic. Analysis has shown that the integrated flux in each harmonic decreases very little, although the peak brightness of course decreases. Such tapered undulators are ideal for spectroscopy, since the flux is relatively constant over hundreds of eV. An APS prototype undulator installed on the CESR storage ring at Cornell was run in tapered mode

and used to collect a Mn EXAFS spectrum, with good results (P.J. Viccaro, personal communication).

2.5 References

Winick, H. 1980. Properties of synchrotron radiation. p. 459-512. *In* H. Winick and S. Doniach (ed.) Synchrotron radiation research. Plenum Press, New York.

Argonne National Laboratory. 1987. 7 GeV Advanced Photon Source - Conceptual Design Report, Report ANL-87-15. Argonne National Laboratory, Argonne, Illinois.

Kim, K. J. 1985. Characteristics of synchroton radiation, *In* D. Vaughn (ed.) X-ray data booklet. Lawrence Berkeley Laboratory PUB-490. Lawrence Berkeley Laboratory, Berkeley, California.

Rarback, H., C. Jacobsen, J. Kirz and I. Mcnulty. 1988. The performance of the NSLS mini-undulator. Nucl. Inst. Meth. A266:96-105.

Chapter 3

X-Ray Absorption Spectroscopy: EXAFS and XANES - A Versatile Tool to Study the Atomic and Electronic Structure of Materials

E. E. Alp, S. M. Mini, and M. Ramanathan

X-ray absorption spectroscopy (XAS) had been an essential tool to gather spectroscopic information about atomic energy level structure in the early decades of this century. It has also played an important role in the discovery and systematization of rare-earth elements (Röhler, 1987). The discovery of synchrotron radiation in 1952, and later the availability of broadly tunable synchrotron based x-ray sources have revitalized this technique since the 1970's. The correct interpretation of the oscillatory structure in the x-ray absorption cross-section above the absorption edge by Sayers *et al.* (1971) has transformed XAS from a spectroscopic tool to a structural technique. EXAFS (Extended X-ray Absorption Fine Structure) yields information about the interatomic distances, near neighbor coordination numbers, and lattice dynamics. An excellent description of the principles and data analysis techniques of EXAFS is given by Teo (1986). XANES (X-ray Absorption Near Edge Structure), on the other hand, gives information about the valence state, energy bandwidth and bond angles. Today , there are about 50 experimental stations in various synchrotrons around the world dedicated to collecting x-ray absorption data from the bulk and surfaces of solids and liquids.

In this chapter, we will give the basic principles of XAS, explain the information content of essentially two different aspects of the absorption process leading to EXAFS and XANES, and discuss the source and sample limitations.

A typical normalized x-ray absorption cross-section as a function of energy is given in Figure 3.1 for a compound with a perovskite structure, La_2CuO_4, measured at the Cu K-edge. The near-edge and extended absorption regions are pointed out. The absorption cross-section, $\mu(E)x$ is measured by determining the attenuation of x-rays by a sample with thickness x:

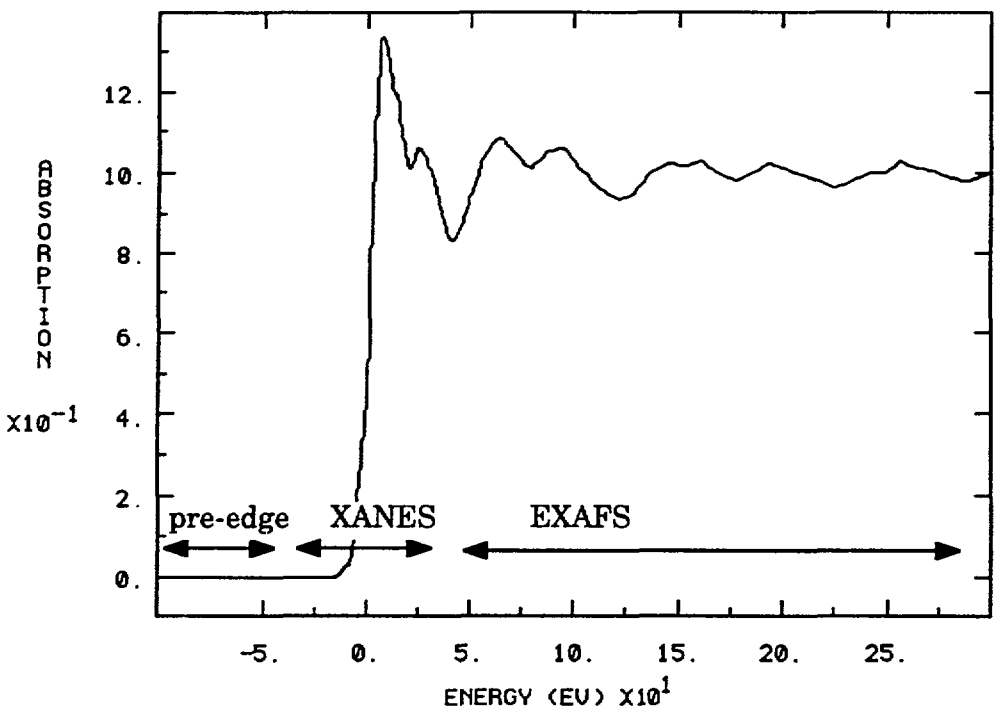

Figure 3.1. Normalized absorption cross section of La_2CuO_4 as a function of energy near the Cu K-edge (E = 8979 eV). XANES and EXAFS regions are pointed out. The zero of the energy is with respect to CuK-edge position.

$$\ln \frac{I_o}{I} = \mu(E)x$$

where I_o and I represent the incident and transmitted beam intensity measured by using ionization chambers.

There are many ways the EXAFS or related data can be obtained. They are shown schematically in Figure 3.2. The *transmission mode* is the most common method of detection, provided that the samples are in the form of a foil or thin single crystal, or a homogenous sample prepared from powders. The thickness of the sample is adjusted such that it is equal to 1 to 2 absorption lengths calculated at the absorption energy of interest, i.e. $\mu \cdot x = 1$. There are tables available to obtain the absorption cross-section of elements (McMaster *et al.*, 1969). For materials with multiple components, one should use the weighted average cross section:

$$\mu(E) = \sum_{i=1}^{n} \mu_i \cdot wt\%\ i$$

Data collection time in the energy scanning mode of operation is between half an hour and 2 hours, while it is 0.1 to 2 seconds for the *energy dispersive* mode, shown in Figure 3.2c, (Dartyge *et al.*, 1986). The measurement time can be cut down to the microsecond level by use of CCD based detectors. The high brightness of the APS will help to improve the signal-to-noise ratio, and will reduce the minimum sample size to micrograms.

3.1 XANES : X-Ray Absorption Near Edge Spectroscopy

The x-ray absorption process is the result of an excitation of an inner level electron to a higher energy level by an incident photon. Since it involves an electronic transition it can be best represented by a transition matrix element coupling the initial state $|i>$ to the final state $<f|$:

$$\mu(E) \approx |\langle f | \varepsilon \cdot r | i \rangle|^2$$

where ε is the polarization vector of the electric field of the photon, and **r** is the position vector of the photoelectron. Since the operator coupling the two states is an electric dipole operator, the selection rules apply and determine the allowable final states for a given initial state. For example, when a 1s level electron is excited, the lowest-lying empty p-states will be occupied and the process is called K-edge-absorption. Each element has a characteristic energy level structure and therefore

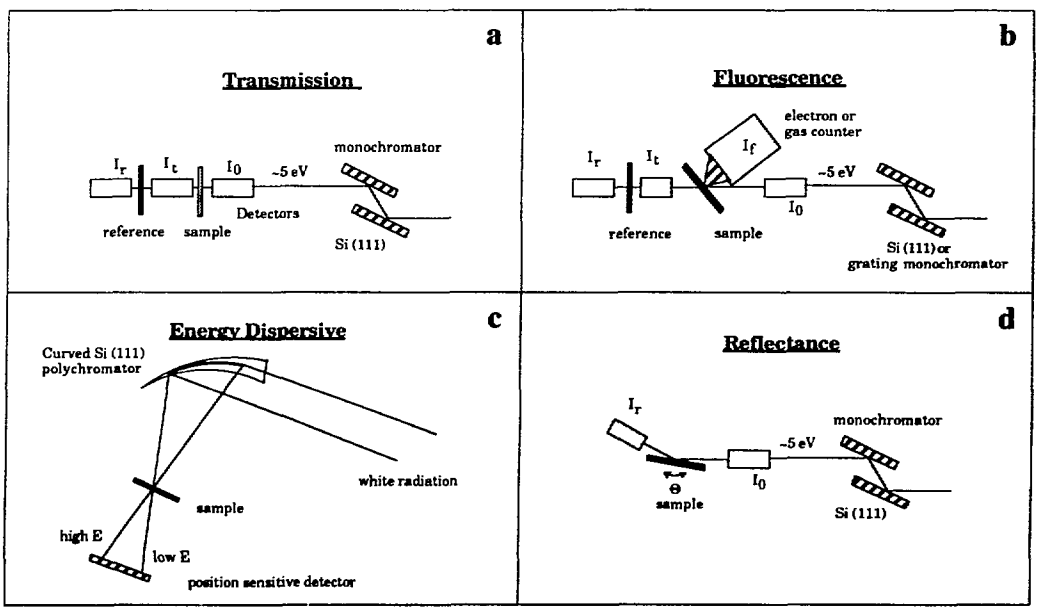

Figure 3.2. Schematic description of various experimental configurations to collect EXAFS and related data.

can be studied separately. The empty energy levels above the Fermi level in a compound are also sensitive to the nature of the chemical bond and valence. This provides a basis for valence determination through *careful measurements* of the position of the absorption edge. Examples are given in Figure 3.3a, b, and c for several copper, iron, and praseodymium compounds. The observed shifts in the position of the absorption edge can be quantitatively related to the valence state of the absorbing atom. These shifts are a few eV per valence change for transition metal element K-edges, and 8-10 eV for rare-earth element L_3-edges. Since changes of the order of 0.5 eV are measurable, fractional changes in the effective charge on atoms can be measured with this technique (Alp *et al.,* 1989). The *careful measurement* implies reproducibility and good energy resolution. Since a typical experimenter collects data at various facilities (i.e. wherever there is light !), it is important to have a common reference point. This can be achieved by collecting a simultaneous measurement of a reference compound in tandem with the unknown compound, as shown in Figure 3.2a.

The atom specific nature of this spectroscopy requires x-ray sources that are broadly tunable in energy. The absorption energies of elements can range from a few electron volts (16 eV for hydrogen 1s to 2p transition) to over 100 kiloelectron volts (115,606 eV for uranium 1s to 7p transition). Naturally, there is no single light source which can provide photons covering this energy range with enough intensity to make a measurement practical. However, with the availability of synchrotron x-ray sources, this problem has been overcome to a large extent. Ultraviolet and soft x-ray sources, as well as hard x-ray sources, are now routinely available in the USA and abroad. On the other hand, there are limitations in our ability to monochromatize this white radiation. The methods used to monochromatize radiation vary as the energy is changed. For example, grating monochromators provide good energy resolution below 1000 eV, while silicon or germanium crystals can be used between 2.5 and 20 keV. This leaves a gap between 1 and 2.5 keV. Unfortunately, this region covers K absorption edges (1s to 2p) of Na, Mg, Al, Si, and P, which are commonly found in many systems. The efforts to use InSb, Beryl, or YB_{66} (Wong, 1988) and artificially grown multilayers with suitable periodicity to monochromatize radiation from synchrotron sources seems to be overcoming this problem.

The electronic information in XANES spectrum is pronounced in different forms. While the relative location of the absorption edge reveals the effective charge on the absorbing atom, the location and intensity of the resolvable features provide additional details about the relative width and occupancy of the final states. Furthermore, the polarized nature of the synchrotron radiation provides an additional dimension in the study of the anisotropy of the final electronic states in single crystals or oriented samples.

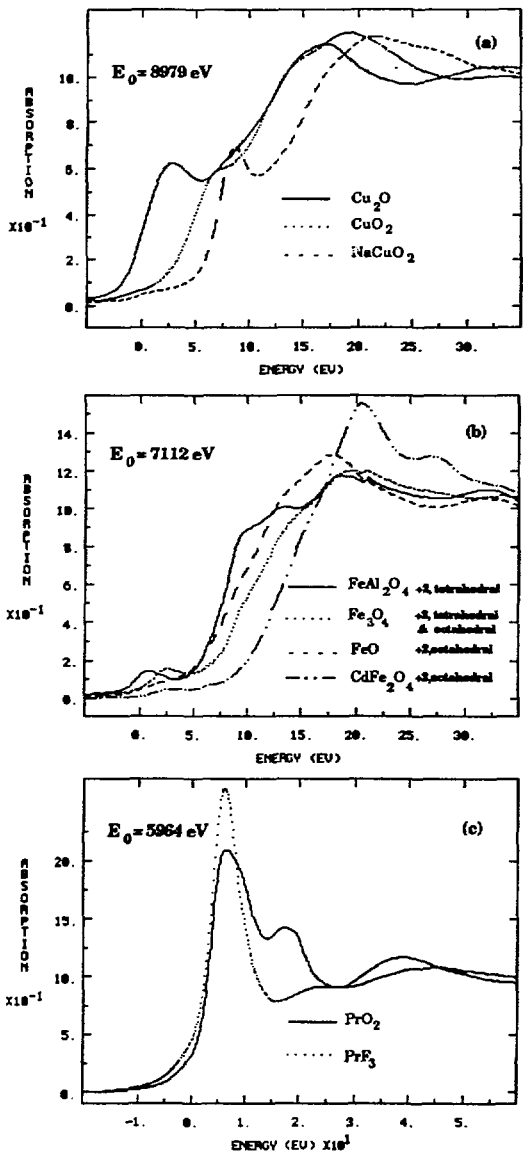

Figure 3.3. The energy shifts observed in XANES spectra of (a) Cu compounds at the Cu K-edge, (b) Fe compounds at the Fe K-edge, and (c) Pr compounds at the Pr L_3-edge. Calibrated comparisons on standard compounds help identifying valence of elements in unknown compounds. The energy scale is referenced to the absorption edge energies given in the insert.

The XANES spectroscopy can be performed in transmission or in *fluorescence mode* when x-rays are detected, or in total electron yield count-mode when secondary conversion electrons are detected, as shown in Figure 3.2b. The transmission experiments provide the best signal-to-noise ratio, and in addition the measurement is representative of the bulk. For dilute samples, the fluorescence mode is necessary. The lowest concentration that can be detected in fluorescence mode depends on various factors such as subtended detection angle, the photon flux, and the ratio of the absorption cross-section of the element of interest to that of the total cross-section of the material. As a rule of thumb, the dilution ratio can be as low as 10^{-5}. The penetration of x-rays below 3 keV requires very thin samples such that not only is it impractical to prepare them, but the signal-to-noise ratio also becomes a problem. In such cases, total electron yield count can be used to measure the absorption spectrum. These measurements require an ultra high vacuum environment, and they are very surface sensitive. Recently, gas detectors operating at low energies have been built and tested. The results indicate that the surface sensitivity problem can be avoided by recording fluoresence yield (Smith *et al.*, 1989).

The current status of calculations regarding the near edge structure is not as well developed as it is for EXAFS. The many-electron self-consistent quantum chemistry code based on representative clusters is the most promising development (Goodman *et al.*, 1989). However, these codes are difficult to use and, in general, they are not in the public domain.

3.2 EXAFS : Extended Absorption Fine Structure Spectroscopy

EXAFS is an interference effect caused by the interaction of the outgoing photoelectrons ejected from inner core levels by the resonant radiation, and the backscattered electrons from the near neighbor atoms, modulating the final state wavefunction of the absorbing atom. It was correctly interpreted by Sayers *et al.* (1971) to be related to the radial distribution function around the central absorbing atom. In its simplest form, traveling electrons can be described by plane waves. In this formalism, the oscillatory part of the absorption coefficient is given by

$$\chi(k) = \sum_{i=1}^{n} \frac{N_i}{kR^2} A_i(k)\, e^{-2\sigma^2 k^2} \sin(2kr_i + \Phi_0)$$

where N_i is the number of atoms in the i^{th} shell, r_i is the interatomic distance between the central atom and i^{th} neighbor, A_i is the amplitude of the backscattered

electron, and Φ_0 is the total phase shift experienced by the electron. The exponential term takes into account the smearing of the interatomic distance due to static and thermal disorder. It is related to the Debye-Waller factor of x-ray scattering. However, it only reflects the change in the bond distance, and not the individual vibrational amplitudes. At higher temperatures this factor tends to smear out the EXAFS oscillations. This has some immediate consequences: First, the data collected at low temperatures will have more accuracy in determining the bond distance than the data collected at higher temperatures. This is shown in Figure 3.4 where two spectra measured at room temperature and 13 K are compared in real space and in k-space. When a sample contains heavy elements like Ba or Bi, then it is possible to collect data up to 20 $Å^{-1}$. The larger the k-range, the higher the accuracy of bond length determination. Second, one can study individual bond strengths in terms of lattice vibrations as a function of temperature. Notice the difference in the temperature dependence of Bi-O vs. Bi-Ba, and Bi-Bi peaks in Figure 3.4b. Finally, data collected from liquids, or solids at high temperature will have limited k-range, thus reducing the accuracy of the technique.

3.3 Polarized EXAFS and XANES

There are other advantages of using synchrotron radiation for EXAFS or XANES spectroscopy. One is the polarization characteristics of this radiation. The radiation emitted from relativistic particles is linearly polarized when observed in the bending plane. However, one can observe elliptical polarization when the measurement is done off-axis. When single crystals or oriented powders are used for absorption experiments, it is possible to selectively excite transitions into orbitals which are along the direction of the polarization (Goodman *et al.*, 1989). In other words, the absorption cross section is anisotropic and can yield additional information (Guo *et al.*, 1990). An example is given in Figure 3.5 where (a) XANES, and (b) EXAFS from oriented crystals of Nd_2CuO_4 are shown. These experiments make it easier to interpret the various peaks observed at the near edge, as well as their shift as a function of chemical doping, pressure, temperature, etc.

The EXAFS signal obtained from polarized measurements also gives enhanced signal for the radial distribution function for the atoms lying in the plane of polarization. An example is given in Figure 3.5b, where for a layered Cu-O compound of Nd_2CuO_4, Fourier transforms of $k^3\chi(k)$ versus interatomic distances are plotted. As shown in the figure, the first near neighbor oxygen atoms and third near neighbor Cu atoms are more visible when the polarization vector of the incident radiation lies in that plane.

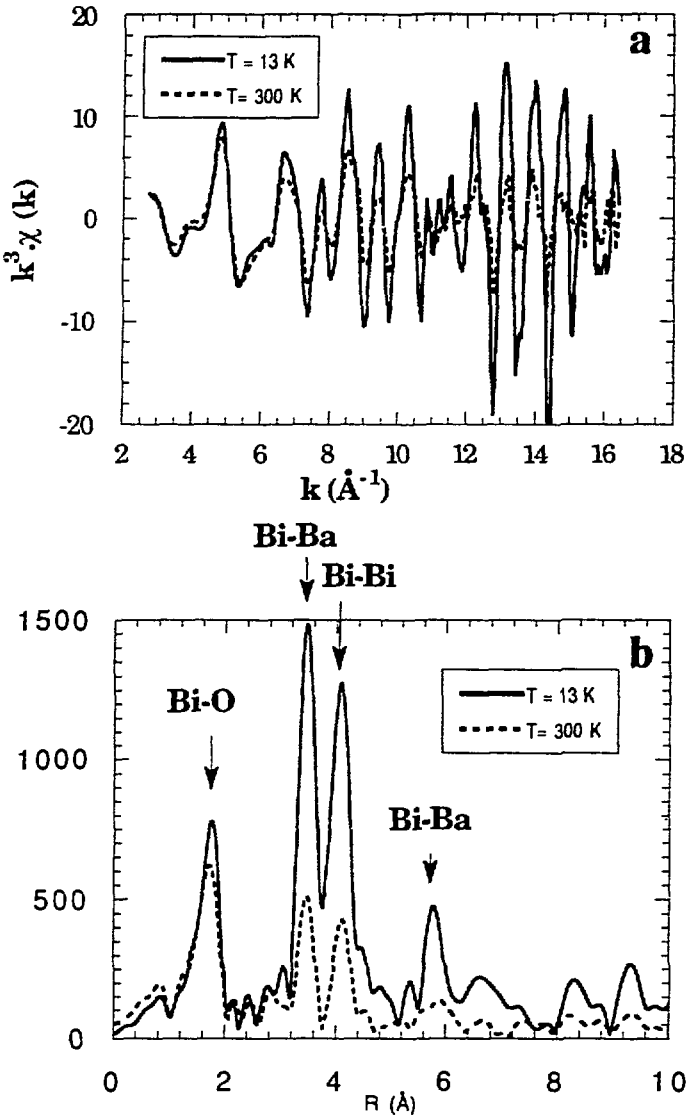

Figure 3.4. The Bi L_3-edge EXAFS of $Ba_{0.6}K_{0.4}BiO_3$ compound at room temperature and at 13 K, (a) in momentum space, and (b) in real space. The stiffness of Bi-O bonds with respect to Bi-Bi and Bi-Ba bonds can be quantitatively determined with proper analysis.

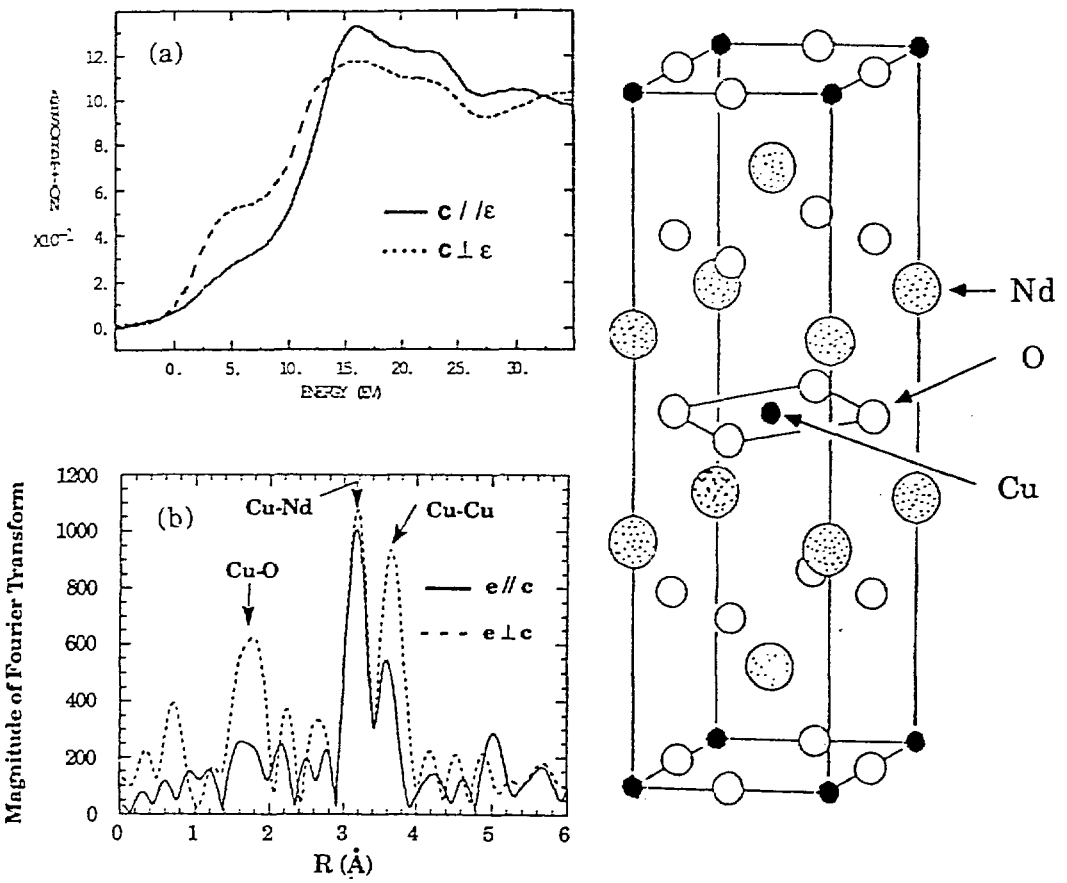

Figure 3.5. (a) The polarized XANES spectra of Nd_2CuO_4, using linearly polarized synchrotron radiation. When the polarization vector of x-rays is along the Cu-O planes ($\mathbf{c} \perp \varepsilon$), the Cu 1s→4p transition requires a few eV more than when it is along the c-axis. This substantial anisotropy indicates the truly 2-dimensional nature of the electron structure along the Cu-O planes. (b) The Fourier transform of Cu K-edge EXAFS spectrum of Nd_2CuO_4. When the polarization vector **e** is along the Cu-O planes, Cu-O and Cu-Cu peaks are enhanced, enabling a more selective study of these bonds.

The EXAFS spectroscopy technique is also used as a surface probe (SEXAFS) or to study buried interfaces by performing the experiment at grazing incidence near the critical angle of total external reflection (REFLEXAFS) (Chen, 1989). Further examples can be found in the proceedings of past EXAFS meetings (Hodgson *et al.*, 1984).

In conclusion, we would like to emphasize the complementary and, in some cases, unique nature of EXAFS and XANES spectroscopies in local atomic and electronic structure determination of solids, liquids, surfaces and very dilute samples.

3.4 Acknowledgments

We would like to thank to Drs. A. Bommannavar for his help during the measurements on Beamline X-18 B at NSLS, and O.B. Hyun for his preparation of oriented copper oxide samples. We also thank B. Dabrowski and D.G. Hinks for providing $Ba_{1-x}K_xBiO_3$ samples. This work is supported by the US DOE, BES-Materials Sciences under contract # W-31-109-ENG-38. SMM is supported by the Science and Technology Center for Superconductivity funded by NSF under contract #STC-8809854.

3.5 References

Alp, E. E., G. Goodman, L. Soderholm, S. M. Mini, M. Ramanathan, G. K. Shenoy, and A. S. Bommannavar. 1989. A new approach to determining the charge distribution in copper compounds. J. Phys.: Condens. Matter 1:6463-6468.

Chen, H. 1989. Studies of Cu-Al interfaces using glancing angle x-ray reflectivity and EXAFS. Ph. D. Thesis, CUNY.

Dartyge, E., C. Depautex, J. M. Dubuisson, A. Fontaine, A. Jucha, P. Leboucher, and G. Tourillon. 1986. X-ray absorption in dispersive mode: A new spectrometer and a data aquisition system for fast kinetics. Nucl. Instr. Meth. A246:452-460.

Goodman, G. L., D. E. Ellis, E. E. Alp, and L. Soderholm. 1989. Charge distribution and valency in copper oxide cyrstals related to superconductivity. J. Chem. Phys. 91:2983-2992.

Guo, J., D. E. Ellis, G. L. Goodman, E. E. Alp, L. Soderholm, and G. K. Shenoy. 1990. Theoretical calculations of x-ray-absorption spectra of copper in La_2CuO_4 and related oxide compounds. Phys. Rev. B 41:82-95.

Hodgson, K. O., B. Hedman, and J. E. Penner-Hahn. 1984. EXAFS and Near Edge Structure III. Springer Verlag. (and the previous volumes).

McMaster, W. H., N. Kerr Del Grande, J. H. Mallet, and J. H. Hubbell. 1969. Compilation of x-ray cross sections. UCRL-50174 Sec. II, Rev. 1. Lawrence Radiation Laboratory, Univ. California, Livermore, California.

Röhler, J. 1987. X-ray absorption and emission spectra. p. 453-545. *In* K. A. Gschneider, J., L. Eyring, and S. Hüfner (ed.) Handbook on the Chemistry and Physics of Rare-Earths. Vol. 10.

Sayers, D. E., E. A. Stern, and F. W. Lytle. 1971. New technique for investigatin noncrystalline structures: Fourier analysis of the extended x-ray-absorption fine structure. Phys. Rev. Lett. 64:1204-1207.

Smith, G. C., A. Krol, and Y. H. Kao. 1989. Proceedings of the 6th synchrotron radiation instrumentation conference, 7-11 Aug. 1989, Berkeley, California. (preprint).

Teo, B. K. 1986. EXAFS: Basic principles and data analysis. Springer Verlag.

Wong, J. 1988. SSRL Activity Report. Stanford, California.

Chapter 4

Applications of X-ray Spectroscopy and Anomalous Scattering Experiments in the Soil and Environmental Sciences

S. J. Anderson, C. C. Ainsworth, P. M. Bertsch, J. M. Bigham, W. F. Bleam, P. R. Bloom, J. B. Harsh, D. G. Schulze, and J.W. Stucki

4.1 Introduction

Chemical reactions in the soil are of interest to agricultural and environmental scientists because such reactions control the availability of plant nutrients and the mobility of environmental contaminants. Knowledge of chemical bonding and of the atomic-level structure of crystalline and non-crystalline solids and of surface-sorbed and soluble species is essential for accurate prediction of the response of soils and natural aqueous systems to environmental perturbations such as fertilization, waste disposal, or treatment of contaminated soil and waters.

X-ray absorption spectroscopy (XAS), x-ray emission spectroscopy (XES), and anomalous scattering methods can provide element-specific information about bonding and structure in both homogeneous and heterogeneous samples. Extended x-ray absorption fine structure (EXAFS) reveals the local atomic arrangement around each type of atom, including average coordination numbers, bond lengths, and bond angles. X-ray absorption near edge structure (XANES) can provide information about symmetry, bonding, and oxidation state of an element (see Chapter 3, this report). X-ray emission spectroscopy may be used to elucidate the electron states that contribute to bonding in minerals or at mineral surfaces. Differential anomalous scattering (DAS), in which the difference between the scattering amplitudes at two energies is measured, yields medium-range, element-specific structural information.

The information gained from XAS experiments (which include EXAFS and XANES) complements that provided by scattering and diffraction methods, XES and

other x-ray spectroscopies, electron spectroscopy, and conventional spectroscopic techniques such as vibrational or resonance spectroscopies. X-ray absorption spectroscopy offers several advantages over other spectroscopic methods for many systems of interest to soil and environmental scientists. First, XAS can provide accurate information about the coordination environment of cations in solids that contain Fe^{3+}, Mn^{2+}, or other paramagnetic cations. In contrast, line broadening limits the interpretation of NMR spectra when paramagnetic materials are present in soils and clays. Second, because of the element-specific nature of x-ray absorption edge spectra, elements in a heterogeneous matrix may be studied with XAS, provided that no element in the sample has an absorption edge (K or L) within about 300 eV of the absorbing atom (Stern, 1988). Although the absorption edge of Si is less than 300 eV above the K-edge for Al, it is possible to obtain Al K-edge EXAFS data for Al in aluminosilicates if the spectra are truncated about 15 eV below the Si absorption edge (McKeown *et al.*, 1985b). A third advantage of x-ray spectroscopic and anomalous scattering methods is that, in contrast to vibrational, resonance, and electron spectroscopies, all of which depend on transitions between energy levels, absorption edge spectra contain a backscattering component that can provide more direct information about interatomic distances (Brown and Parks, 1989).

X-ray spectroscopy can be used to study nearly all elements of the periodic table if a broad spectrum of x-ray energies is available. The x-ray absorption edge energies for elements of interest to soil scientists are listed in Table 4.1. Extended x-ray absorption fine structure often can provide short-range structural information that cannot be obtained by other methods, although the method is subject to a number of limitations. For example, appropriate model or reference compounds are required to determine backscattering amplitudes and phase shifts (Stern, 1988). Experiments utilizing x-ray energies less than about 2.4 keV require ultra-high vacuum or, as a minimum requirement, a non-absorbing atmosphere such as helium. In contrast to low-energy x-rays, x-rays with energies greater than about 2.8 keV are not absorbed significantly by air, and elements with x-ray absorption edges at high energies can be studied in aqueous solutions.

4.2 The Importance of the Advanced Photon Source

In this chapter we shall focus upon those experiments that can be conducted at the Advanced Photon Source (Chapter 2) to be built at Argonne National Laboratory. The Advanced Photon Source (APS) will be best suited for studying elements whose absorption edges can be studied with hard x-rays (E>2.0 eV). The Advanced Light Source to be built at Lawrence Berkeley Laboratory will be better suited than the APS for studying elements whose absorption edges are in the 0.05 to 2.0 keV range (Brown *et al.*, 1988). Although existing synchrotron sources are adequate for static

Table 4.1: K x-ray absorption edges (keV) for elements of interest to soil scientists.

Groups IA to VIIA			Transition Metals and actinides		
Z	element	K edge	Z	Element	K edge
3	Li	0.055	21	Sc	4.500
4	Be	0.112	22	Ti	4.969
5	B	0.187	23	V	5.468
6	C	0.285	24	Cr	5.994
7	N	0.400	25	Mn	6.544
8	O	0.532	26	Fe	7.118
9	F	0.693	27	Co	7.716
11	Na	1.081	28	Ni	8.338
12	Mg	1.304	29	Cu	8.990
13	Al	1.560	30	Zn	9.670
14	Si	1.840	42	Mo	20.018
15	P	2.144	43	Tc	21.068
17	Cl	2.822	48	Cd	26.734
19	K	3.610	80	Hg	83.135
20	Ca	4.041	92	U	115.14
33	As	12.537	93	Np	118.3
34	Se	12.672	94	Pu	121.3
35	Br	13.387	95	Am	124.4
37	Rb	15.214			
38	Sr	16.773			
55	Cs	35.990			
56	Ba	37.441			
82	Pb	88.135			

From Weast (1979).

x-ray spectroscopic and scattering experiments on many systems of interest to soil and environmental scientists, the high flux and brilliance of the APS will offer three main advantages over existing synchrotron storage rings. First, the high flux and brightness will offer the opportunity to study hydrolysis, polymerization, nucleation, and adsorption reactions in aqueous systems at low elemental concentrations. It will be possible to examine the coordination environment of many surface species at realistic surface coverages, even on materials that have low surface areas. Second, the brightness of the source will permit the use of faster, less sensitive detectors and will offer the opportunity to obtain *in situ* kinetic information. The ability to resolve very short time intervals will be of particular use in the study of adsorption, hydrolysis, and nucleation reactions. In addition, the brightness of the APS will provide better energy resolution in XAS and XES spectra and, consequently, more accurate information about bonding in solid, surface, and aqueous species. The enhanced energy resolution also should allow more accurate discrimination between oxidation states of transition metals. The collimated nature and brightness of the radiation should make it possible to obtain spatially resolved spectroscopic data and will permit the study of very small samples. The APS also will offer new opportunities to determine the coordination environment, oxidation state, and bonding in soluble, adsorbed, and solid actinide species.

In the following sections, we shall describe some potential applications of both static and time-resolved EXAFS and XANES experiments on crystalline and amorphous solids, solutions, surface-sorbed species, and the surface layer of bulk solids. In addition, the basis for XES, the complementary nature of XES and electron spectroscopy, and some relevant applications of XES shall be described. Finally, some potential applications of anomalous scattering methods will be discussed.

4.3 Applications of X-ray Absorption Spectroscopy

4.3.1 Cation Environment in Crystalline and Amorphous Solids

X-ray absorption spectroscopy yields structural details that cannot be obtained from a single-crystal or powder Reitveld structural analysis of x-ray diffraction data, which can only give information about the average, long-range three-dimensional structure (Chapter 5). Numerous XAS experiments, reviewed recently by Brown *et al.* (1988) and Brown and Parks (1989), have demonstrated the wealth of information that EXAFS and XANES can provide about the coordination, bonding, and oxidation state of cations in crystalline and amorphous solids. For example, EXAFS experiments can provide valuable information about the coordination environment

of cations in phyllosilicates. In an EXAFS study of the substitution of Co^{2+} ions in the octahedral sites of sepiolite and loughlinite, Fukushima and Okamoto (1987) determined the average Co-O and Co-Co interatomic distances, although the accuracy of their data interpretation has been questioned (Manceau and Decarreau, 1988). Several generally applicable limitations in the interpretation of EXAFS spectra were enumerated in subsequent discussions of the Co EXAFS data (Manceau and Decarreau, 1988; Fukushima, 1988). The coordination environment of Ni in Ni-Mg phyllosilicates has also been studied by EXAFS (Manceau *et al.*, 1984; Manceau and Calas, 1985, 1986). The average number of Ni nearest neighbors was greater than 5 for most samples, which suggested that Ni^{2+} was segregated into discrete domains, not randomly distributed throughout the octahedral sheet (Manceau *et al.*, 1984).

Similar experiments at the Fe absorption edge may indicate whether or not Fe is randomly distributed in smectites. This information would be important in understanding the swelling and ion fixation characteristics of smectites. Based on electron diffraction, x-ray diffraction, and Mössbauer spectroscopic measurements, Mering and Oberlin (1967) and Besson *et al.*, (1983) proposed that Fe-rich smectite (nontronite) is centrosymmetric. In other words, within the limits of experimental accuracy, all octahedral Fe atoms are in *cis* sites (Tsipursky and Drits, 1984). Lear and Stucki (1990) observed frustrated anti-ferromagnetic exchange interactions between Fe atoms in oxidized nontronite. This is evidence that as much as 15% of the octahedral Fe could reside in *trans* sites, thus giving a partial non-centrosymmetric structure. High resolution EXAFS could provide more direct and definitive evidence for the distribution of Fe in smectites. In addition, EXAFS experiments can provide information about the sites occupied by minor constituents of a mineral. For example, Waychunas *et al.* (1986) determined the relative amounts of tetrahedral and octahedral Fe in a plagioclase sample containing 0.2% Fe(III) and 0.09% Fe(II), concentrations too low to be examined with Mössbauer spectroscopy.

The fine structure in x-ray absorption spectra can also provide structural information about amorphous solids. Greaves *et al.* (1981) has determined the coordination environment of Si in silicate glasses. Furthermore, Al EXAFS has revealed that Al is tetrahedrally coordinated in several aluminosilicate glasses (McKeown *et al.*, 1985b). Although truncation of the EXAFS spectrum at about 1.825 keV (to prevent interference by Si) reduces the ability to resolve interatomic distances, it is possible to distinguish between tetrahedral and octahedral Al-O bond lengths in crystalline sillimanite (Al_2SiO_5), which contains both tetrahedral and octahedral Al (McKeown *et al.*, 1985b). Such results suggest that EXAFS could be used to ascertain the local environments of Al and Si in the poorly ordered aluminosilicates allophane and imogolite. Existing ^{27}Al and ^{29}Si NMR data (Goodman *et al.*, 1985; Wilson *et al.*, 1986) are consistent with a model in which a curved or spherical gibbsite sheet is

bonded to monomeric or polymeric silica groups (Cradwick *et al.*, 1972). An EXAFS determination of the bond distances and angles in allophane would allow one to test and refine the models of allophane and imogolite structure.

Aluminum, iron, and manganese hydrous oxides are present in soils as both discrete, well crystalline phases and complex, poorly crystalline admixtures, often containing a number of inorganic or organic contaminants. Numerous investigations have attempted to elucidate the mechanisms of formation of both monomineralic and complex mixed-metal hydrous oxide phases (Hsu, 1989; Schwertmann and Taylor, 1989; McKenzie, 1989). The hydrolysis, polymerization, and nucleation reactions of Al have been studied with a variety of techniques, including NMR (Bertsch *et al.*, 1989a; Fitzgerald *et al.*, 1989) and small angle x-ray scattering (Bottero *et al.*, 1982; Axelos *et al.*, 1985; Bottero *et al.*, 1987). The NMR data suggest the existence of multiple nucleation pathways involving both solid- and solution-phase rearrangements, and EXAFS experiments would provide valuable information to complement the NMR results. Unfortunately, because the absorption edge of Al lies at relatively low energy, Al EXAFS requires ultra-high vacuum conditions. Consequently, *in situ* experiments in aqueous Al solutions cannot be conducted.

The absorption edges of Fe and Mn are of sufficiently high energy that the x-rays are not absorbed significantly by water. Consequently, several Fe EXAFS experiments have been conducted in hydrated systems. It has been demonstrated that ferric hydroxide gels have short-range order, with Fe-O distances (Combes *et al.*, 1986) similar to those observed for octahedral complexes of Fe in solution (Apted *et al.*, 1985). Further studies of the effect of the OH/Al ratio and other synthesis conditions on the coordination environment of Fe^{3+} (Combes *et al.*, 1989; 1990) indicate that the "amorphous" character of the diffraction pattern of two-line ferrihydrite (Chapter 5) is due to extremely small coherently scattering domains, not to a completely random arrangement of Fe-containing octahedra (Combes *et al.*, 1989). A complete understanding of the reaction mechanisms will require time-resolved studies, for which the APS is ideally suited. Although few time-resolved EXAFS studies have been conducted (for a review of time-resolved XAS, see Tourillon *et al.*, 1989), several static studies have monitored temperature-induced structural changes in solids (Taylor and McMillan, 1982; Dumas and Petiau, 1984; Waychunas *et al.*, 1988).

Because synchrotron-based XAS can be used to determine the structural environment of minor components of the solid phase (Ponader and Brown, 1989a, 1989b), EXAFS may be used to elucidate the environment of co-precipitated metals. A recent investigation of Al and Fe coassociation during hydrolysis of relatively dilute solutions suggested that the solid phase apparently contained Fe(III) within the structure and what appeared to be an occluded and surface sorbed Fe(II) fraction. The low yield of solid phase in these experiments precluded conventional

mineralogical characterization (Bertsch *et al.*, 1989b). Synchrotron-based XAS, however, can be used to obtain information about the coordination environment of Fe in the coprecipitate; XAS has been used to determine the coordination environment of Fe in a <30-μg sample of perovskite (Jackson *et al.*, 1987).

Synchrotron-based x-ray absorption spectroscopy is an ideal technique for elucidating the coordination environment of actinides in solid phases because a very small sample is required and the sample can be encapsulated (Bertram *et al.*, 1989). Most actinide EXAFS experiments have been designed to determine the local structure around Np, U, Th, or Pu in silicate glasses such as nuclear-waste storage glasses (Knapp *et al.*, 1984; Petit-Maire *et al.*, 1986; 1989), but the technique can also reveal the atomic and molecular basis for differences in the environmental mobility of different actinides and their isotopes. The pulsed time structure and the high flux of the APS will offer new opportunities to study dynamic changes in actinide solid phases. Ostwald ripening of fresh hydrous oxides of Pu[IV] solids is dependent on the Pu isotope; the $^{238}PuO_2$ solid is more mobile in biological systems than is $^{239}PuO_2$. Crystalline $^{238}PuO_2$(c), unlike $^{239}PuO_2$(c), reverts to an amorphous form in aqueous suspension (Park *et al.*, 1974). Such decrystallization causes an increase in the solubility of PuO_2. The mechanism and cause of the decrystallization are not known, although it may be a radiolytic effect (Rai and Ryan, 1982). The brightness of the APS at high energy may make it possible to use the actinide K absorption edge, but the EXAFS oscillations may be too smeared out due to the short core-hole lifetime. Fast detectors or energy-dispersive design may ameliorate this limitation, however.

4.3.2 Coordination Environment of Surface Species

Surface EXAFS (SEXAFS) and XANES (often referred to as near-edge x-ray absorption fine structure or NEXAFS) are spectroscopic tools for determining the local structure of sorbate-substrate systems or of the surface layers of bulk solids. The main difference between SEXAFS and bulk EXAFS is that the former utilizes a surface-sensitive detection method such as total electron yield (TEY), glancing angle XAS, or fluorescence. X-ray absorption spectroscopy using TEY detection is a surface-sensitive technique that has been used to study Al oxide coatings on Al metal (El-Mashri *et al.*, 1983). Glancing-angle XAS has been applied to surface phases such as Ni oxidation products on Ni metal (Bosio *et al.*, 1984). Fluorescence detection is ideal for studying sorbate-substrate interactions in aqueous suspensions. The fluorescence yield decreases with decreasing atomic number because other processes compete with fluorescence, but fluorescence detection has been shown to be ten times more sensitive than electron yield for studying sulfur surface species (Stöhr, 1985).

Surface EXAFS may provide valuable information about the mechanisms of mineral weathering. Dissolution rates decrease with time, but the cause of this rate decrease is unknown. Does a thin, hydrated silica layer form on mineral surfaces during weathering, thereby inhibiting further dissolution? Or is the decrease in weathering rates caused by preferential release of cations from high-energy sites, as suggested by Blum and Lasaga (1987)? Recent x-ray photoelectron spectroscopy (XPS) data for labradorite seem to indicate that a surface layer is produced during dissolution (Muir *et al.*, 1989), but Inskeep *et al.* (1990) have argued that the existence of a two-phase, exsolved, lamellar structure casts doubt over the interpretation of the XPS data. This uncertainty could be resolved by using EXAFS to determine whether Al and Si exist in an amorphous, hydrated surface layer. In addition, EXAFS experiments may provide information about incongruent weathering of alkali and alkaline earth metals from feldspars. Previous EXAFS studies have determined the coordination environment of Na in bulk silicate glasses (Greaves *et al.*, 1981; McKeown *et al.*, 1985a). The relationship between different cation coordination environments and weathering etch pits might be ascertained by using a microstage to move a sample under a focused x-ray beam. Spatially resolved XAS data would make it possible to correlate changes in the coordination environment of structural ions at mineral surfaces with changes in surface morphology visible with electron microscopy.

The research described above must be conducted in an ultra-high vacuum environment, but the mechanisms of reactions at the water-solid interface can be investigated with fluorescence-yield XAS. Many soil processes are controlled by reactions that occur at the solid/solution interface. The mechanisms of surface reactions are poorly understood, particularly under conditions similar to those found in nature. Surface reactions have been studied with a combination of macroscopic and molecular techniques, each of which has limited applicability to natural soil systems. Soil chemists often study reaction mechanisms or products in soil suspensions. Although this is convenient, unrealistic solid:solution ratios may produce reaction rates and mechanisms that differ from those which would be observed in a natural environment. At the opposite extreme, many spectroscopic methods require that samples be air-dried or maintained under vacuum, conditions that are very different from the aqueous environment in which most soil chemical reactions occur.

Predictive chemical models of ion exchange processes in soils would improve our ability to quantify the mobility and bioavailability of ions, and to predict the response of a natural system to environmental perturbations. Several models have been used to explain cation exchange selectivity differences among metal cations on ion exchange resins, metal oxides, and phyllosilicates. Recently, Xu and Harsh (1990) suggested that a model based on the Principle of Hard and Soft Acids and Bases encompasses the range of electrostatic and covalent bonding that occurs in these

systems, and may be used to quantitatively predict selectivity differences. To develop a comprehensive model of ion exchange on soil surfaces, however, unambiguous information regarding coordination number, bond distances, and covalency of ion-surface bonds is needed. Clearly, XAS offers the potential to obtain the required information.

X-ray absorption spectroscopy offers the opportunity to study surface speciation and to obtain *in situ* structural and mechanistic information under conditions that closely approximate those found in nature. Numerous studies have shown that EXAFS can be used to determine the coordination environment of metals and oxyanions on hydrous oxide surfaces in aqueous suspensions. A recent fluorescence-yield EXAFS study of selenate and selenite adsorption at the goethite/water interface (Hayes *et al.*, 1987) indicated that selenite forms inner-sphere complexes with the surface, whereas selenate does not. An EXAFS study of the adsorption of UO_2^{2+} on an Fe gel (Combes, 1988), and preliminary studies with NpO_2^+ at the goethite/water interface (Eller, personal communication, 1990) have provided information about the molecular structure of adsorbed actinides. In addition, XAS has been used to study Co(II) and Pb(II) adsorption on oxides. Both XANES and EXAFS analyses of the L_{III} edge of Pb yielded information about the coordination environment of Pb adsorbed on γ-Al_2O_3 (Chisholm-Brause *et al.*, 1989b). The EXAFS spectra for Co(II) adsorption on γ-Al_2O_3 (Figure 4.1) and on TiO_2 (Figure 4.2) suggested that Co was adsorbed as a multinuclear metal complex on both Al and Ti oxides, but that more polymerization occurred on γ-Al_2O_3 than on TiO_2 (Chisholm-Brause *et al.*, 1989a). In addition to equilibrium studies such as those summarized here, time-resolved XAS studies will be very useful for determining the mechanisms of adsorption reactions.

X-ray absorption spectroscopy also can distinguish between surface adsorption and precipitation, thereby complementing techniques such XPS. Zachara *et al.* (1988; 1989) used XPS and macroscopic methods to distinguish between adsorption and precipitation of Zn^{2+} on calcite, but the XPS data did not unambiguously verify the existence of a poorly ordered hydrozincite [$Zn_5(OH)_6(CO_3)_2(s)$] surface precipitate. In contrast, EXAFS can distinguish between adsorption and surface precipitation, at least on oxides (Chisholm-Brause *et al.*, 1989a). In addition, XANES may yield information about the covalency of metal-surface bonds, provided that it is possible to assign features of the XANES spectrum to specific orbital transitions (Brown and Parks, 1989). The use of XAS experiments to discriminate between surface adsorption and precipitation in fully hydrated systems represents a great advantage over XPS, which requires an ultra-high vacuum environment.

It may also be possible to use XAS to investigate the surface-charge distribution in minerals such as allophane and imogolite. At pH values common to acidic soils,

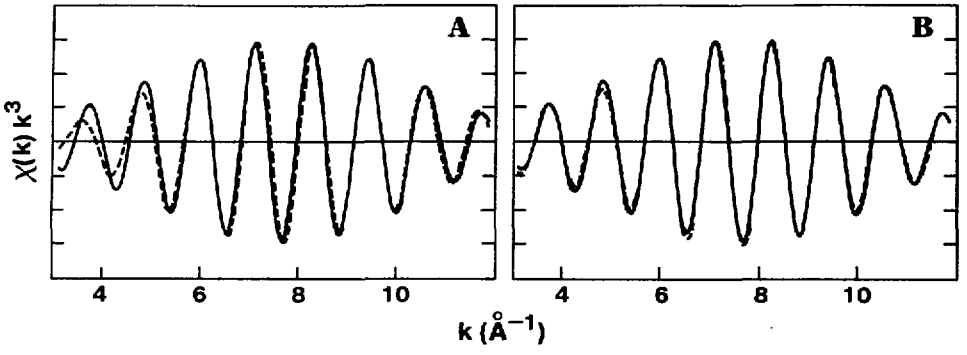

Figure 4.1. Fourier-filtered EXAFS of the second radial distribution peak of Co(II) on γ-Al_2O_3 (solid line) compared with fit (dashed) assuming (a) Co 2nd neighbors or (b) Co + Al second-nearest neighbors. Redrawn from Chisholm-Brause *et al.*, 1989a.

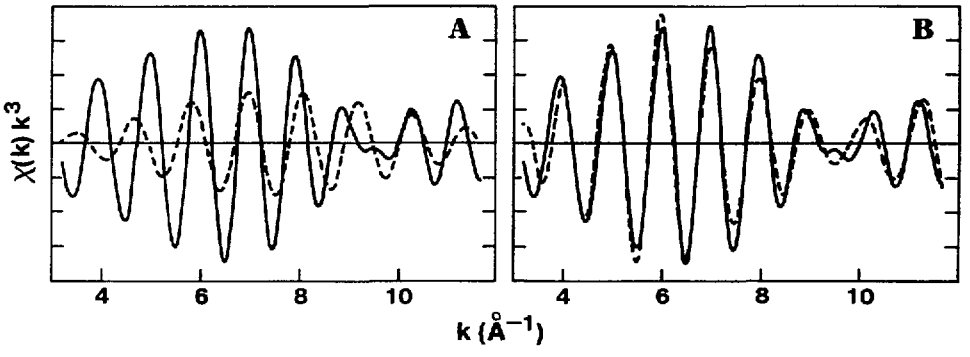

Figure 4.2. Fourier-filtered EXAFS of the second radial distribution function peak of Co(II) on TiO_2 (solid line) compared with calculated fit (dashed line) assuming (a) Co second-nearest neighbors or (b) Co and Ti second-nearest neighbors. The much better fit obtained for Co and Ti second neighbors suggests that most Co is not in multinuclear clusters on TiO_2. Redrawn from Chisholm-Brause *et al.*, 1989a.

these tubular or spheroidal aluminosilicates apparently have positive charge concentrated on the outer surface, and negative charge within the tubes or spherules. Fluorescence quenching experiments have shown that Ce(III) resides in the interior of the imogolite tubes (Harsh *et al.*, 1989). X-ray absorption spectroscopy could probe the coordination environment of adsorbed cations and anions in order to verify the separation of positive and negative charges that apparently permits chemisorption of Na on the inner silica sheet and provides a high anion adsorption capacity at pH values above the point of zero net charge.

4.3.3 Coordination Environment of Soluble Species

The chemistry of many transition metal ions in soils is influenced by their interactions with humic and fulvic acids. Metal ions are immobilized in soil organic matter by formation of complexes with the carboxylate, phenolate, amino, and amide functional groups in humic and fulvic acids. Because of the polymorphous nature of humic and fulvic acids, metal ion complexes have proved to be very difficult to study, although electron spin resonance (ESR) has provided useful information about the nature of Cu^{2+} and Mn^{2+} complexes (Bloom, 1981). The ESR data suggest that Mn^{2+} is bound in an outer-sphere complex, while Cu^{2+} forms a strong inner-sphere bond with carboxylate groups. Most of the studies with these ions have been conducted at much higher concentrations of metal ions than are found in nature. At natural metal loadings, complexation may be dominated by a small number of strongly binding sites that are difficult to observe with ESR. Mössbauer studies of Fe humates have suggested the importance of finely divided FeOOH-like centers in humate-Fe complexes (Bloom and Leenheer, 1989).

X-ray absorption spectroscopy has been used successfully to elucidate the local environment of transition metals in biological compounds (Penner-Hahn *et al.*, 1986). The ability to work with hydrated systems suggest that XAS may provide valuable data on metal-humate complexes. Aqueous inorganic complexes of nearly all first-row transition metals have been studied at high concentrations with XAS (see review by Brown *et al.*, 1988), and the availability of high-flux synchrotron radiation sources such as the APS will make it possible to study aqueous complexes in dilute solutions at or near the concentrations found in soil water. Garcia *et al.* (1986) studied the coordination geometry of Fe^{3+}, Mn^{2+}, Ni^{2+}, and Co^{2+} in dilute chloride solutions. In spite of the low energy of the Cl absorption edge (2.8 keV), the high flux of sources such as the APS permits Cl EXAFS and XANES experiments at concentrations at least as low as 0.001 mol L^{-1} (Brown *et al.*, 1988), and even lower concentrations of heavier elements can be studied.

4.3.4 Cation Oxidation State

Both EXAFS and XANES experiments yield information about the oxidation state of elements in solids or solutions. The positions of certain pre-edge and near-edge features in x-ray absorption-edge spectra are sensitive to the oxidation state of the element. For example, Fe(III) may be distinguished from Fe(II) by a 3-eV shift in a particular pre-edge spectral feature (Waychunas *et al.*, 1983). The XANES spectra are most easily interpreted when the cation of interest is present in tetrahedral coordination and in only one coordination environment. This limits the usefulness of XANES for many systems of interest to soil scientists; Cr-bearing clays do not give a pronounced pre-edge feature because the Cr^{3+} is present in octahedral, rather than tetrahedral, coordination (Calas *et al.*, 1984). Nevertheless, Wong *et al.* (1984) were able to distinguish among several different oxidation states of V in vanadium oxides, including compounds in which V had coordination numbers ranging from 3 to 8. At present, XANES does not permit quantification of each oxidation state, but it is possible to demonstrate whether more than one oxidation state is present (Brown and Parks, 1989). The information about oxidation states contained in EXAFS data is of a different nature than that provided by XANES, and the EXAFS information may be more useful to clay mineralogists. Bond distances, calculated from EXAFS data, reflect the size, and hence the oxidation state, of an element. If the average bond distance is intermediate between those expected for Fe(III) and Fe(II) compounds, then both oxidation states must be present. Petiau *et al.* (1981) showed that if the signal-to-noise ratio of the spectra is sufficiently high, the proportions of Fe(II) and Fe(III) can be obtained by fitting the spectra to coordination shells for both oxidation states.

When Fe(III) in smectites is reduced to Fe(II), cations such as K^+, Na^+, Ca^{2+}, Cu^{2+}, and Zn^{2+} are fixed in the interlayers of undried smectite gels (Khaled and Stucki, 1990; Lear and Stucki, 1989; Chen *et al.*, 1987). The oxidation state of structural iron affects the strength with which interlayer cations are held, yet little is known of the mechanism for increased cation fixation. Because iron resides primarily in the octahedral sheets of smectites, EXAFS rather than XANES might be the best method for determining the qualitative relationship between the change in average oxidation state and changes in Fe bonding.

It should also be possible to investigate the effect of Fe oxidation state upon the coprecipitation of Al and Fe hydrolysis products. At low concentrations, coprecipitation of these metals occurred only when iron was present in the ferrous form. Indirect chemical analyses indicated that coprecipitation proceeded via a surface-induced hydrolysis reaction that facilitated oxidation (Bertsch *et al.*, 1989b). The solid phase initially formed contained Fe(III) within the structure, and also what appeared to be an occluded and surface sorbed Fe(II) fraction. Time-resolved XAS

at the Fe absorption edge would permit simultaneous observation of changes in the average oxidation state, coordination number, and bond distances of coprecipitated Fe.

Many environmentally important organic compounds undergo mineral-surface-enhanced reactions such as hydrolysis, elimination, substitution, oxidation/reduction, and polymerization (Voudrias and Rienhard, 1986). The apparent mechanism for many surface-enhanced transformations involves catalysis by transition metals acting as Lewis acids. Because such reactions are very fast, it is difficult to use vibrational or magnetic resonance spectroscopies to monitor changes in metal oxidation state during the reaction. Information concerning the structural environment, chemical bonding, and oxidation state of Lewis acid/base metal cations may be obtained using EXAFS and XANES. Time-resolved XAS experiments may be used to determine whether Lewis acid catalysts reside on exchange sites or in the mineral structure, and to compare the catalytic efficiency of transition metals located in the octahedral and tetrahedral sheets. Measurements of this kind, coupled with determination of changes in clay interlayer *d*-spacings with reaction time, would be very useful in understanding not only organic reactions at clay and oxide surfaces, but also changes in the fundamental properties of clays caused by oxidation or reduction of structural metal cations.

The environmental mobility of actinides is affected by their oxidation state, yet it is extremely difficult to determine actinide oxidation states at low total Pu concentrations with current wet chemistry methods (Swanson and Rai, 1981; Schramke *et al.*, 1989). The actinides Th, U, Np, and Pu may exist simultaneously in oxidation states ranging from III to VII in solution and in solid phases (Rai *et al.*, 1980; Petit-Maire *et al.*, 1989). Actinide oxidation states are controlled not only by the usual oxidants and reductants (i.e., O_2, Fe, Mn), but also by alpha-particle-induced radiolytic oxidation. The ability to encapsulate very small actinide samples during an XAS experiment allows synchrotron-based XAS investigations of actinide oxidation states. It has been suggested that the L-edge XAS spectra of actinides lack sufficient energy resolution for analysis of pre-edge or near-edge features (Calas *et al.*, 1987), but Bertram and others (1989) recently reported that L_{III}-XANES measurements yield information about occupancies, localization, and covalent mixing of 5f orbitals in actinide compounds. The XANES spectra of Np(V), Np(VI), and Np(VII), but not Np(III) or Np(IV) compounds, exhibited an oxidation-state-dependent energy shift in certain spectral features; the technique should be applicable to all actinides, not just Np (Bertram *et al.*, 1989).

4.4 Applications of Anomalous Scattering Methods

4.4.1 Differential Anomalous Scattering

A major limitation of EXAFS is that multiple scattering becomes important at low values of the scattering vector magnitude, **k**, and quantitative analysis of multiple-scattering effects is not possible at present. Consequently, low-**k** data is not accessible with EXAFS, and EXAFS cannot provide accurate information about coordination shells beyond the nearest-neighbor shell. In addition, EXAFS is best suited for sharp, well-defined peaks and cannot give accurate information about static disordered or anharmonic samples (Kortright *et al.*, 1983).

Anomalous scattering techniques provide information about greater-than-nearest-neighbor interactions. Differential anomalous scattering (DAS) and anomalous small-angle x-ray scattering (ASAXS) are element-specific methods based upon sharp changes in the atomic scattering intensity near an element's x-ray absorption edge (Fuoss *et al.*, 1981; Kortright *et al.*, 1983; Ding *et al.*, 1988). The atomic scattering intensity is related to the atomic scattering factor, f(k,E), which is given by:

$$f(k,E) = f_0(k) + f'(k,E) + f''(k,E) \qquad (4.1)$$

where $k = 4\pi\sin\theta/\lambda$, E is the x-ray energy, f_0 is the energy-independent component of the atomic scattering factor, and both f′ and f″ are strongly energy-dependent near the absorption edge. The magnitude of f′ decreases sharply just below the edge due to resonance of bound electrons. The value of f″ is directly proportional to the x-ray absorption coefficient and increases rapidly at the absorption edge (Ding *et al.*, 1988).

In DAS experiments, scattering is measured at one wavelength far below the absorption edge and one wavelength at the absorption edge. The difference between the two scattering intensities represents scattering by the element of interest. Coordination numbers and interatomic distances are obtained from differential distribution functions (DDFs), which are related to the Fourier transform of the derivative of the scattering intensity with respect to energy (Fuoss *et al.*, 1981). Differential anomalous scattering yields more information about medium-range (5 to 10 Å) structure and about anharmonic and static disordered systems than does EXAFS. Unlike EXAFS, with which nearly all elements of the periodic table may be studied, DAS is limited to elements with atomic numbers greater than 25. The longer-wavelength x-rays required for lighter elements do not permit measurements over a sufficiently broad range of k-space to provide good resolution of interatomic distances (Kortright *et al.*, 1983). The DDFs produced in a DAS analysis do not

show sharp details as well as do the radial distribution functions of an EXAFS analysis. As shown by Kortright *et al.*, (1983), EXAFS and DAS give different results for first neighbor peaks for Mo-Ge alloys, possibly because EXAFS data may only be sensitive to the low-r edge of the first-neighbor shell (Kortright *et al.* 1983). One advantage of DAS is that neither the backscattering phase shifts nor the electron mean-free path are required to determine interatomic distances. The differential distribution functions, however, give no information about the chemical identity of the species in each coordination shell. Clearly, EXAFS and DAS provide complementary information. When possible, particularly with amorphous or disordered samples, both techniques should be used to obtain structural information (Kortright *et al.*, 1983; Kortright and Bienenstock, 1984).

Higher concentrations of an element may be required for DAS than for EXAFS, although high-flux synchrotron radiation should increase the sensitivity of DAS, particularly with strong scatterers or heavy elements in a light matrix. Anomalous scattering from tungsten has been measured in moderately dilute (0.077 mol L^{-1}; 0.13 atom % and 3.9 weight% W) aqueous solutions (Lorentz *et al.*, 1986). The DAS data indicated that tungsten trinuclear clusters were connected by μ-$H_3O_2^-$ bridges. The polymeric forms existed only at high pH, whereas only monomers were found at low pH (Lorentz *et al.*, 1986). At present, there are a number of unanswered questions concerning the configuration of actinide polynuclear species in aqueous solutions at low concentrations. Low concentrations of total U, and hence particular complexes, limit the usefulness of conventional spectroscopic techniques. The high flux of the APS, however, may allow DAS experiments at concentrations as low as 0.001 mol L^{-1} (Lorentz *et al.*, 1986).

4.4.2 Anomalous Small-Angle X-ray Scattering

Anomalous small-angle x-ray scattering (ASAXS) combines anomalous scattering with small-angle scattering techniques. Anomalous small-angle scattering differs from DAS in several ways. First, ASAXS can be used on lighter elements than can DAS (Fuoss *et al.*, 1981). Second, scattering is measured at many, not just two, wavelengths. In addition, ASAXS measurements are made over a very narrow wavelength range just below the absorption edge, so only variation in f' (Equation 4.1) is important. Just below the absorption edge, resonance effects for bound electrons become important. Consequently, f' exhibits a sharp negative peak just below the edge. Anomalous small angle x-ray scattering is a relatively new technique that can be used to eliminate ambiguities in fixed-wavelength SAXS data, to provide information about protein or macromolecule folding (Phillips, 1989), or to determine which components of a system produce particular features in a SAXS pattern. For example, ASAXS has been used to separate the scattering contribution of Ni^{2+}

counterions from the scattering caused by a sulfonated polystyrene ionomer (Ding *et al.*, 1988).

Other ASAXS experiments have demonstrated that the technique can yield information about the location and structural role of metal ions in polymers. Stuhrmann and Notbohm (1981) used ASAXS to determine the coordination geometry of iron atoms in aqueous hemoglobin solutions. It was reported that anomalous scattering could not be detected if the Fe concentration was below 20 mmol L^{-1} (Stuhrmann and Notbohm, 1981), but the high flux of the APS should make it possible to achieve sufficient accuracy with more dilute samples. Furthermore, the APS may allow determination of inter-heavy atom distances in macromolecules (Phillips, 1989). A potential application of ASAXS will be to elucidate medium- and long-range structure around transition metals that are complexed by organic matter.

4.5 Applications of X-ray Emission Spectroscopy to the Study of Structure and Bonding in Minerals and at Mineral Surfaces

4.5.1 Overview

Chemical bonding, resulting from orbital interactions, is an important component in the bonding of oxide minerals, particularly those containing B, Al, Si, P, S, and transition metals. Orbital interactions perturb the electronic states of the atoms composing these minerals, a property directly expressed in the energy distribution of electronic states (the density of states or DOS). Electron spectroscopy directly measures the energy distribution of electronic states (the total DOS), the physical property directly related to bonding in minerals. In contrast, XES measures the different types of electron states contributing to the DOS.

This is best illustrated by the spectra for SiO_2 in Figure 4.3 (adapted from diStefano and Eastman, 1971). The ultraviolet photoelectron spectroscopy (UPS) and XPS spectra reveal two groups of peaks, the O(2p) peak from 0 to -12 eV, and the O(2s) peak from -18 to -23 eV below the uppermost occupied electronic states, *i.e.*, the valence band edge. These peaks lie at lower energy than they would if the bonds in quartz were purely ionic, a result that provides evidence for orbital interactions involving the O(2s) and O(2p) orbitals in quartz. The Si Kβ XES spectrum (Figure 4.3) tells us that non-bonding O(2p) states are found at the top of the valence band, since the Kβ intensity drops off sharply at the band edge. It also tells us that O(2p)-Si(3p) bonding states lie just below non-bonding O(2p) states, since this is where the

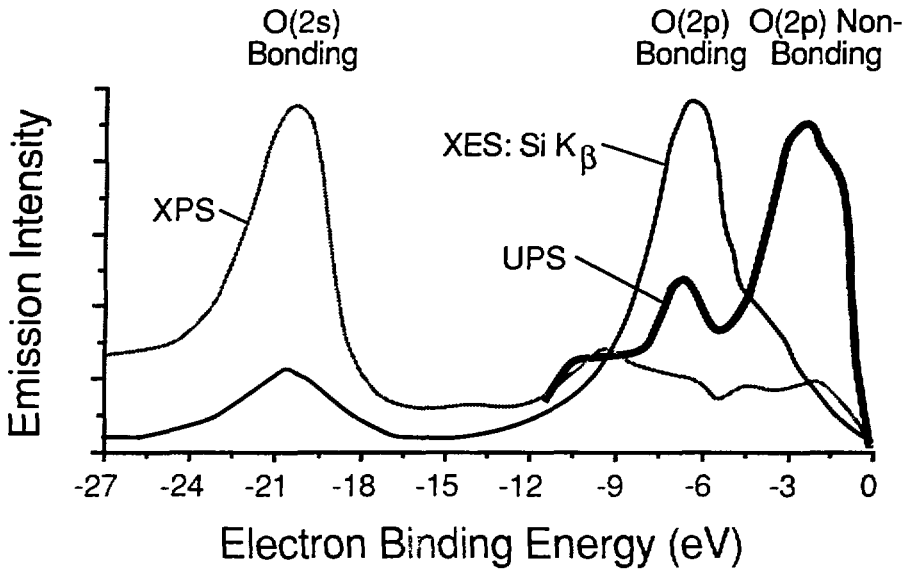

Figure 4.3. X-ray emission, x-ray photoelectron, and ultraviolet photoelectron spectra for amorphous SiO_2. Redrawn from diStefano and Eastman, 1971.

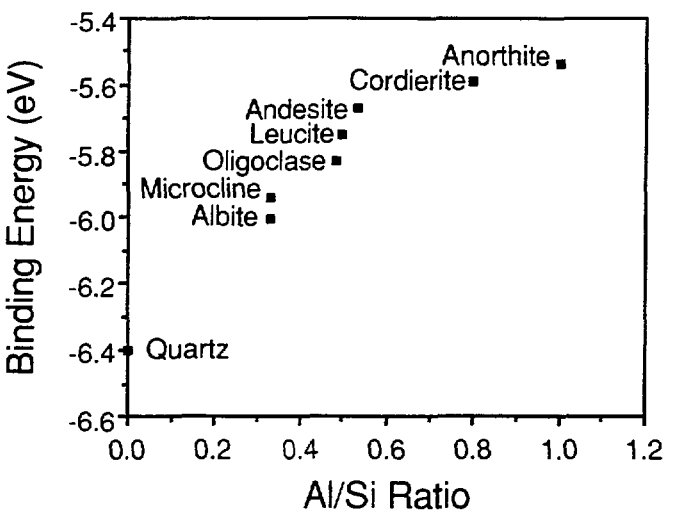

Figure 4.4. Dependence of the SiKβ binding energy as a function of the Al/Si ratio for minerals in which both Si and Al are in tetrahedral sites. Redrawn from White and Gibbs, 1967.

maximum intensity is found, and that O(2s)-Si(3p) bonding occurs in quartz; both the XES and XPS spectra show a peak at -20 eV.

Figure 4.4 (adapted from White and Gibbs, 1967) provides evidence that orbital interactions extend to next-nearest neighbors in minerals, since the major Si $K\beta$ XES peak in aluminosilicates is directly related to the Al/Si ratio. Aluminum valence orbitals lie at higher energy, *viz.* a lower binding energy, than do Si orbitals. This is consistent with the premise that next-nearest-neighbor orbital interactions would predict a decrease in the binding energy of Si $K\beta$ electrons as the Al/Si ratio increases.

4.5.2 Solid-State Physics of Oxide Minerals

Figure 4.5 illustrates the results of theoretical calculations of orbital interactions in phyllosilicates (Bleam and Hoffmann, 1988a; 1988b). These calculations predict the DOS as it would be measured in electron spectroscopic studies. Notice, for instance, how the Si states match with the O(2s) states, indicating the mixing of these electronic states to form crystal orbitals in phyllosilicates. Figure 4.6 illustrates the energy distribution of bonding interactions (Crystal Orbital Overlap Populations, or COOP) in phyllosilicates for various types of bonds. Figure 4.6a is for an isolated tetrahedral sheet, whereas Figures 4.6b and 4.6c are for tetrahedral sheets in actual minerals. Al-O bonding is quite similar to Si-O bonding. Notice that the large peak at -14.8 eV in the DOS of oxygen states (Figure 4.5) is missing in the COOP curves. This is because the -14.8 eV peak is due to non-binding states.

The valence electronic states of oxide minerals retain the general features of atomic oxygen, *viz.* O(2s) and O(2p) states. These states are perturbed by orbital interactions with atoms, mainly Group IIB through VIB elements, with the result that O(2s) states and a third of the O(2p) states are stabilized and shift to lower energies. Non-bonding, O(2s) states, fully half of all valence states in oxides, are found at the top of the valence band. Reactivity is associated with those O(2p) and O(2s) states that are least stabilized through orbital interactions. These are found at the *top* of the "O(2s)" group of bands and within and just below the *top* of the "O(2p)" group of bands lying at the valence band edge.

These ideas also can be illustrated through band-structure diagrams, which represent the energies of the electronic states in a solid for certain special values of the wave vector κ. Band-structure diagrams for SiO_2 and $AlPO_4$ appear in Figure 4.7. The energies of O(2s) states, perturbed by orbital interactions with cations, are presented in Figure 4.7a-b, while the O(2p) bands, also perturbed by interactions with cation orbitals, are found in Figure 4.7c-d. Clearly, the energies of the electronic states,

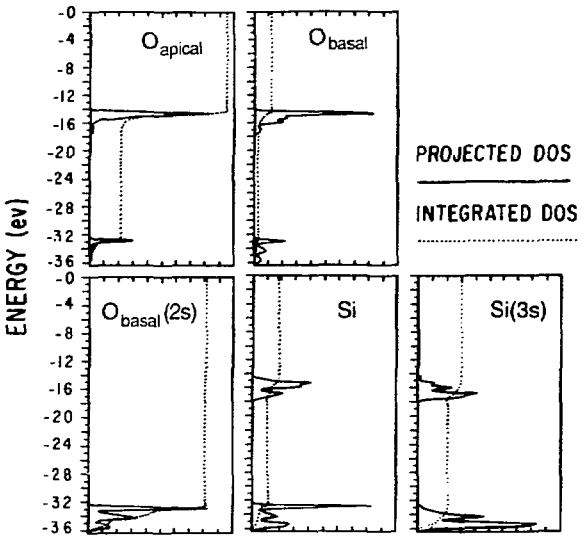

Figure 4.5. Density of states for Si and O atoms in different sites of a *p6mm* tetrahedral sheet. Redrawn from Bleam and Hoffmann, 1988a.

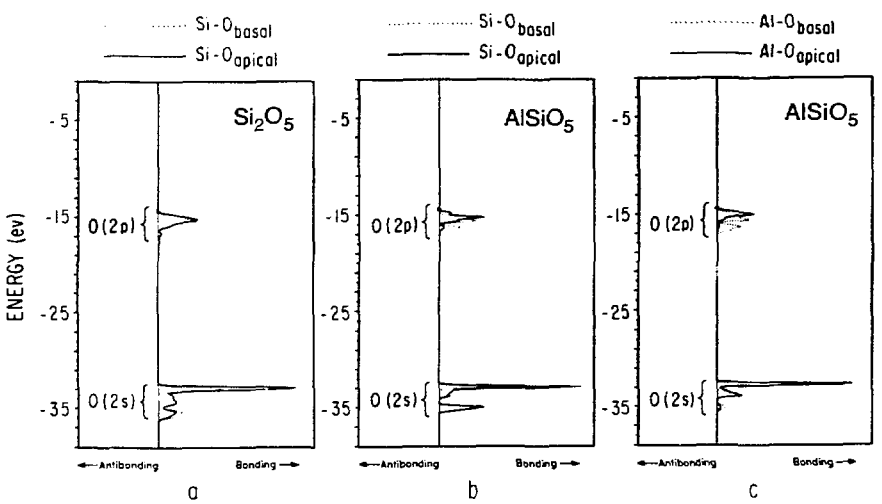

Figure 4.6. Calculated crystal orbital overlap population curves for *p6mm* tetrahedral sheets with varying Al substitution.

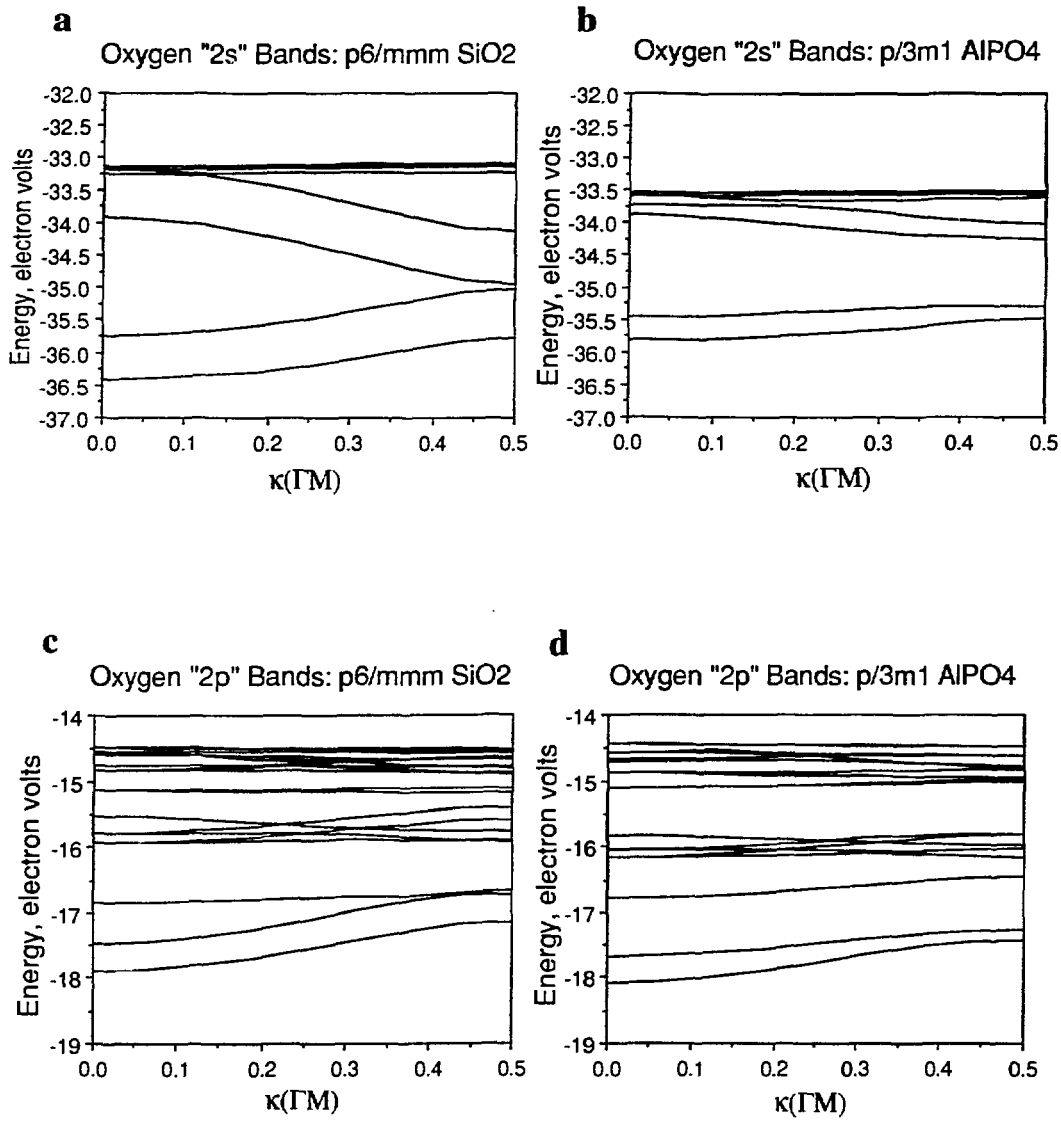

Figure 4.7. Band structure diagrams for O(s) and O(2p) orbitals. (a) O(2s) of SiO_2; (b) O(2s) of $AlPO_4$, (c) O(2p) of SiO_2, (d) O(2p) of $AlPO_4$.

represented by these band-structure diagrams, vary as a result of the composition of the material. In this case, the variations can be traced to the energies of the cation valence orbital (a property reflected in the electronegativity of an element). The overall appearance of the band-structure diagram of $AlPO_4$ resembles that of SiO_2, indicating that the oxygen orbitals are perturbed by some average of the orbital energies for the cations bound to them. This equivalent to saying that there is extensive orbital interactions between next-nearest neighbor cations. Cation-cation, next-nearest neighbor interactions are the basis for the compositional dependence of the XES spectra of the sort shown in Figure 4.4.

4.5.3 Applications of Synchrotron X-ray Sources

The applications presented in this section focus upon systems wherein the species of interest are present at very low concentration. The surface excess of an adsorbate may be in the range of 10^{-8} to 10^{-7} moles per square meter. Given that the upper limit on the surface area of oxide minerals is in the range of 200 to 300 $m^2\ g^{-1}$, one can imagine the challenge a surface chemist faces in obtaining high-resolution spectra. The significance of synchrotron radiation, therefore, derives from the high intensity of the radiation; the APS will offer much higher fluxes and better energy resolution than existing synchrotron storage rings.

Electron spin resonance spectroscopy studies of transition metal ions adsorbed onto oxide surfaces suggest that Cu^{2+} adsorbed on TiO_2 (Figure 4.7a) and Mn^{2+} adsorbed on γ-AlOOH form ion clusters on the surfaces (Bleam and McBride, 1985; 1986). X-ray emission spectra, in particular the $L_{2,3}$ transitions of these ions, should be sensitive to the electronegativity of next-nearest neighbor metal ions. If the structure that gives a ferromagnetic resonance in ESR experiments is truly a cluster, the XES transition should be shifted less by interactions with metal atoms of the adsorbent than if it were dispersed sufficiently to have only adsorbent metal atoms as next-nearest neighbors.

Most detailed surface chemistry studies of adsorption on oxides use pristine adsorbents. By contrast, mineral surfaces in soils and other natural systems have a variety of ions adsorbed on their surfaces that are not major components of the bulk phase. It is important to elucidate the manner in which these impurity atoms alter the oxide source chemistry. As an example, the experimental picture of phosphate adsorption on pristine aluminum oxides is fairly complete and consistent. Suppose the aluminum oxide is "dressed" with some other cation and we observe a change in the adsorption capacity of the oxide. Can this be attributed to the direct influence of the impurity ion? Both XES and EXAFS experiments should reveal whether the adsorbate nucleus (PO_4-P in this example) is interacting directly with the impurity

cations. If so, the impurity cation will be a next-nearest neighbor of the adsorbate ion. This would be revealed in both EXAFS data and in shifts in the XES transition energy (P Kβ in this example).

4.6 Beam Line Requirements and Instrumentation

The x-ray spectroscopy and anomalous scattering experiments of interest to soil scientists are similar in many respects to experiments conducted by geologists, except that soil and environmental scientists are interested primarily in low-temperature processes occurring at or near the earth's surface. Consequently, both the beam line and instrumentation requirements of soil scientists closely parallel those of earth scientists (Brown and Waychunas, 1988). A continuously tunable x-ray source with a high flux and a stable output will be required for all spectroscopy and scattering experiments. For anomalous scattering experiments, it is desirable that the source have a bandwidth ($\Delta E/E$) of approximately 10^{-4} at about 10 keV, with no harmonics (Hoyt, 1989). The Type "B" wiggler magnet insertion device will provide the appropriate beam characteristics for most experiments at low energies (1.5 to 20 keV). The type "A" wiggler will provide greater brightness at higher energies. The type "A" undulator, which has been designed to provide extremely high brilliance and is expected to irradiate a very small ($<1\ \mu m^2$) spot, might be very useful for spatially resolved EXAFS (microEXAFS) investigations, although limitations may be imposed by the fact that the output from undulators is not continuously tunable. Appropriate optics, such as a moveable grazing-incidence mirror or crystal monochromators, will also be required. Fluorescence detection will be needed for experiments in aqueous solutions or suspensions; electron yield or grazing incidence would be best for studying surface defects on minerals, and transmission detection will be the preferred method for many studies on bulk solids. Time-resolved studies, particularly ASAXS experiments, will require a fast, position-sensitive detector such as a photodiode array detector. To reduce thermal anharmonicity during EXAFS experiments, it will be useful to have access to a sample-cooling chamber.

4.7 References

Apted, M. J., G. A. Waychunas, and G. E. Brown, Jr. 1985. Structure and specification of iron complexes in aqueous solutions determined by x-ray absorption spectroscopy. Geochim. Cosmochim. Acta. 49:2081-2089.

Axelos, M., D. Tchoubar, J. Y. Bottero, and F. Fiessinger. 1985. Détermination par D.P.A.X. de la structure fractale d'agrégats obtenus par collage d'amas. Etude de deux solutions d'hydroxyde d'aluminium $Al(OH)_x$ avec x=2,5 et 3. J. Physique. 46:1587-1593.

Bertram, S., G. Kaindl, J. Jové, and M. Pagès. 1989. L-edge x-ray absorption studies of neptunium compounds. Physica B. 158:508-510.

Bertsch, P. M., M. A. Anderson, and W. J. Layton. 1989a. Aluminum-27 nuclear magnetic resonance studies of ferron-hydroxo-polynuclear Al interactions. Magn. Res. Chem. 27:283-287.

Bertsch, P. M., W. P. Miller, M. A. Anderson, and L. W. Zelazny. 1989b. Coprecipitation of iron and aluminum during titration of mixed Al^{3+}, Fe^{3+}, and Fe^{2+} solutions. Clays Clay Miner. 37:12-18.

Besson, G., A. S. Brookings, L. G. Daynyak, M. Rautaureau, S. I. Tsipursky, C. Tchoubar, and V. A. Drits. 1983. Use of diffraction and Mössbauer methods for the structural and crystallochemical characterization of nontronites. J. Appl. Cryst. 16:374-383.

Bleam, W. F., and R. Hoffmann. 1988a. Orbital interactions in phyllosilicates: Perturbations of an idealized two-dimensional, infinite silicate frame. Phys. Chem. Minerals. 15:398-408.

Bleam, W. F., and R. Hoffmann. 1988b. Isomorphous substitution in phyllosilicates as an electronegativity perturbation: Its effect on bonding and charge distribution. Inorg. Chem. 27:3180-3186.

Bleam, W. F., and M. B. McBride. 1985. Cluster formation versus isolated adsorption. A study of Mn(II) and Mg(II) on boehmite and goethite. J. Colloid Interface Sci. 103:124-132.

Bleam, W. F., and M. B. McBride. 1986. The chemistry of adsorbed Cu(II) and Mn(II) in aqueous titanium dioxide suspensions. J. Colloid Interface Sci. 110:335-346.

Bloom, P. R. 1981. Metal-organic matter interaction in soil. p. 129-159. *In* R.H. Dowdy (ed.) Chemistry in the soil environment. ASA Special Publication No. 10. ASA, CSSA, and SSSA, Madison, WI.

Bloom, P. R., and J. A. Leenheer. 1989. Vibrational, electronic, and high-energy spectroscopic methods for characterizing humic substances. p. 410-445. *In* M. H. B. Hayes, P. McCarthy, R. L. Malcolm, and R. S. Swift (ed.) Humic substances. Vol II. John Wiley and Sons, London.

Blum, A. E., and A. C. Lasaga. 1987. Monte Carlo simulations of surface reaction rate laws. p. 255-312. *In* W. Stumm (ed.) Aquatic surface chemistry: Chemical processes at the particle-water interface. Wiley Interscience, New York.

Bosio, L., R. Cortes, and M. Froment. 1984. ReflEXAFS studies of protective oxide formation on metal surfaces. p. 484-486. *In* K.O. Hodgson, B. Hedman, and J. E. Penner-Hahn (ed.) EXAFS and Near-Edge Structure III. Springer Proc. Phys. 2. Springer-Verlag, New York.

Bottero, J.Y., M. Axelos, D. Tchoubar, J.M. Cases, J.J. Fripiat, and F. Fiessinger. 1987. Mechanism of formation of aluminum trihydroxide from keggin Al_{13} polymers. J. Colloid Interface Sci. 117:47-57.

Bottero, J. Y., D. Tchoubar, J. M. Cases, and F. Fiessinger. 1982. Investigation of the hydrolysis of aqueous solutions of aluminum chloride. 2. Nature and structure by small-angle x-ray scattering. J. Phys. Chem. 86:3667-3673.

Brown, G. E. Jr., G. Calas, G. A. Waychunas, and J. Petiau. 1988. X-ray absorption spectroscopy and its applications in mineralogy and geochemistry. p. 432-512. *In* F.C. Hawthorne, (ed.) Reviews in Mineralogy Vol. 18. Mineral. Soc. Amer.,Washington, D.C.

Brown, G., and G. A. Parks. 1989. Synchrotron-based x-ray absorption studies of cation environments in earth materials. Rev. Geophys. 27:519-533.

Brown, G., and G. A. Waychunas. 1988. Synchrotron-based spectroscopic and anomalous scattering studies of earth materials. p. 69-92. *In* J. V. Smith and M. H. Manghnani (co-chairs), Synchrotron x-ray sources and new opportunities in the earth sciences: workshop report. Agronne National Laboratory ANL/APS-TM3, Argonne, Illinois.

Calas, G., G. E. Brown, Jr., G. A. Waychunas, and J. Petiau. 1987. X-ray absorption spectroscopic studies of silicate glasses and minerals. Phys. Chem. Minerals. 15:19-29.

Calas, G., A. Manceau, A. Novikoff, and H. Boukili. 1984. Comportement du chrome dans les mineaux d'alteration du gisement de Campo Formoso (Bahia, Bresel). Bull. Minéral. 107:755-766.

Chen, S. A., P. F. Low, and C. B. Roth. 1987. Relation between potassium fixation and the oxidation state of octahedral iron. Soil Sci. Soc. Amer. J. 51:82-36.

Chisholm-Brause, C. J., G. E. Brown, Jr., and G. A. Parks. 1989a. EXAFS investigation of aqueous Co(II) adsorbed on oxide surfaces *in situ*. Physica B. (Amsterdam) 158:646-648.

Chisholm-Brause, C. J., A. L. Roe, K. F. Hayes, G. E. Brown, Jr., G. A. Parks, and J. O. Leckie. 1989b. XANES and EXAFS study of aqueous Pb(II) absorbed on oxide surfaces. Physica B. (Amsterdam) 158:674-675.

Combes, J.-M. 1988. Evolution de la structure locales des polymeres et geis feriques lors de la cristallisation de oxydes der fer. Application au plegeage de l'uranium. Ph.D. Dissertaiton, University of Paris, Paris, France.

Combes, J.-M., A. Manceau, and G. Calas. 1986. Study of the local structure in poorly-ordered precursors of iron oxyhydroxides. J. Physique 47:697-701.

Combes, J.-M., A. Manceau, and G. Calas. 1990. Formation of ferric oxides from aqueous solutions: A polyhedral approach by x-ray absorption spectroscopy. II. Hematite formation from ferric gels. Geochim. Cosmochim. Acta. 54:1083-1091.

Combes, J.-M., A. Manceau, G. Calas, and J. Y. Bottero. 1989. Formation of ferric oxides from aqueous solutions: A polyhedral approach by x-ray absorption spectroscopy. I. Hydrolysis and formation of ferric gels. Geochim. Cosmochim. Acta. 53:583-594.

Cradwick, P. D. B., V. C. Farmer, J. D. Russell, C. R. Masson, K. Wada, and N. Yoshinaga. 1972. Imogolite, a hydrated aluminium silicate of tubular structure. Nature Phys. Sci. 240:187-189.

Ding, Y. S., S. R. Hubbard, K. O. Hodgson, R. A. Register, and S. L. Cooper. 1988. Anomalous small-angle x-ray scattering from a sulfonated polystyrene ionomer. Macromolecules 21:1698-1703.

diStefano, T. H., and D. E. Eastman. 1971. Photoemission measurements of the valence levels of amorphous SiO_2. Phys. Rev. Lett. 27:1560-1562.

Dumas, T., and J. Petiau. 1984. Structural organization around nucleating elements (Ti,Zr) and Zn during crystalline nucleation process in silica-aluminate glasses. p. 311-313. *In* K.O. Hodgson, B. Hedman, and J.E. Penner-Hahn, (ed.) EXAFS and Near-edge structure III. Springer-Verlag, New York.

Eller, P. G. 1990. Personal communication. "Neptunium sorbed on α-FeOOH: Preliminary Report of an XAS study". G.E. Brown *et al.* at SLAC, and P.G. Eller at LANL.

El-Mashri, S. M., R. G. Jones, and A. J. Forty. 1983. An electron-yield EXAFS study of anodic-oxide and hydrated-oxide films on pure aluminum. Philosophical Mag. A. 48:665-685.

Fitzgerald, J. J., L. E. Johnson, and J. S. Frye. 1989. Temperature effects on the ^{27}Al NMR spectra of polymeric aluminum hydrolysis species. J. Mag. Res. 84:121-133.

Fukushima, Y. 1988. Extended x-ray absorption fine structure study of cobalt-exchanged sepiolite: Reply. Clays Clay Miner. 36:384.

Fukushima, Y., and T. Okamoto. 1987. Extended x-ray absorption fine structure study of cobalt-exchanged sepiolite. p. 9-16. *In* L.G. Schultz, H. van Olphen, and F.A. Mumpton (ed.) Proceedings of the International Clay Conference, Denver, 1985. The Clay Minerals Society, Bloomington, Indiana.

Fuoss, P. H., P. Eisenberger, W. K. Warburton, and A. Bienenstock. 1981. Application of differential anomalous x-ray scattering to structural studies of amorphous materials. Phys. Rev. Lett. 46:1537-1540.

Garcia, J., A. Bianconi, M. Benfatto, and C. R. Natoli. 1986. Coordination geometry of transition metal ions in dilute solutions by XANES. J. Physique 47:49-54.

Goodman, B. A., J. D. Russell, B. Montez, E. Oldfield, and R. J. Kirkpatrick. 1985. Structural studies of imogolite and allophanes by aluminum-27 and silicon-29 nuclear magnetic resonance spectroscopy. Phys. Chem. Miner. 12:342-346.

Greaves, G. N., A. Fontaine, P. Lagarde, D. Raoux, and S. J. Gurman. 1981. Local structure of silicate glasses. Nature 293:611-616.

Harsh, J. B., S. J. Traina, C. Su, and J. Boyle. 1989. Surface properties of allophane and imogolite. Inter. Clay Conf. of AIPEA. Strasbourg, France (Abstract).

Hayes, K. F., A. L. Roe, G. E. Brown, Jr., K. O. Hodgson, J. O. Leckie, and G. A. Parks. 1987. *In situ* x-ray absorption study of surface complexes: Selenium oxyanions on α-FeOOH. Science 238:783-786.

Hoyt, J. J. 1989. Applications of anomalous small-angle x-ray scattering. p. 115-126. *In* M. Beno and S. Rice (Co-chairs) Chemical applications of synchrotron radiation: Workshop report. Argonne National Laboratory. ANL/APS-TM-4.

Hsu, P. H. 1989. Aluminum hydroxides and oxyhydroxides. p. 331-378. *In* J. B. Dixon and S. B. Weed (ed.) Minerals in soil environments. 2nd ed. Soil Science Soc. Am., Madison, WI.

Inskeep, W. P., E. A. Nater, D. S. Vandervoort, P. R. Bloom, and M. S. Erich. 1990. Characterization of laboratory weathered surfaces using x-ray photoelectron spectroscopy and transmission electron microscopy. Geochim. Cosmochim. Acta. (accepted for publication).

Jackson, W. E., E. Knittle, G. E. Brown, Jr., and R. Jeanloz. 1987. Partitioning of Fe within high pressure silicate perovskite: Evidence for unusual geochemistry in the lower mantle. Geophys. Res. Lett. 14:224-226.

Khaled, E. M., and J. W. Stucki. 1990. Effect of iron oxidation state on cation fixation in smectites. Soil Sci. Soc. Am. J. (accepted for publication).

Knapp, G. S., B. W. Veal, A. P. Paulikas, A. W. Mitchell, D. J. Lam, and T. E. Klippert. 1984. EXAFS studies of sodium silicate glasses containing dissolved actinides. p. 305-307. *In* K.O. Hodgson, B. Hedman, and J.E. Penner-Hahn, (ed.) EXAFS and Near-Edge Structure III. Springer Proc. Phys. 2. Springer-Verlag, New York.

Kortright, J., and A. Bienenstock. 1984. Structural study of metallic amorphous Mo-Ge alloys. J. Non-Crystalline Solids. 61&62:273-278.

Kortright, J., W. Warburton, and A. Bienenstock. 1983. Anomalous x-ray scattering and its relationship to EXAFS. p. 362-372. *In* A. Bianconi, L. Incoccia, and S. Stipcich. EXAFS and near-edge structure. Springer-Verlag, Berlin.

Lear, P. R., and J. W. Stucki. 1989. Effect of iron oxidation state on the surface area of smectites. Clays Clay Miner. 37:547-552.

Lear, P. R., and J. W. Stucki. 1990. Magnetic properties and site occupancy of iron in nontronite. Clay Miner. 25:3-13.

Lorentz, R. D., A. Bino, and J. E. Penner-Hahn. 1986. Differential anomalous scattering evidence for the existence of μ-H_3O_2-bridging ligands in solution. J. Amer. Chem. Soc. 108:8116-8117.

Manceau, A., and G. Calas. 1985. Heterogeneous distribution of nickel in hydrous silicates from New Caladonian ore deposits. Am. Miner. 70:549-558.

Manceau, A., and G. Calas. 1986. Nickel-bearing clay minerals. 2. Intracrystalline distribution of nickel: An x-ray absorption study. Clay Miner. 21:341-360.

Manceau, A., G. Calas, and J. Petiau. 1984. Cation ordering in Ni-Mg phyllosilicates of geological interest. p. 358-361. *In* K.O. Hodgson, B. Hedman, and J.E. Penner-Hahn (ed.) EXAFS and near-edge structure III. Springer-Verlag, New York.

Manceau, A., and A. Decarreau. 1988. Extended x-ray absorption fine structure study of cobalt-exchanged sepiolite: Comment on a paper by Y. Fukushima and T. Okamoto. Clays Clay Miner. 36:382-383.

McKenzie, R.M. 1989. Manganese oxides and hydroxides. p. 439-465. *In* J. B. Dixon and S. B. Weed (ed.) Minerals in soil environments. 2nd ed. Soil Science Soc. Am., Madison, Wisconsin.

McKeown, D. A., G. A. Waychunas, and G. E. Brown, Jr. 1985a. EXAFS and XANES study of the local coordination environment of sodium in a series of silica-rich glasses and selected minerals within the Na_2O-Al_2O_3-SiO_2 system. J. Non-Crystalline Solids. 74:325-348.

McKeown, D. A., G. A. Waychunas, and G. E. Brown, Jr. 1985b. EXAFS study of the coordination environment of aluminum in a series of silicon-rich glasses and selected minerals within the Na_2O-Al_2O_3-SiO_2 system. J. Non-Crystalline Solids. 74:349-371.

Mering, J., and J. Oberlin. 1967. Electron-optical study of smectites. Clays Clay Miner. 15:3-25.

Muir, I. J., G. M. Bancroft, and H. W. Nesbit. 1989. Characteristics of altered labradorite surfaces by SIMS and XPS. Geochim. Cosmochim. Acta. 53:1235-1241.

Park, J. F., D. L. Catt, D. K. Craig, R. L. Olson, and R. J. Smith. 1974. Solubility changes of ^{238}Pu oxide in water suspensions and effect on biological behavior after inhalation by beagle dogs. p. 719-724. *In* Proceedings of the Third Int. Radiation Protection Association Conference. CONF-730907-P1.

Penner-Hahn, J. E., K. Smith, J. H. Dawson, and K. O. Hodgson. 1986. Structural characterization of high valent intermediates in horseradish peroxidases. J. Physique C8:1137-1142.

Petiau, J., C. Lapeyre, P. Levitz, and G. Loupias. 1981. EXAFS and near-edge structure of some transition elements and germanium in silicate glasses. *In* EXAFS for inorganic systems. NERC. p. 127-129.

Petit-Maire, D., J. Petiau, G. Calas, and N. Jacquet-Francillon. 1986. Local structure around actinides in borosilicate glasses. J. Physique 47, C8:849-852.

Petit-Maire, D., J. Petiau, G. Calas, and N. Jacquet-Francillon. 1989. Insertion of neptunium in borosilicate glasses. Physica B. (Amsterdam) 158:56-57.

Phillips, J. C. 1989. Macromolecular structure changes in solution observed by time-resolved synchrotron x-ray scattering. p. 101-114. *In* M. Beno and S. Rice. (Co-chairs) Chemical applications of synchrotron radiation: Workshop report. Argonne National Laboratory. ANL/APS-TM-4.

Ponader, C. W., and G. E. Brown, Jr. 1989a. Rare earth elements in silicate glass/melt systems: I. Effects of composition on the coordination environments of La, Gd, and Yb. Geochim. Cosmochim. Acta. 53:2893-2903.

Ponader, C. W., and G. E. Brown, Jr. 1989b. Rare earth elements in silicate glass/melt systems: II. Interactions of La, Gd, and Yb with halogens. Geochim. Cosmochim. Acta. 53:2905-2914.

Rai, D., and J. L. Ryan. 1982. Crystallinity and solubility of Pu(IV) oxide and hydrous oxide in aged aqueous suspensions. Radiochimica Acta. 30:213-216.

Rai, D., R. J. Serne, and J. L. Swanson. 1980. Solution species of plutonium in the environment. J. Environ. Qual. 9:417-420.

Schramke, J. A., D. Rai., R. W. Fulton, and G. R. Choppin. 1989. Determination of aqueous plutonium oxidation states by solvent extraction. J. Radioanal. Nuc. Chem. 130:333-346.

Schwertmann, U., and R. M. Taylor. 1989. Iron Oxides. p. 379-438. *In* J. B. Dixon and S. B. Weed (ed.) Minerals in soil environments. 2nd ed. Soil Science Soc. Am., Madison, Wisconsin.

Stern, E. A. 1988. Theory of EXAFS. *In* D. C. Koningsberger and R. Prins (ed.) X-ray absorption. Principles, applications, techniques of EXAFS, SEXAFS, and XANES. Chem. Anal. 92:3-51.

Stöhr, J. 1985. Geometry and bond lengths of chemisorbed atoms and molecules: NEXAFS and SEXAFS. Z. Physik B 61:439-445.

Stuhrmann, H. B., and H. Notbohm. 1981. Configuration of the four iron atoms in dissolved human hemoglobin as studied by anomalous dispersion. Proc. Natl. Acad. Sci. USA. 78:6216-6220.

Swanson, J. L., and D. Rai. 1981. Spectrophotometric measurement of ionic plutonium species in solution at low concentrations. Radiochem. Radioanal. Letter. 50:89-98.

Taylor, J. M., and P. W. McMillan. 1982. EXAFS investigation into the role of ZrO_2 as a nucleating agent in $MgO\text{-}Al_2O_3\text{-}SiO_2$ glass. p. 589-596. *In* P.H. Gaskell, J.M. Parker, and E.A. Davis (ed.) Structure of non-crystalline materials II. Taylor and Francis, London.

Tourillon, G., E. Dartyge, A. Fontaine, and H. Tolentino. 1989. Time resolved x-ray absorption spectroscopy. Physica B 158:287-290.

Tsipursky, S. I., and V. A. Drits. 1984. The distribution of octahedral cations in the 2:1 layers of dioctahedral smectites studied by oblique-texture electron diffraction. Clay Miner. 19:177-193.

Voudrias, E. A., and M. Reinhard. 1986. Abiotic uranic reactions at mineral surfaces. p. 462-486. *In* J.A. Davis and K.F. Hayes (ed.) Geochemical processes at mineral surfaces. ACS Symposium Series 323. Am. Chem. Soc., Washington, D.C.

Waychunas, G. A., G. E. Brown, Jr., and M. J. Apted. 1983. X-ray K-edge absorption spectra of Fe minerals and model compounds: Near-edge structure. Phys. Chem. Minerals 10:1-9.

Waychunas, G. A., G. E. Brown, Jr., and M. J. Apted. 1986. X-ray K-edge absorption spectra of Fe minerals and model compounds: II. EXAFS. Phys. Chem. Minerals 13:31-47.

Waychunas, G. A., G. E. Brown, Jr., C. W. Ponader, and W. E. Jackson. 1988. Evidence from x-ray absorption for network-forming Fe^{2+} in molten alkali silicates. Nature 332:251-253.

Weast, R. C. (ed.). 1979. CRC Handbook of chemistry and physics. p. E-206. CRC Press, Inc., Boca Raton, Forida.

White, E. W., and G. V. Gibbs. 1967. Structural and chemical effects on the SiKβ x-ray line for silicates. Am. Mineral. 52:985-993.

Wilson, M. A., S. A. McCarthy, and P. M. Redericks. 1986. Structure of poorly-ordered aluminosilicates. Clay Miner. 21:879-897.

Wong, J., F. W. Lytle, R. P. Messmer, and D. H. Maylotte. 1984. K-edge absorption spectra of selected vanadium compounds. Phys. Rev. B. 30:5596-5610.

Xu, S., and J. B. Harsh. 1990. Monovalent cation selectivity quantitatively modeled according to hard/soft acid/base theory. Soil Sci. Soc. Am. J. 54:357-363.

Zachara, J. M., J. A. Kittrick, L. S. Dake, and J. B. Harsh. 1989. Solubility and surface spectroscopy of zinc precipitates on calcite. Geochim. Cosmochim. Acta. 53:9-19.

Zachara, J. M., J. A. Kittrick, and J. B. Harsh. 1988. The mechanism of Zn^{2+} adsorption on calcite. Geochim. Cosmochim. Acta. 52:2281-2291.

Chapter 5

Synchrotron-Based X-Ray Diffraction and Scattering Studies of Soil Materials

D. G. Schulze, J. E. Amonette, S. J. Anderson, P. M. Bertsch, J. M. Bigham, J. B. Dixon, C. T. Johnston, J. W. Stucki, M. L. Thompson, and S. J. Traina

5.1 Introduction

Soils are important to society from agricultural, environmental, and engineering perspectives. Traditionally, soils have been relied on to help produce food and fiber. More recently, environmental concerns have increased, and the importance of soils in controlling ground-water pollution, safe use of pesticides, and nuclear waste storage has become evident. Modification and control of soil physical behavior to improve streets, roads, and airports continues to be important.

The behavior of soils is controlled, to a large extent, by constituent minerals that have special sets of properties developed in the soil weathering environment. Clay minerals in soils have adsorbed hydroxy-aluminum polymers that influence their chemical and physical properties. The oxides of iron and manganese in soils have foreign ions substituted in their structures that influence their behavior, influence crystal growth, and fingerprint the geochemical environment in which they formed.

Characterization of the properties of soil minerals relies heavily on information obtained from x-ray diffraction studies to supplement chemical and engineering data. Conventional x-ray diffractometry is limited, however, by the low intensity, poor collimation, and polychromatic nature of the source. Synchrotron x-ray sources offer a means of solving several important problems in soil and clay mineralogy. For example, the shrinking and swelling of clay minerals influences the availability of two major plant nutrients (nitrogen and potassium), the movement of water through soils, the mobility of environmentally sensitive ions and molecules (e.g., heavy metals, radionuclides, pesticides, and nitrogen compounds), and the stability of structures

built on them. Synchrotron-based techniques extend our ability to detect changes in the crystal structures of clay minerals as they shrink or swell, and improve our ability to identify trace quantities of toxic elements and compounds associated with these minerals.

Soil minerals must often be studied under aqueous conditions to determine their behavior in the presence of water; this can often be done with synchrotron-based techniques, whereas many other techniques require exposure of the specimen to high vacuum. The high intensity of synchrotron x-ray sources permits investigation of the extremely small crystals in soil clays to determine their behavior at the low concentrations at which they often occur in nature. Synchrotron-based techniques also provide unique opportunities to study the mechanisms of certain chemical reactions in real-time.

5.2 Importance of the Advanced Photon Source

The unique advantages of synchrotron radiation are 1) the very high intensities available, 2) the highly collimated nature of the radiation, 3) the ability to select monochromatic radiation from a continuous range of energies, and 4) the ability to conduct kinetic studies with time resolutions on the order of micro- and nanoseconds. Many of these features are available at existing synchrotron facilities, but full implementation of these features will be realized when the Advanced Photon Source (APS) is completed in the mid-1990s. In particular, because of the incorporation of various undulator and wiggler insertion devices into the design of the APS, photon fluxes several orders of magnitude above those at existing facilities will be available.

In general, the extremely intense collimated radiation produced by the APS should result in a dramatic lowering of the detection limits for trace and poorly ordered phases in soils and man-made wastes. Thus, trace compounds of environmental significance can be more readily identified, and general analyses of very small samples or of surface compounds are more feasible. Microdiffraction of soil thin sections may make it possible to identify local concentrations of trace phases which would be diluted below the detection limit by conventional procedures. Resolution on the order of 0.002° 2θ will be attainable for well-crystallized samples, which is one order of magnitude greater than that at existing synchrotron facilities and two orders of magnitude better than for conventional x-ray diffractometers (Waychunas *et al.*, 1988). This will allow powder patterns to be used routinely for structural refinements, as well as for quantitative analysis by the Rietveld technique.

The high brightness of the APS will allow rapid collection of diffraction data at ambient conditions, and make it possible to observe structural changes over very

short time intervals, typically milli- and microseconds. For example, kinetic studies of the behavior of soil suspensions could lead to better understanding of K-depletion/fixation reactions in soils, clay swelling during organic sorption and cation exchange reactions, and the incipient precipitation of oxides on the interior and exterior surfaces of clays.

Both small-angle neutron scattering (SANS) and small-angle x-ray scattering (SAXS) have been used to study the structure of inorganic and organic polymers in aqueous suspensions, as well as the structure of disordered solids. Neutron scattering has been used more commonly because multiple Bragg scattering effects are much smaller and scattering length density differences are greater for neutron scattering than for x-ray scattering (Henderson *et al.*, 1989). Unfortunately, with presently available neutron densities, most SANS studies must be conducted at relatively high concentration.

The APS will make it more feasible to conduct SAXS studies on a variety of systems. SAXS produces less incoherent scattering than does neutron scattering; therefore, x-ray scattering profiles may be measured at higher values of the scattering vector with less interference from the background (Henderson *et al.*, 1989). SAXS is a weak effect, and the high intensity of the APS will make it possible to study more dilute systems. In addition, the brilliance and the low divergence will make it possible to use smaller specimens with better depth resolution (Russell, 1988). The high-intensity source will make it possible to obtain much better time resolution (up to nanosecond resolution) without sacrificing energy resolution (Russell, 1989).

Some examples of specific research areas which would benefit from the techniques which will be available at the APS are outlined below. Other areas of research will undoubtedly evolve as synchrotron x-ray sources become more widely used by the soil and environmental sciences communities.

5.3 Potential Applications of Synchrotron-based X-ray Diffraction and Scattering Techniques

5.3.1 Clay Microstructure

Layer silicate clay minerals are largely responsible for many chemical and physical properties of soils and sediments. In water, these layer silicates develop a gel-like microstructure. This microstructure, used here to denote the organization of individual clay layers relative to one another within a particle, is characterized by the distances between, and the relative orientations of, adjacent clay layers. The

microstructure is commonly considered to be a dominant factor in determining a number of bulk physical and chemical properties of clays, such as permeability, mechanical strength, water-holding capacity, and chemical reactivity.

Several important gaps exist in our understanding of clay microstructure and its effect on the macroscopic behavior of soils and sediments. First, the relationship between basic structural and surface properties of the clay (such as iron oxidation state, isomorphous substitution, hydration energy, van der Waal's forces, and coulombic interactions) and inter-layer or inter-particle arrangements are still poorly characterized and under dispute (Norrish and Rausell-Colom, 1963; Derjaguin and Churaev, 1974; Israelachvili and Pashley, 1983; Low, 1987). Second, the dynamics of microstructure formation and modification are unknown. Third, methods for modifying microstructure *in situ* are unpredictable because the governing forces are not understood. Fundamental to filling these gaps is the ability to characterize the clay-water system *in situ*.

The direct observation of clay microstructure is difficult, particularly when the clay is highly expanded, because of the small size of particles and their disordered arrangement while in a suspended or gel state. Recent studies by Tessier, Pons, and co-workers (e.g., Pons *et al.*, 1987, 1982b; Tessier, 1984; Ben Rhaiem *et al.*, 1986, 1987), using the methods detailed by Plançon and Tchoubar (1975, 1977), examined the microstructure of low- to moderately expanded clay gels using high-resolution electron microscopy (HRTEM) and SAXS techniques. HRTEM is less direct than SAXS because the water in the clay gel must be replaced with a hardened resin and the sample must be cut with a thin-sectioning device prior to placement in the microscope. This process could introduce changes in the microstructure, and thus call into question the ultimate value of HRTEM for characterizing the gel-state of highly swelling clays.

Small-angle x-ray scattering, on the other hand, is able to observe clay gels directly in the water state without modification. Using synchrotron radiation, Pons *et al.* (1981, 1982a) observed that swelling in water forms a gel in which the clay layers are kept parallel with stacking units of about four to five layers, but these layers are disoriented in the lateral directions. Further studies (de la Calle *et al.*, 1988) also showed that in some systems, the lateral orientation can be differentiated by appropriate comparisons between theoretical and experimental scattering patterns.

Experimental procedures for SAXS experiments of clays are already developed for laboratory x-ray sources. A sample chamber for obtaining x-ray scattering data from aqueous smectite suspensions was described by Viani *et al.* (1983) and by Wu *et al.* (1989), and such chambers could be easily mounted on a diffractometer on an APS beam line. The experimental patterns can be analyzed by comparing them with

theoretical curves derived by the method used by Pons (Plançon and Tchoubar, 1975, 1977). Variations in microstructure due to different saturating cations (namely, Ca, K, Cu, Zn, Mn, and Na) can be determined using homoionic smectites, and the effect of isomorphous substitution can be identified without further experimentation by choosing smectites with different octahedral and tetrahedral cation composition. The effect of iron oxidation state can be studied using an iron-rich and an iron-poor Na-saturated smectite. Procedures for reducing structural Fe to different levels, and procedures for handling the reduced samples under an inert atmosphere are described by Stucki *et al.* (1984a, 1984b), Komadel *et al.* (1990), and Wu *et al.* (1989), while the effect of water content can be measured by varying the He pressure inside the sample chamber as described by Viani *et al.* (1983, 1985).

The very high intensity of an APS beam line will enable completion of an x-ray scattering pattern in less than 1 minute. This unique and powerful attribute can be exploited to obtain a rapid sequence of patterns of smectite gels as they transform either under increasing pressure or, in the case of a reduced sample, during oxidation as oxygen is introduced into the surrounding atmosphere. Thus, both static and dynamic properties of gel formation can be studied.

5.3.2 Structural Properties of Clay-Sized Minerals

The crystal structures of minerals determine many of the macroscopic chemical and physical properties of soils. Powder diffraction analysis of soil clay minerals is usually confined to identifying and obtaining semiquantitative estimates of phases, measuring unit cell dimensions, and estimating crystallite size. Synchrotron x-ray sources provide new approaches for obtaining a more complete understanding of the structural properties of soil minerals.

5.3.2.1 Rietveld Structural Refinement of Powder Patterns

The full pattern fitting method of Rietveld (1969) makes it possible to refine the crystal structures of powdered phases. Although widely used to refine crystal structures using neutron diffraction data, the Rietveld method has only recently been applied to clay-sized minerals of interest to soil and environmental scientists. Bish (Bish and Von Dreele, 1989; Bish, 1989) recently used the Rietveld method to refine the kaolinite structure. Other recent applications of the method to clay-sized minerals include structural refinements of Mn-substituted goethite (Bish and Ebinger, 1989), birnessite (Post and Veblen, 1989), chlorite (Walker, 1989), hollandite, todorokite, and zeolites (Post and Bish, 1989).

Although Rietveld refinements can be done using laboratory x-ray sources, synchrotron x-ray sources provide unique advantages (Finger, 1989, Will *et al.*, 1987). The use of a synchrotron x-ray beam eliminates many geometrical aberrations inherent to focusing methods, because the beam is highly collimated and consists of only a single sharp spectral line. Thus, line profiles are much easier to handle in profile fitting procedures. The narrow spectral bandwidth of the synchrotron x-ray beam is an order of magnitude improvement over conventional laboratory x-ray sources, and thus there is a dramatic improvement in the resolution of overlapping diffraction lines for well-crystallized samples (Parrish *et al.*, 1986). This will make it possible to extend the Rietveld procedure to increasingly complex natural mixtures. Finally, the ability to chose wavelengths between about 0.5 and 2Å makes it possible to choose the wavelength which produces the best peak-to-background ratio.

The Rietveld method may provide significant new insights on the influence of foreign ion substitution in iron oxide minerals. The substitution of Al for Fe in the crystal structures of goethite and hematite can be used as an indicator of the conditions under which the minerals formed (Fitzpatrick and Schwertmann, 1982). The presence of the smaller Al ions in these minerals causes a decrease in the size of the unit cell dimensions, which is easily detected by shifts in the x-ray line positions. The unit cell dimensions of synthetic, Al-substituted goethites and hematites have been studied extensively to develop accurate relationships between cell dimensions and Al substitution. The unit cell dimensions of these minerals are not, however, solely a function of Al substitution. There is considerable variation in the goethite *a* dimension, and in the hematite *a* and *c* dimensions, which has been correlated to the synthesis temperature of the minerals (Schulze, 1984; Schulze and Schwertmann, 1987; Schwertmann, 1988). The Rietveld method may make it possible to determine the cause of this unit cell variation. Current Rietveld programs (Von Dreele, 1989; Larson and Von Dreele, 1988) make it relatively easy to extract strain-broadening information from powder diffraction patterns, allowing one to determine whether structural strain is the cause of the unit cell variability.

Structural data on other clay minerals, for example vermiculites and illites, might also benefit from Rietveld refinement. The ability of current Rietveld programs to refine up to nine phases simultaneously (Von Dreele, 1989; Larson and Von Dreele, 1988) makes it possible to obtain detailed information on specific phases even when they occur in complex mixtures. The Rietveld method is also likely to make significant improvements in the quantitative analysis of soil minerals from powder x-ray patterns (see Section 5.3.5).

5.3.2.2 Single-Crystal Refinement of the Kaolinite Structure

The hydroxyl groups of kaolin subgroup minerals have attracted considerable attention as sensitive indicators of structural disorder and as indicators of changes resulting from the presence of guest species in the interlayer region (Barrios *et al.*, 1977; Johnston *et al.*, 1984; Brindley *et al.*, 1986; Raupach *et al.*, 1987; Bookin *et al.*, 1989; Prost *et al.*, 1989). In particular, the OH stretching and deformation vibrational modes have been shown to correlate strongly with the degree of disorder (Barrios *et al.*, 1977; Prost *et al.*, 1989), the Hinckley index (Brindley *et al.*, 1986), and changes in interlayer bonding (Wieckowski and Wiewiora, 1976; Giese, 1982; Johnston and Stone, 1990). Controversy remains, however, regarding the assignment of these bands to the four distinct structural OH groups present in kaolinite and dickite (Giese, 1988). The best available structural data for the OH groups, recently summarized by Johnston *et al.* (1990), indicate that there is relatively poor agreement regarding the bond length and overall positions of the hydrogen atoms. There has been little effort to reconcile the suggested hydrogen positions obtained from neutron-, electron-, and x-ray diffraction studies with the observed infrared (IR) and Raman spectra of kaolin polymorphs. Polarized single-crystal fourier transform infrared (FT-IR) spectra provide insight into the location of the OH groups in kaolinite and dickite.

Polarized single-crystal FT-IR spectra of the ν(O-H) region of Ouray dickite (Figure 5.1a-b) and the corresponding kaolinite spectra (Figure 5.2a-b) represent the first reported single-crystal vibrational spectra for kaolinite or dickite (Johnston *et al.*, 1990). Unambiguous assignment of the *a*- and *b*-crystallographic axes of dickite was determined using a cross-polarizing optical microscope fitted with a 550 nm quartz retardation plate. Polarized single-crystal FT-IR spectra were then obtained for a dickite crystal of known orientation (Figure 5.1a-b). Figure 5.1a presents the FT-IR spectra with no y-offset and the absolute intensity scale shown on the y-axis; the same data are shown in Figure 5.1b with polarization of the electric vector defined by the angle between the electric vector and the *a*-axis (Figure 5.3). The band at 3623 cm^{-1} has been assigned to the inner-hydroxy OH_1 group located between the tetrahedral and octahedral sheets. The angle (θ) between the transition moment of the inner hydroxyl group and the crystallographic *b*-axis was found to be 49°, based upon the dichroic ratio (Turrell, 1972). The band at 3710 cm^{-1} is attributed to the OH_3 inner-surface hydroxyl, with $\theta = 11°$. The band at 3656 cm^{-1} is assigned to the OH_2 and OH_4 inner surface hydroxyls; θ was found to be 45 ±5° (Johnston *et al.*, 1990).

Polarized single-crystal FT-IR spectra of Keokuk kaolinite in the ν(O-H) region are shown in Figure 5.2a-b. The spectral components of kaolinite could not be resolved into individual components due to the lower signal-to-noise ratio obtained for kaolinite in comparison with that for dickite, and because kaolinite has at least four

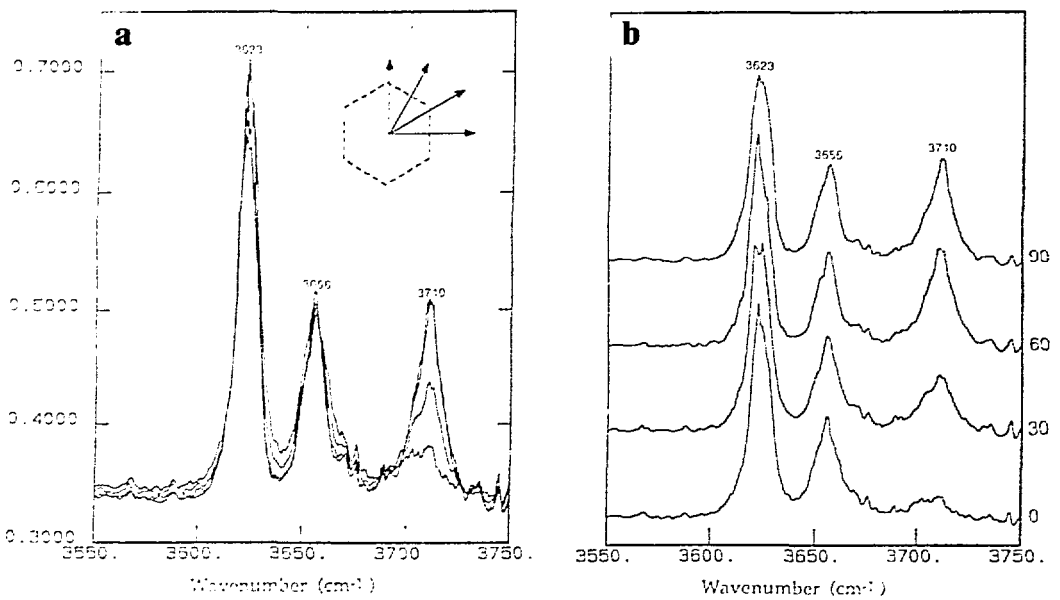

Figure 5.1. Polarized single-crystal FT-IR spectra of Ouray dickite in the 3550 to 3750 cm-1 region: (a) stack plot showing the spectra with no y-offset with the absorbance scale shown on the left, (b) same spectra as shown in (a) where the listed polarization angles correspond to the angle between the electric vector of the transmitted IR beam and the crystallographic b-axis of the dickite crystal.

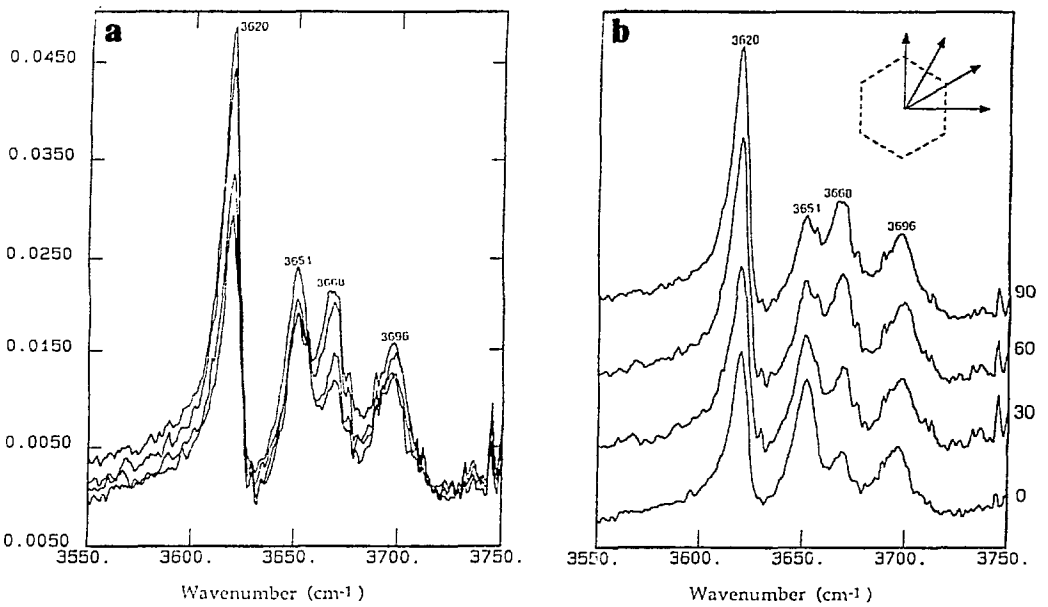

Figure 5.2. Polarized single-crystal FT-IR spectra of Keokuk kaolinite in the 3550 to 3750 cm-1 region: (a) stack plot showing the spectra with no y-offset is shown on the left, (b) the same spectra are shown on the right where the listed polarization angles correspond to the angle between the electric vector of the transmitted IR beam and an arbitrary side of the kaolinite crystal.

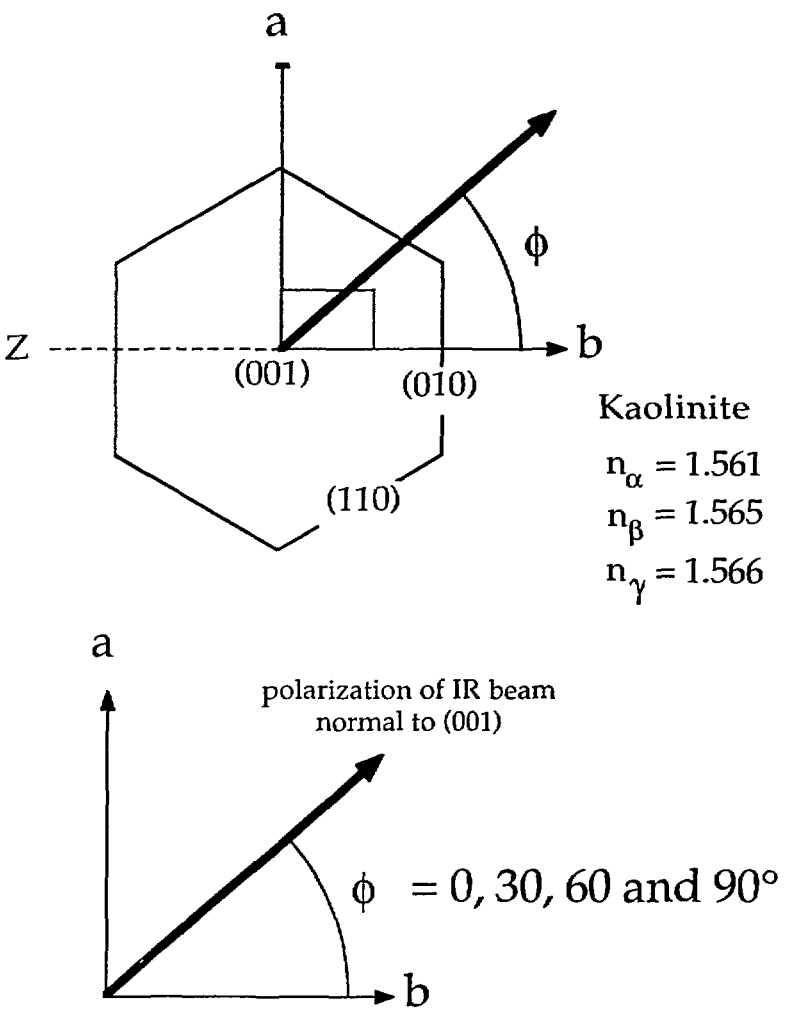

Figure 5.3. Conceptual diagram showing the optical orientation of the crystallographic axes.

ν(O-H) bands in comparison to only three for dickite. Unfortunately, the single-crystal FT-IR data presented here for kaolinite do not provide unambiguous information regarding the assignment and orientation of the hydroxyl groups. The crystallographic axes of kaolinite could not be determined in this study due to the small size of the kaolinite crystals, and the likely presence of kaolinite twins.

The dickite crystals examined in this study were approximately 50 μm on edge, while the kaolinite crystals were about 20 μm on edge. Conventional single crystal x-ray diffraction studies are limited to crystals larger than 50 or 60 μm on edge. At present, only powder diffraction data are available for kaolinite, and poor agreement exists among the various x-ray and neutron diffraction structures of kaolinite and dickite (Johnston *et al.*, 1990). There is a need to obtain accurate single-crystal structural information on these and related minerals to better understand their physicochemical properties. Given the large uncertainties in the position of the hydrogen atoms in the best available kaolinite and dickite structures, it is suggested that vibrational data be used to constrain the coordinates of the hydroxyl groups in future structural refinements of dickite and kaolinite.

Synchrotron radiation would clearly provide a unique structural tool to probe the stacking defaults in phyllosilicates. Single crystal structure determinations have been made on MnO crystals as small as 2.5 x 2.5 x 2.5 μm using synchrotron radiation (Sueno *et al.*, 1987), thus, single crystal studies of kaolin group minerals should be possible.

5.3.4 Spatial Distribution of Soil Minerals

Soils are highly organized, natural bodies. Full understanding of the chemical, physical, and biological reactions that occur in soils depends to a large degree on knowledge of soil organization at the scale of millimeters to centimeters. Many soil minerals are distributed in discrete pedological features. For example, phyllosilicate clays may be concentrated as coatings or fillings in pores, iron oxides may be localized as nodules or as coatings on aggregates, and secondary calcite may occur pseudomorphosed after root cells or as finely divided crystals in the groundmass. The spatial organization of such pedological features must be characterized to better understand how they form and how they function in both agricultural and nonagricultural ecosystems.

Identification of soil minerals by light microscopy, typically carried out on thin sections (25-30 μm thick) of resin-impregnated blocks of undisturbed soil, is usually limited by the size of the mineral grains, their opacity or association with opaque minerals, and the similarity of optical properties of many minerals. Some

investigators have physically removed bits of thin sections with microdrills to obtain x-ray diffraction patterns (Verschuren, 1978; Beaufort *et al.*, 1983; Feijtel *et al.*, 1989). Besides being tedious, such efforts result in only small amounts of sample which require long periods of analysis using laboratory x-ray sources.

By performing x-ray diffraction studies directly on thin sections, the spatial relationships of minerals in undisturbed soil samples may be documented (Wilson and Clark, 1978). Not only does this increase efficiency over optical methods alone, but the accuracy of such characterizations is improved. Unfortunately, standard x-ray diffraction techniques are not well adapted for this task, primarily because the x-ray beam is too broad and the intensity is too low for diffraction patterns to be collected from localized, individual mineral grains or small clusters of crystals. On the other hand, a synchrotron x-ray beam is ideal because it can be collimated to a fine spot (a few micrometers in size) with high spatial resolution, but without significantly losing intensity (Prewitt *et al.*, 1987). Two examples of soil mineral characterization by synchrotron x-ray microdiffraction are: (1) studies of clay coatings, and (2) mica-smectite transformations.

Coatings of clay minerals occur along pore walls in subsurface horizons of many soils (Bullock and Thompson, 1985). Although they may compose only 1-2% of the soil volume, clay coatings have significant impact on root growth, plant nutrition, and transport of pollutants because of their large specific surface areas, large cation exchange capacities, and slow permeabilities (e.g., Soileau *et al.*, 1964). By using synchrotron x-ray diffraction techniques on soil thin sections, it should be possible to identify the clay minerals which occur in pores of different soils or even in different kinds of pores of the same soil. With standard techniques, c-axis parameters are most often used in the identification of clay minerals, but the high resolution allowed by the synchrotron beam and the ability to easily perform diffraction analyses in both reflection and transmission mode (Parrish *et al.*, 1986), will facilitate identification of clay minerals in thin section by using a- and b-axis parameters as well.

Micas are thought to be transformed to vermiculites and/or smectites in certain soils. Little is known about the speed of the process, and it is not clear which environmental factors favor solid-phase transformation versus precipitation of soluble constituent species. Silt-size mica grains in the process of decomposition can be identified in thin sections of soils. Subsequent synchrotron x-ray diffraction analyses of contiguous segregations of clay could determine if transformation has occurred. Synchrotron x-ray fluorescence microprobe analysis of the same sample area could provide quantitative elemental analyses of the original mineral and its weathering products (Chapter 6 of this volume) and x-ray absorption spectroscopy would allow the identification of the oxidation state(s) of Fe atoms in the minerals (Chapters 3 and 4 of this volume).

5.3.5 Identification and Quantification of Mineral Phases

Natural soils and man-made inorganic waste materials such as fly ashes usually consist of a complex assembly of crystalline and poorly ordered mineral phases. Assessment and prediction of the geochemical and physical processes that occur in these materials require qualitative and quantitative information about the mineral phases that are present. Conventional procedures rely on x-ray powder diffraction in combination with chemical and spectroscopic analyses to provide information about crystalline phases present in major and minor proportions. Trace constituents and poorly ordered phases, however, are not easily analyzed by these procedures due to inherent limitations in the intensity of conventional x-ray sources. Synchrotron radiation sources promise to remove these limitations and allow detection and quantification of phases present at very low levels.

5.3.5.1 Poorly Crystallized Minerals

The role of poorly crystallized minerals in soils and waste materials has only recently come to be more fully appreciated. Iron oxide minerals such as ferrihydrite, aluminosilicate minerals such as allophane and imogolite, and some of the Mn oxide minerals exhibit only short-range ordering and thus produce very weak and diffuse x-ray patterns. These minerals occur as very small particles with high surface areas, and they are very reactive chemically. Phosphate, for example, can be so strongly adsorbed by these minerals that it is unavailable to plants. Chromium(III) can substitute for iron in ferrihydrite resulting in a compound that is much less soluble than pure $Cr(OH)_3$. These minerals, therefore, can have a profound influence on soil chemical properties even when they are present in only small amounts.

The identification of these poorly crystallized minerals in the complex matrix of soil minerals has been difficult. Ferrihydrite, for example, was first identified in samples from special environments, such as the ocherous deposits often found in ditches draining wet soils, where the mineral often occurs in an almost pure form.

A differential x-ray diffraction technique (DXRD) based on the selective chemical dissolution of one or more components from the sample (Schulze, 1981, 1986) has made progress in lowering the detection limits for ferrihydrite. Two diffraction patterns must be collected--one pattern is collected of the untreated sample, while a second pattern is collected from a sample that has been treated by a selective chemical dissolution procedure to remove the constituent(s) of interest. After appropriate scaling of the treated pattern to match intensities of peaks common to both samples, the pattern of the treated sample is subtracted from the pattern of the untreated sample. The resulting difference diffraction pattern is that of the

mineral(s) dissolved by the selective dissolution procedure. Figure 5.4 illustrates this procedure for a sample containing about 23% ferrihydrite (Schwertmann *et al.*, 1982). Ferrihydrite is soluble in 0.2 M NH_4-oxalate, and the difference between the untreated and oxalate-treated patterns yields the characteristic 6-line diffraction pattern of ferrihydrite.

Long counting times are required with conventional x-ray diffraction equipment to obtain spectra with the large signal-to-noise ratio needed for DXRD. For example, the patterns illustrated in Figure 5.4 required about 12 hours each to collect. Even with these long counting times, the lower detection limit for ferrihydrite in soil materials is only about 15 wt% by DXRD (Campbell and Schwertmann, 1984) and additional improvements using laboratory x-ray sources seem unlikely. The high brightness of the APS would make it possible to obtain DXRD patterns in a shorter period of time and should make it possible to lower the detection limits for poorly crystallized minerals even further.

Another differential x-ray diffraction technique is based on the anomalous scattering of specific elements in a sample. In this technique, diffraction patterns are taken using two different x-ray wavelengths, one just before, and one at the absorption edge of the element of interest. The resulting change in the scattering factor of the element whose absorption edge was crossed results in a change in the diffraction pattern of the minerals containing the element. For example, if diffraction patterns are taken just before and just after the Fe absorption edge, the intensities of the Fe-containing minerals should change relative to the minerals which do not contain Fe. Subtraction of the two patterns, after appropriate normalization to the same 2θ scale, results in the pattern of the Fe-containing minerals. Wood *et al.* (1986) demonstrated the feasibility of this technique using a mixture of Co_3O_4 and kaolinite, and diffraction patterns collected using CoKα and CoKβ radiation. The technique should be applicable to Fe-containing minerals if the appropriate wavelengths are used. The advantage of the anomalous scattering approach is that the same sample is used for both patterns. Although Wood *et al.* (1986) used a laboratory x-ray source, synchrotron x-ray sources will make this approach much more practical because it is easy to select monochromatic radiation of the desired wavelength.

5.3.5.2 Trace Phases

The chemistry of heavy metals in soils is of considerable agronomic and environmental importance. Many heavy metals (Ni, Zn, Ba, Co, Pb, etc.) are adsorbed by or incorporated into the structures of manganese oxides, which occur in soils as very fine particles of variable structure, stoichiometry, and crystallinity. The oxidation states of some of these metals are controlled by manganese oxides as well.

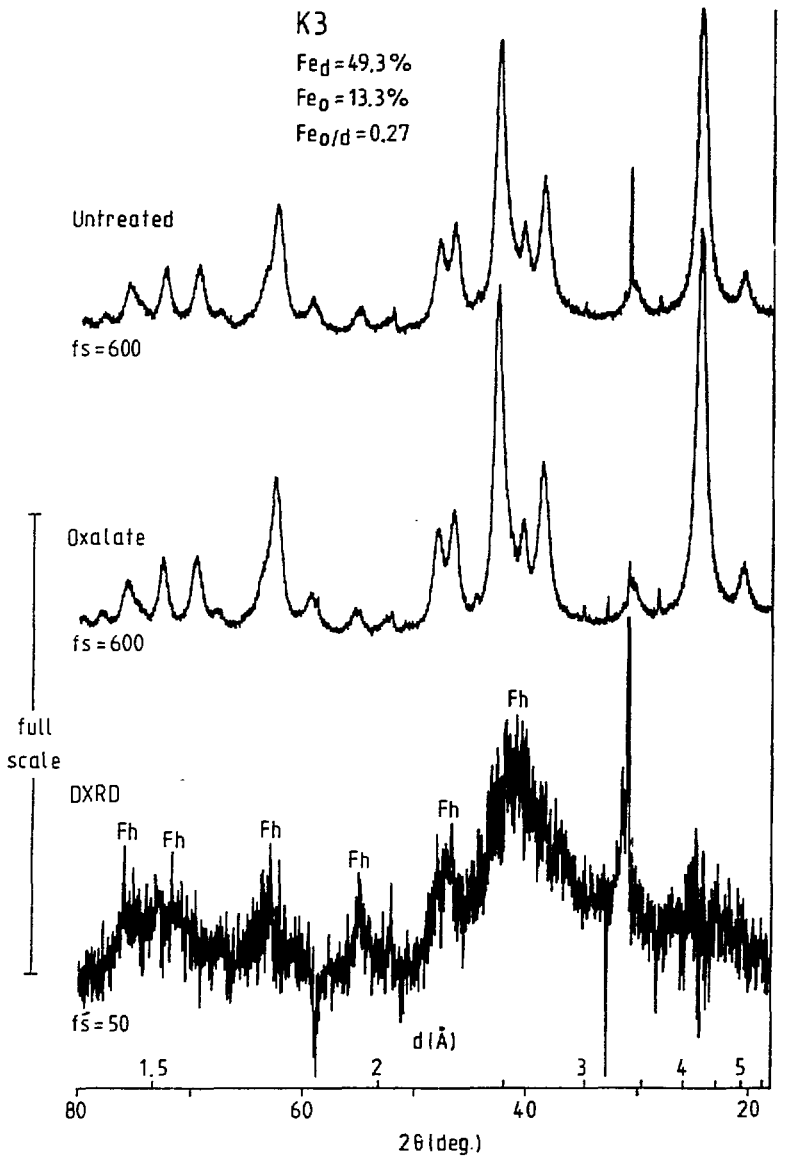

Figure 5.4. X-ray diffraction diagrams of a sample containing approximately 23% ferrihydrite (Fh). Patterns of the untreated sample and the oxalate treated sample appear almost identical, but subtraction of the oxalate pattern from the untreated pattern yields the differential x-ray diffraction pattern (DXRD) of ferrihydrite (Fh). fs=full scale counts/second. (From Schwertmann *et al.*, 1982, with permission.)

Cr(III), for example, is readily oxidized to the more soluble (and hence mobile) Cr(VI) form by manganese oxides (Bartlett and James, 1979; Eary and Rai, 1987). With conventional techniques, identification of the reactive manganese oxide phases in soils and wastes is difficult because of their low abundance, variable crystallinity, high mass absorption coefficients for CuKα radiation, and interferences by abundant layer silicate minerals. Consequently, most investigators have studied the less reactive manganese oxide nodules (Senkayi *et al.*, 1986; Uzochukwu and Dixon, 1986; Tokashiki *et al.*, 1986) or synthetic specimens (Eary and Rai, 1987), or have used the bulk soil without being able to identify the exact phases that are reacting (Bartlett and James, 1979). The application of the Rietveld method is likely to greatly improve the quantitative phase analysis using x-ray diffraction data (Bish and Chipera, 1988). Bish and Howard (1988) have shown how this approach can yield high-precision quantitative results with the added benefit of producing precise cell parameters and approximate chemical compositions. In addition, the use of an internal standard will allow the determination of the total amorphous content of a sample.

The application of high-intensity high-resolution synchrotron radiation should lower the detection limits and remove many of the interferences that currently limit the identification and careful study of the reactive manganese oxide fraction in soils and wastes. This type of information should add greatly to our knowledge of the chemistry of trace metals in the soil environment and allow better selection of soils for particular agronomic and environmental uses.

5.3.6 Time-Resolved Scattering and Diffraction Studies of Mineral Formation and Transformation

5.3.6.1 Time-Resolved Studies of Fe-Containing Systems

Soils and sediments represent "open" systems wherein numerous chemical, physical, and biological factors combine to induce alterations of the mineral fabric over a time scale ranging from millennia to, perhaps, milliseconds. The most reactive components in these systems include an array of oxides, hydroxides, and oxyhydroxides of Fe and Mn whose properties are described in a number of excellent review articles (Murray, 1979; McKenzie, 1989; Schwertmann and Taylor, 1989). These minerals have been widely recognized for their ability to scavenge various trace metals (Chao and Theobald, 1976), inorganic anions (Hingston, 1981) and organic compounds (Oades and Tipping, 1989) from associated waters and for their sensitivity to local environmental factors. Changes in soil or sediment chemistry may induce fairly rapid modifications in composition, spatial distribution, and even

structure among these minerals. Because of these properties, the Fe and Mn oxides are often implicated as important agents affecting aqueous geochemistry and environmental quality through both surface- and precipitation-controlled reactions.

The nature of the crystalline phases produced within the Fe and Mn systems depends strongly on the physicochemical conditions of gel formation from solution and the evolution or aging of these gels over time. Factors such as pH, temperature, H_2O activity, oxidation rate, electrolyte concentration, and foreign ions have been described in numerous "cause and effect" studies of mineral formation (e.g., Schwertmann, 1959; Giovanoli *et al.*, 1975; Torrent *et al.*, 1982; Schwertmann and Murad, 1983; Brady *et al.*, 1986; Cornell *et al.*, 1989). The actual mechanisms by which these variables influence crystal nucleation and development are largely unknown because differences among solutions and gels at various stages of evolution have not generally been distinguishable with conventional diffraction or spectroscopic methods due to limitations imposed by rapid kinetics and/or low sensitivity. This situation could change dramatically when high energy synchrotron radiation with a pulsed time structure becomes available at the APS.

For example, direct structural studies of solutions containing metal complexes using non-element specific methods have generally been viewed as impractical or ambiguous, primarily because of poor signal-to-noise ratios. Preliminary studies of Fe^{2+}, Fe^{3+}, and Mn^{2+} chloride solutions using synchrotron-based XANES and EXAFS have yielded promising results (Apted *et al.*, 1985; Garcia *et al.*, 1986). In the work of Apted *et al.* (1985), Fe^{3+}-O and Fe^{3+}-Cl bond distances were measured and changes in these distances with decreasing Cl- concentration were interpreted to mean a shift from tetra-chloro complexes (d(Fe-Cl)=2.25Å) to either hexa-aquo ($Fe(H_2O)_6^{3+}$) or trans-$Fe(H_2O)_4Cl^{2+}$ complexes (d(Fe-O)=2.10Å). Fe K-EXAFS has also been used to study the local structure of Fe^{3+} gels (Combes *et al.*, 1986, 1989). These gels were amorphous to x-ray diffraction but were shown to have short range order with Fe-O distances similar to those observed for octahedral complexes of Fe in solution (Apted *et al.*, 1985). Interestingly, gels precipitated by oxidation of Fe^{2+} solutions yielded FeO_6 octahedra linked primarily by edge sharing; whereas, those produced from ferric nitrate solutions exhibited a higher proportion of corner sharing. Extensions or modifications of such experiments to follow the evolution of polyhedral "clusters" using x-ray diffraction and XAS on APS beam lines could yield valuable insight into pathways and environmental controls leading to the formation of various Fe and Mn oxides.

Experimental requirements for such studies at the APS should be fairly simple. Sandstrom *et al.* (1981) have described solution sample cells consisting of a thin-walled Teflon container with Kapton windows. Such cells should be adequate for XAS analyses of electrolyte solutions and gels in aqueous media. Time-dependent

diffraction studies are primarily limited by x-ray flux for weakly scattering samples. To date, kinetic studies using diffraction techniques have been constrained to relatively slow phenomena. Faster kinetics associated with phase transformations and precipitation reactions will probably require that data collection be several orders of magnitude faster. With the use of an APS undulator, the available x-ray flux from a single radiation bunch in the storage ring should be adequate for the collection of a complete diffraction pattern with time resolution on a microsecond scale (Waychunas *et al.*, 1988).

5.3.6.2 Time-Resolved Studies of Aluminosilicate Systems

Both static and time-resolved SAXS and diffraction studies have provided information about mineral formation and transformations. Recently, Henderson *et al.* (1989) used SAXS to study the nucleation and crystallization of zeolites. Axelos *et al.* (1989) studied the effects of solution pH on the structure of the silica-H_2O interface for silica Ludox HS. Measurements of the vector scattering amplitude showed a decrease in particle radius and volume as pH increased from 7 to 10. At pH 7, the SAXS data suggested the presence of angular crystal facets on the particle surfaces. In contrast, at pH 10 the particles appeared to have a smooth, spheroidal shape, and the electron density exhibited a more gradual transition from the surface to the bulk solution, suggesting the presence of a gel-like surface (Axelos *et al.*, 1989).

Small-angle x-ray scattering studies have shown that the properties of colloidal solid phases formed from Al_{13} polynuclear species depend upon the OH/Al ratio and the age of the solution (Bottero *et al.*, 1982; Axelos *et al.*, 1985; Bottero *et al.*, 1987). Complementary magic angle spinning - nuclear magnetic resonance (NMR) results suggested that the initial Al_{13} containing colloidal phase underwent solid-state rearrangement to a structure resembling $Al(OH)_3$. The infrared spectra of the material were characteristic of the $Al(OH)_3$ mineral bayerite, thus supporting the NMR data (Bottero *et al.*, 1987). Small-angle x-ray scattering experiments utilizing a synchrotron source would permit time-resolved experiments during the neutralization process under a range of synthesis conditions.

The hydrolysis of aluminum may proceed by a different mechanism in the presence of clay minerals than when negatively charged phyllosilicates are absent. The properties of hydroxy interlayers formed when cations are neutralized in the presence of the clay are different from interlayers that form when clays are equilibrated with preneutralized solutions (Barnhisel and Bertsch, 1989). In addition, the physicochemical properties of hydroxy-interlayered clays and the interlayer materials depend upon the identity of the clay mineral, the concentration and nature of the saturating cation, the type and concentration of base, and the rate

of neutralization. Furthermore, Si and organic acids have been shown to influence the nature of the hydroxy-Al interlayer (e.g., Sterte and Shabtai, 1987; Buondonno *et al.*, 1989). Another factor which may influence the nature of the interlayer material is the specific arrangement of clay particles into isolated clay crystallites, tactoids, quasicrystals, or even larger aggregates, either prior to or concurrent with hydroxy-cation introduction.

The nature of these species has been determined only partially by NMR spectroscopy. NMR is limited by the failure to identify most polymeric species and by the fact that most soil clay minerals contain significant paramagnetic Fe, which causes line-broadening and poor resolution of the Al spectra. Static x-ray scattering studies with a rotating anode source have provided insight into the effect of the ratio of pillar charge to clay surface charge on the packing of organometallic pillars in the interlayers of fluorhectorite and montmorillonite (Tsvetkov and White, 1988).

Time-resolved scattering or diffraction studies during the introduction of hydroxy-cations or during the neutralization process will be a powerful tool for studying the effect of different synthesis methods or different clay minerals on the properties of interlayers. The ability to obtain high-resolution diffraction data at low angles will be useful in this regard. Furthermore, the more intense x-rays will allow for the determination of the distribution of lower atomic weight polynuclears (e.g., Al, Si). With small angle scattering techniques, the important questions concerning clay particle arrangement during the interlayering process could be followed.

Henderson *et al.* (1989) demonstrated that SAXS may be used to study colloid organization, tactoid formation, and intercalation in synthetic perfluorohectorite suspensions. As these authors point out, rapid time-resolved measurements require the high intensities available from synchrotron sources. The availability of undulator x-ray sources such as the APS should allow for data collection in the 1 to 100 ms range.

5.3.6.3 Static and Time-Resolved Studies of Organic Molecules in Mineral Systems

The complex, long-chain, polyelectrolytic macromolecules known as humic and fulvic acids are important moieties in soils and natural waters. The propensity of these predominantly anionic molecules to form aqueous complexes with a number of environmentally hazardous solutes has been widely documented. At present, it is thought that humic and fulvic acids can facilitate the movement of complexed contaminants through porous soils and geologic materials.

Recent research by Traina *et al.* (1989) and Lee and Farmer (1989) suggests that the complexation of dissolved anthropogenic organic solutes by humic and fulvic acids is affected by the macromolecular configuration of dissolved humic substances, with the extent of complex formation decreasing with increased counter ion valence or ionic strength. Clearly, an understanding of the conformational behavior of these macromolecules in aqueous environments is important.

The concentration and type of counter ions associated with dissolved humic and fulvic acids can greatly influence their chemical and physical behavior. Gosh and Schnitzer (1980) used solution viscometry to study the effects of ionic strength, solution pH, and humic substance concentration on the macromolecular structures of dissolved humic acids. Under conditions of low ionic strength, high pH, and low total C concentration, the humic and fulvic acid molecules existed in solution as ionized, easily deformable, linear polymers. In contrast, acidic pH values, high ionic strength, and large concentrations of C caused the humic and fulvic acids to exhibit coiled or spheroidal configurations (Figure 5.5). Similar results were reported by Cummins *et al.* (1989) in SANS studies of the effects of different inorganic electrolytes on the geometries of micelles of poly(oxyethylene) nonionic surfactants. The above results indicate that humic and fulvic acids behave in a manner similar to other polyanionic macromolecules, and thus should be amenable to many analytical methods used to study other macromolecules in aqueous solutions. In particular, it is likely that steady-state and time-resolved SAXS methods can be used to elucidate the conformations of dissolved humic and fulvic acids.

Synchrotron-based, static SAXS studies of a variety of polymer systems provide examples of the information that may be obtained about fulvic and humic acids. Russell *et al.* (1988b) used SAXS to compare interactions between anionic and cationic polymers. The data not only provided information about the interface between the two types of polymers, but also indicated that polymers terminated with a sulfonate group interact more strongly with tertiary amines than do analogous carboxyl-terminated polymers (Russell *et al.*, 1988b). Similar steady-state studies of fulvic and humic acids, including the interaction of anthropogenic organic solutes with fulvic and humic acids, may be possible in the future. In addition, synchrotron-based anomalous small-angle x-ray scattering experiments (Chapter 4, this volume), should provide detailed information about the role of metal cations in the coagulation of humic substances (see, e.g., Stuhrmann and Notbohm, 1981; Ding *et al.*, 1988).

Static SAXS experiments will provide new information about the morphology of fulvic and humic acids and the binding between natural organic material and anthropogenic organic solutes, but time-dependent experiments will be necessary for a more complete understanding of the interaction of the many variables which affect

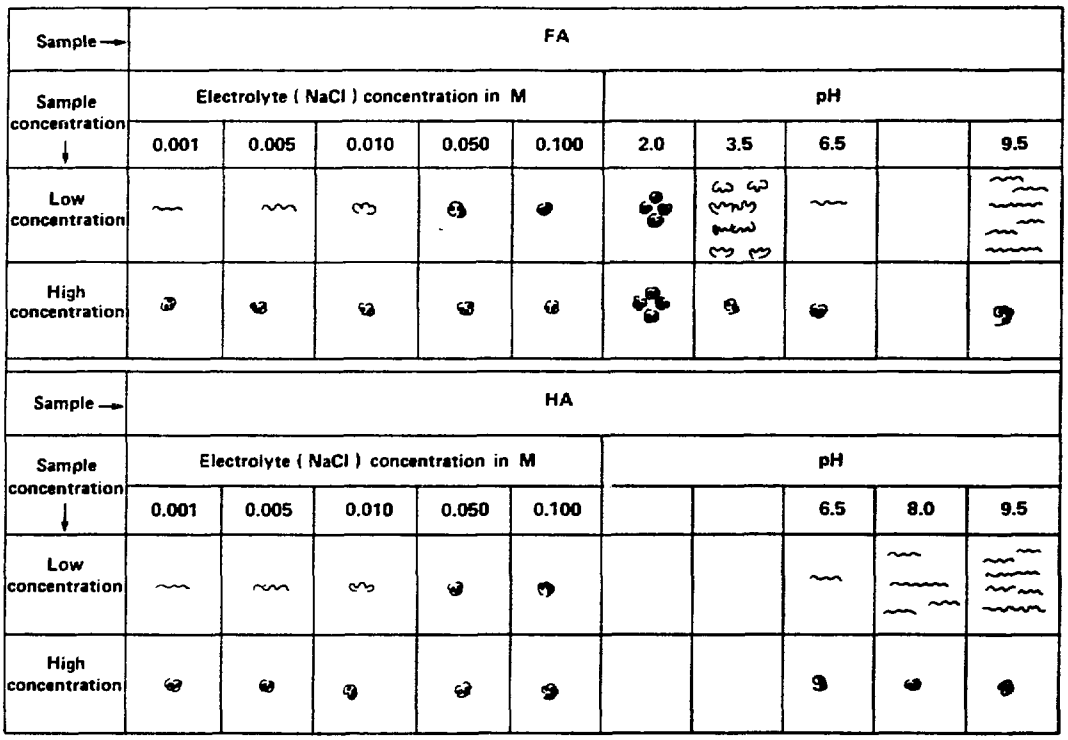

Figure 5.5. Model macromolecular structures of humic and fulvic acid (Gosh and Schnitzer, 1980, with permission).

fulvic and humic acid conformation and reactivity. Time-dependent measurements of changes in the complexation of anthropogenic organic solutes by humic substances can readily be made with standard analytical methods such as fluorescence quenching and fluorescence lifetime measurements, but time-dependent measurements of the conformations of fulvic and humic acids will require the use of a combination of techniques, including time-resolved SAXS. Recent work at the NSLS has demonstrated the feasibility of measuring the effect of some variable, such as temperature, upon the macromolecular conformation (and hence the small-angle scattering profile) of proteins in solution on the 10 s time scale (Phillips, 1989). The greater intensity of the APS will make it possible to obtain better time resolution and should allow measurements to be made on more dilute systems.

Other methods may provide information about natural and anthropogenic organic compounds adsorbed on phyllosilicate or oxide surfaces. For example, a combination of SAXS and SANS experiments on a mixture of semicrystalline and amorphous (noncrystallizable) polymers (Russell *et al.*, 1988a) revealed that the non-crystallizable polymer resided between the lamellae of the crystalline polymer, poly(ethylene oxide). Furthermore, the data suggested the existence of an interfacial zone containing amorphous polyethylene oxide, but none of the noncrystallizable polymer (Russell *et al.*, 1988a). Another x-ray technique that may yield valuable information about organic molecules on mineral surfaces is glancing-angle x-ray scattering (GIXS). Glancing angle x-ray scattering is a surface-sensitive scattering technique that has been used to obtain information about the molecular structure and ordering of phospholipids deposited on single-crystal silicon (Seul *et al.*, 1983). Although most such studies have involved dried materials, a more recent high-resolution x-ray scattering study conducted in a water-saturated, He atmosphere demonstrated that the hydration of lipid bilayers deposited on Si is temperature dependent, and that the individual bilayers are solvated by an integral number of water molecules. X-ray reflectivity has also been used to study interactions between a solvent and polymers adsorbed on a solid substrate (Sirota, 1989). To minimize interference from the solvent, a thin solvent film was trapped on the solid by stretching Mylar over the wet substrate. The air-Mylar and solvent-Mylar interfaces produce no specular peaks because the Mylar surface is rougher than the surface of the quartz substrate (Sirota, 1989). Similar techniques may be suitable for studying mineral-organic-water interactions.

5.4 Projected Instrumentation Needs

Most of the x-ray diffraction needs of the soil and environmental science community can be met with a two-circle powder diffractometer equipped with a diffracted-beam monochromator. This instrument should have the capability of being configured for

both low and medium resolution data collection. The instrument should be capable of very rapid data collection in low resolution operation for phase identification and quantification, and for routine structural refinement using the Rietveld technique. It should be possible to collect a pattern in minutes. It is important that the diffractometer be able to scan from very low angles, beginning at 0.5° 2θ, to obtain low-angle scattering data and to measure large d-spacings of expanded layer silicates. Important accessories include: (1) a beryllium-domed sample chamber to allow diffraction experiments at various relative humidities and in various atmospheres (such as He, N_2 or CO_2), and (2) heating and cooling stages to allow collection of spectra at sample temperatures ranging from liquid He to 1000°C. For routine fast scans, a linear, position-sensitive detector would be adequate but, for higher resolution, an intrinsic-Ge detector would be necessary. Kinetic studies at very short time intervals would require one of the new generation of ultrafast x-ray detectors such as the charge-coupled device detector described by Clarke *et al.* (1988). A computer-controlled x-y sample stage and the appropriate incident-beam focusing apparatus would allow microdiffraction studies of thin sections.

For surface diffraction studies, and for single-crystal work, access to a large-radius five-circle diffractometer similar to that described by Vlieg *et al.* (1987) would be useful. It is anticipated that the four- or five-circle instrument proposed by the Geosync User's Group (Waychunas *et al.*, 1988) could be used for these types of studies.

Small-angle x-ray scattering studies of minerals and organic polymers will require a SAXS camera with a position-sensitive detector; a photodiode array detector may be best for time-resolved SAXS (Song *et al.*, 1988). It will be necessary to have electronics that can monitor experimental parameters and the scattering intensity as a function of time (Phillips, 1989). A vertically polarized beam is preferable for some SAXS studies (Dutta, 1989). The APS undulator may be best suited for SAXS experiments on clay and polymer suspensions; the narrow bandwidth of the undulator and the horizontal and vertical collimation of the beam may eliminate the need for a monochromator. This would eliminate scattering from optical elements. For anomalous small angle x-ray scattering studies it is necessary to have a beam free of harmonics and a bandwidth of $\Delta E/E \leq 10^{-4}$ at 10 keV (Hoyt, 1989).

5.5 References

Apted, M. J., G. A. Waychunas, and G. E. Brown, Jr. 1985. Structure and specification of iron complexes in aqueous solutions determined by x-ray absorption spectroscopy. Geochim. Cosmochim. Acta 49:2081-2089.

Axelos, M., D. Tchoubar, J. Y. Bottero, and F. Fiessinger. 1985. Détermination par D.P.A.X. de la structure fractale d'agrégats obtenus par collage d'amas. Etude de deux solutions d'hydroxyde d'aluminium $Al(OH)_x$ avec x=2,5 et 3. J. Physique 46:1587-1593.

Axelos, M. A. V., D. Tchoubar, and J. Y. Bottero. 1989. Small-angle x-ray scattering investigation of the silica/water interface: Evolution of the structure with pH. Langmuir 5:1186-1190.

Barnhisel, R. I., and P. M. Bertsch. 1989. Chlorites and hydroxy-interlayered vermiculite and smectite. p. 729-788. *In* J. B. Dixon and S. B. Weed (ed.) Minerals in soil environments. 2nd ed. Soil Sci. Soc. Am., Madison, Wisconsin.

Barrios, J., A. Plançon, M. I. Cruz, and C. Tchoubar. 1977. Qualitative and quantitative study of stacking faults in a hydrazine treated kaolinite. Relationship with the infrared spectra. Clays Clay Miner. 25:422-429.

Bartlett, R., and B. James. 1979. Behavior of chromium in soils--III. Oxidation. J. Environ. Qual. 8:31-35.

Beaufort, D., P. Dudoignon, D. Proust, J. C. Parneix, and A. Meunier. 1983. Microdrilling in thin section: A useful method for the identification of clay minerals *in situ*. Clay Miner. 18:219-222.

Ben Rhaiem, H., C. H. Pons, and D. Tessier. 1987. Factors affecting the microstructure of smectites: Role of cation and history of applied stresses. p. 292-297. *In* L. G. Schultz, H. van Olphen, and F. A. Mumpton (ed.) Proc. Int. Clay Conf., Denver, 1985, The Clay Minerals Society, Bloomington, Indiana.

Ben Rhaiem, H., D. Tessier, and C. H. Pons. 1986. Comportement hydrique et évolution structurale et texturale des montmorillonites au cours d'un cycle de desiccation-humectation: Partie I. Cas des montmorillonites calciques. Clay Miner. 21: 9-29.

Bish, D. L. 1989. Rietveld refinement of the kaolinite structure at 88, 294, and 573K. p. 17. *In* Abstracts, Clay Minerals Society 26th Annual Meeting, Sacramento, California. The Clay Minerals Society, Bloomington, Indiana.

Bish, D. L., and S. J. Chipera. 1988. Problems and solutions in quantitative analysis of complex mixtures by x-ray powder diffraction. Adv. X-ray Anal. 31:295-308.

Bish, D. L., and M. H. Ebinger. 1989. Rietveld refinement of synthetic goethite and Mn-substituted goethite. p. 18. *In* Abstracts, Clay Minerals Society 26th Annual Meeting, Sacramento, California. The Clay Minerals Society, Bloomington, Indiana.

Bish, D. L., and S. A. Howard. 1988. Quantitative phase analysis using the Rietveld method. J. Appl. Cryst. 21:86-91.

Bish, D. L., and R. B. Von Dreele. 1989. Rietveld refinement of non-hydrogen atomic positions in kaolinite. Clays Clay Miner. 37:289-296.

Bookin, A. S., V. A. Drits, A. Plançon, and C. Tchoubar. 1989. Stacking faults in kaolin-group minerals in the light of real structural features. Clays Clay Miner. 37:297-307.

Bottero, J. Y., D. Touchbar, J. M. Cases, and F. Fiessinger. 1982. Investigation of the hydrolysis of aqueous solutions of aluminum chloride. 2. Nature and structure by small-angle x-ray scattering. J. Phys. Chem. 86:3667-3673.

Bottero, J. Y., M. Axelos, D. Tchoubar, J. M. Cases, J. J. Fripiat, and F. Fiessinger. 1987. Mechanism of formation of aluminum trihydroxide from Keggin Al_{13} polymers. J. Colloid Interface Sci. 117:47-57.

Brady, K., J. M. Bigham, W. F. Jaynes, and T. J. Logan. 1986. Influence of sulfate on Fe-oxide formation: comparisons with a stream receiving acid mine drainage. Clays Clay Miner. 34:266-274.

Brindley, G. W., C. Kao, J. L. Harrison, M. Lipsicas, and R. Raythatha. 1986. Relation between structural disorder and other characteristics of kaolinites and dickites. Clays Clay Miner. 34:239-249.

Bullock, P., and M. L. Thompson. 1985. Micromorphology of Alfisols. p. 17-47. *In* L.A. Douglas and M.L. Thompson (eds.) Soil micromorphology and soil classification. Spec. Pub. 15. Soil Sci. Soc. Amer., Madison, Wisconsin.

Buondonno, A., D. Felleca, and A. Violante. 1989. Properties of organo-mineral complexes formed by different addition sequences of hydroxy-Al, montmorillonite, and tannic acid. Clays Clay Miner. 37:235-242.

Campbell, A. S., and U. Schwertmann. 1984. Iron oxide mineralogy of placic horizons. J. Soil Sci. 35:569-582.

Chao, T. T., and P. K. Theobald, Jr. 1976. The significance of secondary iron and manganese oxides in geochemical exploration. Econ. Geol. 71:1560-1569.

Clarke, R., B. Rodricks, and R. Smither. 1988. CCD x-ray detectors. p. 19-21. *In* R. Clarke, P. Sigler, and D. Mills (ed.) Time-resolved studies and ultrafast detectors: Workshop report. ANL/APS-TM-2, Argonne National Laboratory, Argonne, Illinois.

Combes, J. M., A. Manceau, and G. Calas. 1986. Study of the local structure in poorly-ordered precursors of iron oxihydroxides. J. Physique 47:697-701.

Combes, J. M., A. Manceau, G. Calas, and J. Y. Bottero. 1989. Formation of ferric oxides from aqueous solutions: A polyhedral approach by x-ray absorption spectroscopy: I. Hydrolysis and formation of ferric gels. Geochim. Cosmochim. Acta 53:583-594.

Cornell, R. M., W. Schneider, and R. Giovanoli. 1989. The transformation of ferrihydrite into lepidocrocite. Clay Miner. 24:549-553.

Cummins, P. G., E. Staples, J. Penfold, and R. K. Heenan. 1989. Geometry of micelles of the poly(oxyethylene) nonionic surfactants C16E6 and C16E8 in the presence of electrolyte. Langmuir. 5:1195-1199.

de la Calle, C., H. Suquet, and C. H. Pons. 1988. Stacking order in a 14.30-Å Mg-vermiculite. Clays Clay Miner. 36: 481-490.

Derjaguin, B. V., and N. V. Churaev. 1974. Structural component of disjoining pressure. J. Colloid Interface Sci. 49:249-255.

Ding, Y. S., S. R. Hubbard, K. O. Hodgson, R. A. Register, and S. L. Cooper. 1988. Anomalous small-angle x-ray scattering from a sulfonated polystyrene ionomer. Macromolecules. 21:1698-1703.

Dutta, P. 1989. The structure of lipid monolayers on water: A summary of recent x-ray diffraction results. p. 21-25 *In* M. Beno and S. Rice (Co-chairs) Chemical applications of synchrotron radiation: Workshop report. Argonne National Laboratory. ANL/APS-TM-4. Argonne, Illinois.

Eary, L. E., and D. Rai. 1987. Kinetics of chromium(III) oxidation to chromium(VI) by reaction with manganese dioxide. Environ. Sci. Technol. 21:1187-1193.

Feijtel, T. C., A. G. Jongmans, and J. D. J. van Doesburg. 1989. Identification of clay coatings in an older Quaternary terrace of the Allier, Limagne, France. Soil Sci. Soc. Amer. J. 53:876-882.

Finger, L. W. 1989. Synchrotron powder diffraction. p. 309-331. *In* D. L. Bish and J. E. Post (ed.) Modern powder diffraction. Reviews in Mineralogy, Vol. 20. Miner. Soc. Amer., Washington, D. C.

Fitzpatrick, R. W., and U. Schwertmann. 1982. Al-substituted goethite, an indicator of pedogenic and other weathering environments in South Africa. Geoderma 27:335-347.

Garcia, J., A. Bianconi, M. Benfatto, and C. R. Natoli. 1986. Coordination geometry of transition metal ions in dilute solutions by XANES. J. Physique 47:49-54.

Giese, R. F. 1982. Theoretical studies of the kaolin minerals: Electrostatic calculations. Bull. Mineral. 105:417-424.

Giese, R. F. 1988. Kaolin minerals: structures and stabilities. p. 29-66. *In* S. W. Bailey (ed.) Hydrous phyllosilicates (exclusive of micas). Reviews in Mineralogy, Vol. 19. Miner. Soc. of Amer., Washington, D. C.

Giovanoli, R., P. Burki, M. Giuffredi, and W. Stumm. 1975. Layer structured manganese oxide hydroxides. IV. The buserite group; structure stabilization by transition elements. Chimia 29:517-520.

Gosh, K., and M. Schnitzer. 1980. Macromolecular structures of humic substances. Soil Sci. 129:266-276.

Henderson, S. J., D. Dai, and J. W. White. 1989. Some applications of small angle scattering in chemistry. p. 57-96. *In* M. Beno and S. Rice (Co-chairs) Chemical applications of synchrotron radiation: Workshop report. Argonne National Laboratory. ANL/APS-TM-4. Argonne, Illinois.

Hingston, F. J. 1981. A reveiw of anion adsorption. p. 51-90. *In* M. A. Anderson and A. J. Rubin (ed.) Adsorption of inorganics at solid-liquid interfaces. Ann Arbor Science Publishers, Ann Arbor, Michigan.

Hoyt, J. J. 1989. Applications of anomalous small angle x-ray scattering. p. 115-126. *In* M. Beno and S. Rice (Co-chairs) Chemical applications of synchrotron radiation: Workshop report. Argonne National Laboratory. ANL/APS-TM-4. Argonne, Illinois.

Israelachvili, J. N., and R. M. Pashley. 1983. Molecular layering of water at surfaces and origin of repulsive hydration forces. Nature 306:249-250.

Johnston, C. T., and D. A. Stone. 1990. Influence of hydrazine on the vibrational modes of kaolinite, Clays Clay Miner. (in press).

Johnston, C. T., G. Sposito, and D. F. Bocian. 1984. Vibrational spectroscopic study of the interlamellar kaolinite-dimethylsulfoxide complex. J. Phys. Chem. 88:5959-5964.

Johnston, C. T., S. F. Agnew, and D. L. Bish. 1990. Polarized single crystal FT-IR microscope study of Ouray Dickite and Keolkuk kaolinite. Clays Clay Miner. (in press).

Komadel, P., P. R. Lear, and J. W. Stucki 1990. Reduction and reoxidation of nontronite: extent of reduction and reaction rates. Clays Clay Miner. 38:203-208.

Larson, A. C., and R. B. Von Dreele. 1988. Generalized structure analysis system (GSAS) user manual. LAUR 86-748, Los Alamos National Laboratory, Los Alamos, New Mexico.

Lee, D. Y., and W. J. Farmer. 1989. Dissolved organic matter interaction with napropamide and four other non-ionic pesticides. J. Environ. Qual. 18:468-474.

Low, P. F. 1987. Structural component of the swelling pressure of clays. Langmuir 3:18-25.

McKenzie, R. M. 1989. Manganese oxides and hydroxides. p. 439-465. *In* J. B. Dixon and S. B.. Weed (ed.) Minerals in soil environments, 2nd ed. Soil Sci. Soc. Amer., Madison, Wisconsin.

Murray, J. W. 1979. Iron oxides. p. 47-98. *In* R. G. Burns (ed.) Short course notes, Vol. 6. Marine minerals. Miner. Soc. Amer., Washington, D.C.

Norrish, K., and J. A. Rausell-Colom. 1963. Low-angle x-ray diffraction studies of the swelling of montmorillonite and vermiculite. p. 123-149. *In* A. Swineford (ed.) Clays and Clay Minerals, Proc. 10th Natl. Conf., Austin, Texas, 1961. Pergamon Press, New York.

Oades, J. M., and E. Tipping. 1989. Interactions of humic substances with oxides. *In* Humic substances. III. Metals, minerals, and organic chemicals. Proc. 2nd Conf. Int. Humic Substances Soc. John Wiley and Sons, Chichester, Great Britian.

Parrish, W., M. Hart, and T. C. Huang. 1986. Synchrotron x-ray polycrystalline diffractometry. J. Appl. Cryst. 19:92-100.

Phillips, J. C. 1989. Macromolecular structure changes in solution observed by time-resolved synchrotron x-ray scattering. p. 101-114. *In* M. Beno and S. Rice. (Co-chairs) Chemical applications of synchrotron radiation: Workshop report. Argonne National Laboratory. ANL/APS-TM-4. Argonne, Illinois.

Plançon, A., and C. Tchoubar. 1975. Etude des fautes d'empilement dans les kaolinites partiellement désordonées--I. Modèle ne comportant que des fautes par translation. J. Appl. Cryst. 8:582-588.

Plançon, A., and C. Tchoubar. 1977. Determination of structural defects in phyllosilicates by x-ray powder diffraction -- I. Principle of calculations of the diffraction phenomenon. Clays Clay Miner. 25:430-435.

Pons, C. H., H. Ben Rhaiem, D. Tessier, and C. Clinard. 1987. Apport de la diffusion aux petits angles des rayons X à l'étude de la microstructure des matériaux argileux. Soil Micromorphology 1987:37-42.

Pons, C. H., F. Rousseaux, and D. Tchoubar. 1981. Utlisation du rayonnement synchrotron en diffusion aux petits angles pour l'étude du gonflement des smectites. I. Étude du système eau-montmorillonite-Na en fonction de la température. Clay Miner. 16:23-42.

Pons, C. H., F. Rousseaux, and D. Tchoubar. 1982a. Utlisation du rayonnement synchrotron en diffusion aux petits angles pour l'étude du gonflement des smectites. I. Étude des différents systèmes. Clay Miner. 17:327-338.

Pons, C. H., D. Tessier, H. Ben Rhaiem, D. Tchoubar. 1982b. A comparison between x-ray studies and electron microscopy observations of smectite fabric. p. 177-185. *In* H. van Olphen and F. Veniale (eds.) Proc. Int. Clay Conf., Bologna and Pavia, 1981. Elsevier, Amsterdam.

Post, J. E., and D. L. Bish. 1989. Rietveld refinement of crystal structures using powder x-ray diffraction data. p. 277-308. *In* D. L. Bish and J. E. Post (ed.) Modern powder diffraction. Reviews in Mineralogy, Vol. 20. Miner. Soc. Amer., Washington, D. C.

Post, J. E., and D. R. Veblen. 1989. Crystal structure determinations for Na-, K- and Mg-birnessites using TEM and the Rietveld method. p. 55. *In* Abstracts, Clay Minerals Society 26th Annual Meeting, Sacramento, California. The Clay Minerals Society, Bloomington, Indiana.

Prewitt, C. T., P. Coppens, J. C. Phillips, and L. W. Finger. 1987. New opportunities in synchrotron x-ray crystallography. Science 238:312-319.

Prost, R., A. Dameme, E. Huard, J. Driard, and J. P. Leydecker. 1989. Infrared study of structural OH in kaolinite, dickite, nacrite, and poorly-crystalline kaolinite at 5 to 600 K. Clays Clay Miner. 37:464-468.

Raupach, M., P. F. Barron, and J. G. Thompson. 1987. Nuclear magnetic resonance, infrared, and x-ray powder diffraction study of dimethylsulfoxide and dimethylselenoxide intercalates with kaolinite. Clays Clay Miner. 35:208-219.

Rietveld, H. M. 1969. A profile refinement method for nuclear and magnetic structures. J. Appl. Cryst. 2:65-71.

Russell, T. P. 1988. Time-resolved SAXS studies on polymers. p. 29. *In* R. Clarke, P. Sigler, and D. Mills (Co-chairs) Time-resolved studies and ultrafast detectors: Workshop report. Argonne National Laboratory. ANL/APS-TM-2. Argonne, Illinois.

Russell, T. P. 1989. Synchrotron radiation studies on polymers. p. 97-100. *In* M. Beno and S. Rice (Co-chairs) Chemical applications of synchrotron radiation: Workshop report. Argonne National Laboratory. ANL/APS-TM-4. Argonne, Illinois.

Russell, T. P., H. Ito, and G. D. Wignall. 1988a. Neutron and x-ray scattering studies on semicrystalline polymer blends. Macromolecules 21:1703-1709.

Russell, T. P., R. Jerome, P. Charlier, and M. Foucart. 1988b. The microstructure of block copolymers formed via ionic interactions. Macromolecules. 21:1709-1717.

Sandstrom, D. R., B. R. Stults, and R. B. Greegor. 1981. Structural evidence for solutions from EXAFS measurements. p. 139-157. *In* B. K. Teo and D.C. Cory (eds.) EXAFS spectroscopy: techniques and applications. Plenum Press, New York.

Schulze, D. G. 1981. Identification of soil iron oxide minerals by differential x-ray diffraction. Soil Sci. Soc. Am. J. 45:437-440.

Schulze, D. G. 1984. The influence of aluminum on iron oxides. VIII. Unit-cell dimensions of Al-substituted goethites and estimation of Al from them. Clays Clay Miner. 32:36-44.

Schulze, D. G. 1986. Correction of mismatches in 2θ scales during differential x-ray diffraction. Clays Clay Miner. 34: 681-685.

Schulze, D. G., and U. Schwertmann. 1987. The influence of aluminium on iron oxides: XIII. Properties of goethites synthesized in 0.3M KOH at 25°C. Clay Miner. 22:83-92.

Schwertmann, U. 1959. Über die Synthese definierter Eisenoxyde unter verschiedenen Bedingungen. Z. Anor. Allg. Chem. 298:337-348.

Schwertmann, U. 1988. Some properties of soil and synthetic iron oxides. p. 203-250. *In* J. W. Stucki, B. A. Goodman, and U. Schwertmann (ed.), Iron in soils and clay minerals. D. Reidel Publishing Co., Boston, Massachusetts.

Schwertmann, U., and E. Murad. 1983. The effect of pH on the formation of goethite and hematite from ferrihydrite. Clays Clay Miner. 31:277-284.

Schwertmann, U., and R. M. Taylor. 1989. Iron oxides. p. 379-438. *In* J. B. Dixon and S. B. Weed (ed.) Minerals in soil environments, 2nd ed., Soil Sci. Soc. Am. Madison, Wisconsin.

Schwertmann, U., D. G. Schulze, and E. Murad. 1982. Identification of ferrihydrite in soils by dissolution kinetics, differential x-ray diffraction, and Mössbauer spectroscopy. Soil Sci. Soc. Am. J. 46:869-875.

Senkayi, A. L., J. B. Dixon, and L. R. Hossner. 1986. Todorokite, goethite, and hematite: Alteration products of siderite in East Texas lignite overburden. Soil Sci. 142:36-41.

Seul, M., P. Eisenberger, and H. M. McConnell. 1983. X-ray diffraction by phospholipid monolayers on single-crystal silicon substrates. Proc. Natl. Acad. Sci. USA 80:5795-5797.

Sirota, E. B. 1989. The use of x-ray reflectivity as a surface probe. p. 5-20. *In* M. Beno and S. Rice (Co-chairs) Chemical applications of synchrotron radiation: Workshop report. Argonne National Laboratory. ANL/APS-TM-4. Argonne, Illinois.

Soileau, J. M., W. A. Jackson, and R. J. McCracken. 1964. Cutans (clay films) and potassium availability to plants. J. Soil Sci. 15:117-123.

Song, H. H., R. S. Stein, D.-Q. Wu, M. Ree, J. C. Phillips, A. LeGrand, and B. Chu. 1988. Time-resolved SAXS on crystallization of a low-density polyethylene/high-density polyethylene polymer blend. Macromolecules 21:1180-1182.

Sterte, J., and J. Shabtai. 1987. Cross-linked smectites. V. Synthesis and properties of hydroxy silico-aluminum montmorillonites and fluorhectorites. Clays Clay Miner. 35:429-439.

Stucki, J. W., D. C. Golden, and C. B. Roth. 1984a. The preparation and handling of dithionite-reduced smectite suspensions. Clays Clay Miner. 32:191-197.

Stucki, J. W., P. F. Low, C. B. Roth, and D. C. Golden. 1984b. Effects of oxidation state of octahedral iron on clay swelling. Clays Clay Miner. 32:357-362.

Stuhrmann, H. B., and H. Notbohm. 1981. Configuration of the four iron atoms in dissolved human hemoglobin as studied by anomalous dispersion. Proc. Natl. Acad. Sci. USA. 78:6216-6220.

Sueno, S., M. Kimata, I. Nakai, M. Ohmasa, K. Ohsumi, and S. Sasaki. 1987. Recent activities of the mineralogy gropu in Photon Factory, KEK, Japan. Abstracts, Proc. Geol., Soc. Amer. Ann. Mtg. 19:859.

Tessier, D. 1984. Etude expérimentale de l'organisation des matéraux argileux. Thesis. University of Paris, Paris, France, I.N.R.A. Versailles Publ., 360p.

Tokashiki, Y., J. B. Dixon, and D. C. Golden. 1986. Manganese oxide analysis in soils by combined x-ray diffraction and selective dissolution methods. Soil Sci. Soc. Amer. J. 50:1079-1084.

Torrent, J., R. Guzman, and M. A. Parra. 1982. Influence of relative humidity on the crystallization of Fe(III) oxides from ferrihydrite. Clays Clay Miner. 30:337-340.

Traina, S. J., D. Spontak, and T. J. Logan. 1989. Effects of cations on the complexation of naphthalene by water-soluble organic carbon. J. Environ. Qual. 18:221-227.

Tsvetkov, F. and J. W. White. 1988. Aggregation of organometallic complex pillars in synthetic fluorhectorite and montmorillonite. J. Am. Chem. Soc. 110:3183-3187.

Turrell, G. 1972. Infrared and Raman spectra of crystals. Academic Press, London.

Uzochukwu, G. A., and J. B. Dixon. 1986. Mineralogical and chemical properties of black concretions in two soils of east Texas and north Alabama. Soil Sci. Soc. Amer. J. 50:1358-1363.

Verschuren, R. H. 1978. A microscope-mounted drill to isolate microgram quantities of mineral material from polished thin section. Mineral. Mag. 42:499-503.

Viani, B. E., P. F. Low, and C. B. Roth. 1983. Direct measurement of the relation between interlayer force and interlayer distance in the swelling of montmorillonite. J. Colloid Interface Sci. 96:229-244.

Viani, B. E., Low, P. F., and Roth, C. B. 1985. Direct measurement of the relation between swelling pressure and interlayer distance in Li-vermiculite. Clays Clay Miner. 33, 244-250.

Vlieg, E., J. F. Van Der Veen, J. E. Macdonald, and M. Miller. 1987. Angle calculations for a five-circle diffractometer used for surface x-ray diffraction. J. Appl. Cryst. 20:330-337.

Von Dreele, R. B. 1989. Neutron powder diffraction. p. 333-369. *In* D. L. Bish and J. E. Post (ed.) Modern powder diffraction. Reviews in Mineralogy, Vol. 20. Miner. Soc. Amer., Washington, D. C.

Walker, J. R. 1989. Rietveld refinement of IIb chlorite. p. 73. *In* Abstracts, Clay Minerals Society 26th Annual Meeting, Sacramento, California. The Clay Minerals Society, Bloomington, Indiana.

Waychunas, G. A., G. E. Brown Jr., and L. W. Finger. 1988. Synchrotron x-ray scattering studies of earth materials. p. 25-43. *In* J. Smith and M. Manghnani (ed.) Synchrotron x-ray sources and new opportunities in the earth sciences: Workshop report. ANL/APS-TM-3, Argonne National Laboratory, Argonne, Illinois.

Wieckowski, T., and A. Wiewiora. 1976. New approach to the problem of the interlayer bonding in kaolinite. Clays Clay Miner. 24:219-223.

Will, G., N. Masciocchi, W. Parrish, and M. Hart. 1987. Refinement of simple crystal structures from synchrotron radiation powder diffraction data. J. Appl. Cryst. 20:394-401.

Wilson, M. J., and D. R. Clark. 1978. X-ray identification of clay materials in thin sections. J. Sediment. Petrol. 48:656-660.

Wood, I. G., L. Nicholls, and G. Brown. 1986. X-ray anomalous scattering difference patterns in qualitative and quantitative powder diffraction analysis. J. Appl. Cryst. 19:364-371.

Wu, J., P. F. Low, and C. B. Roth. 1989. Effects of octahedral-iron reduction and swelling pressure of interlayer distances in Na-nontronite: Clays Clay Miner. 37:211-218.

Chapter 6

X-ray Fluorescence Microprobe and Microtomography

S. V. Mattigod, M. L. Rivers, and S. R. Sutton

6.1 Introduction

Chemical techniques have played an important role in a wide variety of research areas in soil science. The attractiveness of synchrotron radiation-based microanalytical techniques lies in their capabilities for non-destructive, trace-level analyses of a wide range of elements with fine spatial resolution. High elemental sensitivity makes it possible to study the behavior of many elements within a given physical and chemical system. Perhaps most significant to soil and environmental science, fine spatial resolution offers the possibility to analyze minute particles and microscopic regions within individual mineral phases. In addition, mineralogical studies in this field rely heavily on the ability to follow the course of reactions with fine time resolution. The high intensity of synchrotron radiation sources allows rapid data acquisition for such research.

A major complication in soil mineralogical and geochemical research is the need to use chemical pretreatments and physical separations to concentrate phases of interest. Such treatments undoubtedly alter the specimens from their natural states. Microtomographic techniques have the potential for noninvasive *in situ* studies of soils and other environmentally important specimens.

Although little geochemical research on sedimentary systems has used synchrotron radiation, extensive applications on other earth materials suggest that this approach should have significant impact on a wide variety of soil science applications. These applications fall into three general categories:

(i) Clay Mineralogy - Understanding the formation and properties of clay minerals requires knowledge of the effects of trace elements on clay mineral structures and reactivities.

(ii) Soil Genesis - The development of soils is a complex phenomenon that is very sensitive to many environmental parameters, including mineralogy, hydrology, temperature, and organic constitution.

(iii) Environmental Science - The current surge of interest in transport and containment mechanisms for toxic species in the geosphere and atmosphere requires detailed information on the fixation of these species on clay mineral surfaces, and an understanding of remobilization reactions that take place in nature. Progress on this topic can only be made by studying existing soil specimens under conditions that closely approximate those in nature.

Many of these applications are currently hampered by the lack of the spatial resolution required to study these very-fine-grained (sub-micrometer) samples, and the lack of sensitivity needed to follow reactions with sufficiently rapid data acquisition. The Advanced Photon Source (APS) will provide the technological quantum leap in these two characteristics, allowing soil and environmental scientists to seriously consider these experiments for the first time.

6.2 Experimental Techniques

6.2.1 X-ray Fluorescence Microprobe

The very intense, collimated, and polarized synchrotron x-ray beam allows the extension of conventional x-ray fluorescence (XRF) techniques to analysis of trace elements at very high spatial resolution. In this technique, x-rays are used to eject inner shell electrons from the atoms in a sample. The subsequent refilling of each vacancy by an outer shell electron results in the emission of a fluorescence x-ray whose energy is characteristic of the emitting atom. Measurement of the intensity of fluorescence x-rays at specific transition energies is used to determine the abundance of the emitting atoms.

A white-light, energy-dispersive x-ray microprobe (XRM) has been in operation for over three years at the National Synchrotron Light Source (NSLS), Brookhaven National Laboratory. The XRM consists of a collimator, sample stages, and Si(Li) x-ray detector (Gordon *et al.*, 1988). Practical spot sizes of less than 10 μm and elemental detection limits of better than 1 ppm for many elements can be achieved. Single spot analyses and 1-D and 2-D scanning are available (Spanne and Rivers, 1987). A petrographic microscope is used for optical specimen viewing under transmitted, reflected, and/or polarized illumination. A frame grabber with a freeze frame peripheral unit provides image display, image enhancement, and hard copy

capabilities. Data acquisition, processing, and motor control are performed with a dedicated MicroVAX II computer, with a VAXStation GPX as the principal analysis terminal.

Elemental sensitivities with this simple yet powerful instrument have been demonstrated to be near the 1 ppm level for most elements using either K or L transitions (Hanson *et al.*, 1987). Accuracy was demonstrated in a study of 21 feldspars and synthetic glasses (Lu *et al.*, 1989) in which SXRF concentrations were compared with electron microprobe analyses of the same thick section of each feldspar, and with atomic absorption analyses of a fragment or slice. Concentrations determined by the three techniques agreed to within about 2%.

In addition to routine elemental analyses with this instrument, technical upgrades are in progress to improve spatial resolution, energy resolution, and elemental sensitivity. An 8:1 critical reflectance, ellipsoidal, focusing mirror (Jones *et al.*, 1987) has been installed and initial tests show an increase in photon flux of about a factor of 30 over the direct beam. This enhancement will allow wavelength dispersive detectors to be used on the microprobe. Design and construction of an incident beam monochromator is in progress.

A different microprobe approach is being developed at the X26 beamline by Lawrence Berkeley Laboratory (Thompson *et al.*, 1988). This instrument uses a pair of multilayer coated concave spherical mirrors arranged in the Kirkpatrick-Baez geometry to focus the beam to less than 10 μm. Femtogram sensitivities for elements from K to Zn have been achieved.

6.2.2 Applications of the XRM

A wide variety of geochemical and biochemical studies have been performed using the XRM. In the biological sciences, the XRM is advantageous for determining trace element compositions for micron-sized structures. In one study, a 2-D map of the gallium distribution in a bone biopsy demonstrated that Ga from a gallium nitrate treatment concentrated in regions of new bone growth (Bockman *et al.*, 1990).

In the earth sciences, the XRM is valuable in determining trace element distributions at high spatial resolution and the compositions of minute specimens. For example, analyses on glass inclusions in volcanic rocks from California, Italy, and Alaska are being used to track the geochemical evolution of magma chambers and the role of the volatile components in establishing trace element partitioning between the vapor and melt phases. Some examples of applications in sedimentary geochemistry and environmental science are given below.

6.2.2.1 Trace-Element Distributions in Coal Mineralization

Synchrotron radiation is being used to investigate trace element microdistributions in coal as a means of understanding diagenetic processes in sedimentary basins. By analyzing authigenic minerals in coal and using data on fluid/mineral trace element partitioning behavior, changes in fluid chemistry during burial and diagenesis are being examined (Kolker *et al.*, 1990; Suen *et al.*, 1989). Minerals of particular interest include calcite, kaolinite (Figure 6.1), and sulfides (White *et al.*, 1989). Trace element characteristics of specific maceral (organic) components of coal are also being examined and systematic differences in the chemistry of vitrinite and inertinite components have been identified. The SXRF method offers an opportunity to study fine-scale variations in concentrations of trace element, which were otherwise obscured by conventional bulk analyses, for a variety of natural materials.

6.2.2.2 Authigenic Clay Minerals in Anthracite-rank Coal

Authigenic clay minerals in anthracite coal cleats from carboniferous strata of eastern Pennsylvania indicate that metasomatic, hydrothermal fluids flowed through these fractures. The distribution, texture, and composition of these clay minerals allow insight into the relationships among coalification, tectonic deformation, and clay mineral authigenesis. It has been hypothesized that the hydrothermal circulation was largely driven by Alleghenian-age orogeny and associated deep basinal flow, and that the fluids may have significantly increased coal rank in this region. This model is being tested using the trace element compositions of individual clay minerals to constrain the temperature and composition of the hydrothermal solutions and, together with petrographic textural data, to document the relative timing of these hydrothermal episodes.

Three clay minerals have been analyzed in initial work (Jones *et al.*, 1989). Rectorite and tosudite fragments were obtained from different fracture sets within the same coal sample, while NH_4-illite was from the same seam in a different locality. Elements detected included Al, Si, K, Ca, Ba, Cr, Mn, Fe, Ni, Cu, Zn, Ga, Rb, and Sr. The following observations were made: K contents are similar for tosudite and rectorite (300 ppm), but they are about an order of magnitude greater in illite (0.3%). Barium shows an analogous variation suggesting that the Ba concentrations are controlled by ionic-size-dependent substitution. Strontium is correlated qualitatively with the Ca trend (expected based on their similar chemical behavior), but the rectorite Sr content is higher than one would predict from simple substitution (Ca/Sr is less than unity). Given that Sr can be enriched in fluids by the weathering of limestones, one possibility is that this is a signature of the non-local hydrothermal

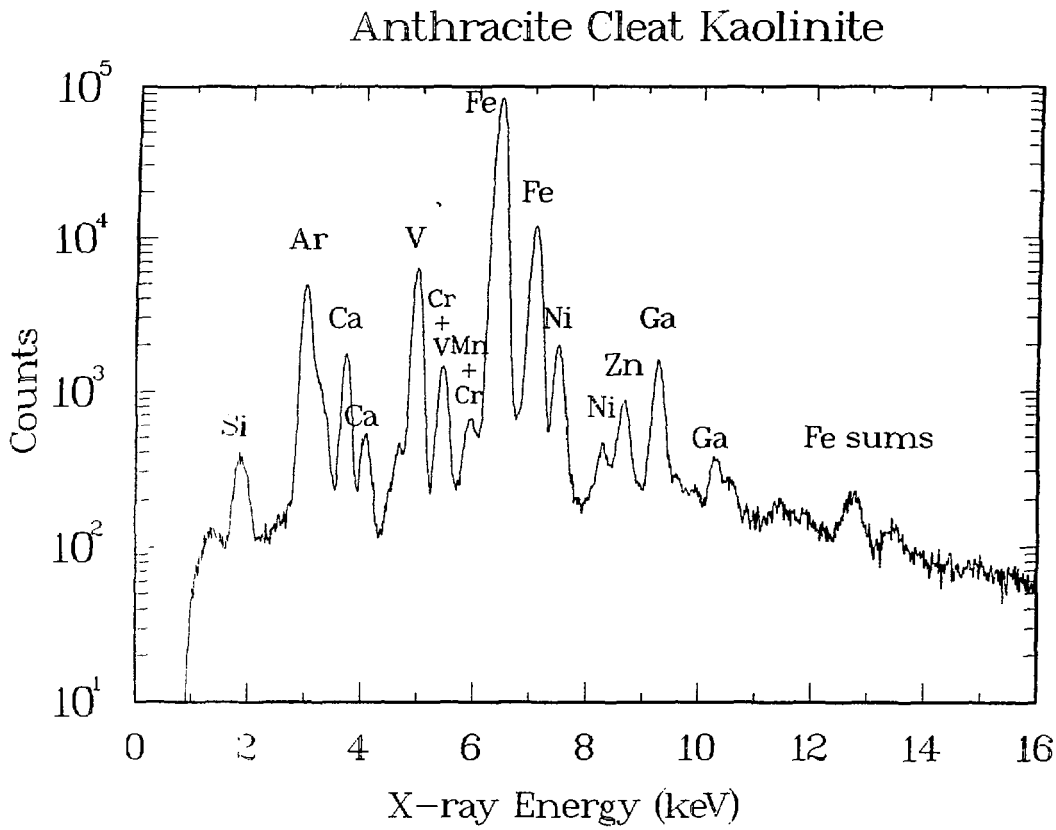

Figure 6.1. Trace element composition of kaolinite in anthracite coals.

intrusion. The similar Fe contents for phases from the two different fracture sets support the idea that Fe is locally derived.

6.2.2.3 Metal-rich Precipitates from Deep Sea Vents

"Black smoke" particles from seafloor hot springs on the East Pacific Rise and Mid-Atlantic Ridge consist primarily of elemental sulfur and sulfides (pyrrhotite, chalcopyrite, and sphalerite). Preliminary results (Campbell *et al.*, 1989) show Fe-sulfides (pyrrhotite and pyrite) contain Cu, Zn, and As at levels near 1000 ppm. Chalcopyrite contains Se in addition to these other trace elements. Knowledge of trace element compositions of these particles is important to understanding the processes that occur in hydrothermal plumes and their effects on the formation of metalliferous sediments.

6.2.2.4 Petrogenesis of Gold in Carlin-Type Ore Specimens

Carlin-type ores have proved to be important sources of gold from an economic standpoint, with bulk assays typically 1 to 10 ppm, but little has been known regarding the location of gold, its chemical/mineralogical speciation, and its petrogenesis. Such information is essential for developing extraction techniques and identifying new deposits. Previous electron microprobe and mineral separation studies have suggested that the gold is intimately associated with euhedral pyrite crystals in these specimens and existing ore-processing techniques are based on this belief. The synchrotron x-ray microprobe has allowed, for the first time, direct detailed studies of the microdistribution of Au in this material. The results of these studies (Chen *et al.*, 1987; 1988) demonstrated that pyrite crystals contain little Au compared to the matrix material: pyrite Au was undetectable at the detection limit of about 5 ppm while the siliceous/carbonaceous matrix contained up to 40 ppm Au. The matrix was found to be heterogeneous. Subsequent scanning electron microscopy and energy-dispersive x-ray (EDX) analyses have identified the mineralogic speciation as Au metal, in association with the clay mineral illite. These studies are continuing to unravel the complex sedimentary history of these ores.

6.2.3 X-ray Fluorescence Measurements with the X17 Superconducting Wiggler

The X17 superconducting wiggler (SCW) at NSLS is an extremely important x-ray source for synchrotron x-ray fluorescence microprobe analyses for two reasons. First, the energy hardness is ideal for excitation of K fluorescence from high-Z

elements, such as rare earth elements (REE) and toxic metals. Second, the SCW spectrum is very similar to that of an APS bending magnet so that one can gain experience now using high power devices somewhat similar to those that will be built at the APS. For the SCW at NSLS, the increase in the flux of high-energy photons from the device versus that from a bending magnet is a factor of 100 to 1000 in the region of the REE K edges (30-60 keV). Some preliminary experiments were performed with the ring restricted to low-current mode during operation of the SCW (Rivers and Sutton, 1989). Detection limits for the USGS manganese crust standard P-1 indicate < 5 ppm detection limits for the light REE (250 μm beam, 400 second acquisition, 250 μm Ta filter on incident wiggler radiation).

Encouraging results were obtained in an experiment aimed at ascertaining the feasibility of making noninvasive, *in vivo* measurements of lead in the human tibia. Comparable sensitivity with a 25μm beam is expected when the SCW is commissioned to operate at high-ring current. These conditions will then be attractive for studies of high-atomic-number elements in a wide range of materials.

6.2.4 Microtomography

Microtomography is the extension to finer spatial resolution of the tomographic imaging techniques developed in the medical community in recent years (CAT scanning). Medical scanners typically have spatial resolutions in the 1 to 2-mm range. By using the very-high-intensity beam from a synchrotron radiation source, the spatial resolution can be taken to the μm range.

The basic principle of tomography is to record the line integral of some property for a large number of rays that intersect the object of interest at a variety of angles. In the simplest case, this can be done with a pencil beam of radiation, by translating the object through the beam and recording the intensity at each translation step. The object is then rotated a small amount and the translation process is repeated. The rotate/translate process is continued until the object has been rotated 180 degrees. There is then sufficient information in the line integrals that have been measured to reconstruct a cross section of the object, using such techniques as filtered back-projection. In transmission tomography, one measures the x-ray transmission for each ray, and the reconstruction produces an image of the linear attenuation coefficient (μ^{ρ}). This type of image is typically produced in medical imaging and is useful in studies of biological samples, porosity, and other things. Images of elemental distributions can be produced in two ways. In digital subtraction tomography, two images are produced, one with an x-ray beam just above the absorption edge of the element and one with an x-ray beam just below. The difference between the images will then show the distribution of the element of

interest. Because this technique requires subtraction of one signal from another, it is limited mainly to elements present at relatively high concentrations (>1%) in the specimen.

In fluorescence microtomography, a fluorescence detector is used to measure directly the characteristic x-ray emission from one or more elements in the sample. Again, the line integral of the emission is being measured along the rays through the sample. The reconstruction image in this case is a direct map of the distribution of the element in the specimen. By counting longer, one can obtain images for even trace elements in the specimen.

6.2.4.1 Advantages

The principal advantage of microtomography is that it allows one to make images of slices through an object without having to actually section it. This has the obvious advantages for imaging living organisms. However, even with inanimate or inorganic objects tomography, not sectioning the object is useful. For instance:

(a) Imaging fragile objects where sectioning would damage features such as porosity. The imaging of soils is an application where this is important.

(b) Imaging very small objects, such as 30 to 50 μm fly ash particles.

(c) Imaging objects in environmental chambers.

(d) Imaging multiple slices simultaneously using 2-D array detectors.

Microtomographic technology will probably improve in the near future, allowing a dramatic reduction in the time needed to collect the many slices needed to build 3-D images.

6.2.4.2 Applications

Microtomography can also be used for nondestructive analyses of voids in ceramics. In preliminary experiments, Krieger (1988) made a 300 x 300 pixel image of a 3 x 3 mm ceramic with 10 x 10 μm pixel size (Figure 6.2). Voids down to 10 to 20μm in size can be revealed in this way. The second application of image reconstruction techniques is fluorescence imaging of sectioned samples. A demonstration experiment mapped the distribution of Au evaporated on a Kapton foil. A biomedical application of interest is the study of light elements in sciatic nerves, since longitudinal variations in concentration can be studied without any physical

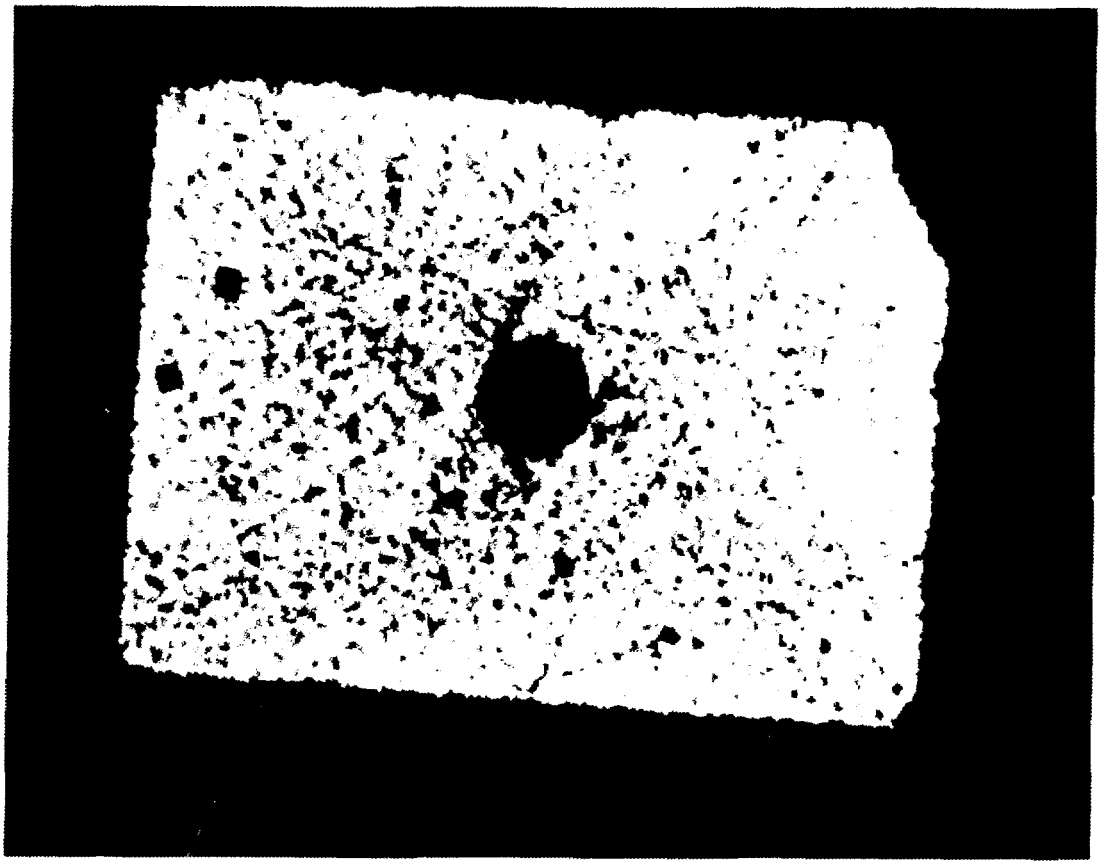

Figure 6.2. Microtomograph of a ceramic material showing the distribution of voids. The circular void in the center is a 75 μm test object drilled there intentionally.

sectioning. A pilot experiment on a freeze dried leech ganglion showed that it is feasible to study K distributions in nerves on the micrometer scale using this technique.

6.3 Potential Applications in Soil and Environmental Sciences

6.3.1 Elemental Distribution in Pedogenic Manganese Nodules

Manganese oxide and hydroxide-rich nodules occur in many soil profiles (McKenzie, 1989). Manganese is an essential nutrient element for plants and animals, and considerable attention has been focussed on the soil chemistry of this element. The redox and adsorption chemistry of Mn minerals in soils may also affect the chemistry of other nutrient elements and of potentially toxic trace elements. These nodules are considered to be a pedogenic indicator because they occur more frequently in soil horizons affected by seasonal waterlogging. Based on a number of studies, McKenzie (1989) hypothesized that the Mn nodules form as reduced Mn is mobilized from waterlogged soil horizons, and subsequently precipitated on Mn oxide-rich substrates during drying periods. The mineral forms of Mn most commonly identified in soil nodules are birnessite, vernadite, and lithiophorite.

Significant concentrations of Fe, Co, Cu, Ni, V, Pb, and Zn are also present in these nodules, and actinides at a radioactive waste site have been found to be associated mainly with Mn oxides. In Mn nodules, the total concentrations of Fe can be as high as 17% (Tokashiki *et al.*, 1986), whereas H_2O_2-extractable concentrations approach 1.4% for Co, 0.14% for Ni, 0.3% for V, 0.25% for Pb, 0.24% for Cr, and 0.12 % for Zn (McKenzie, 1989).

Studies of marine manganese nodules have shown that Mn and Fe are zonally distributed and that the accessory trace elements may preferentially associate with one of these major oxide components. Similar data for soil Mn nodules are not available. The accessory trace elements can exist in either adsorbed or substituted form. Use of the XRM, microtomography, and x-ray diffraction (XRD) can provide detailed data about the concentrations, distributions and solid phase associations of trace elements. Such data will help understand better the role of soil Mn nodules in nutrient availability and their presence as a reflection of pedogenic conditions.

6.3.2 Secondary Carbonate Accumulations in Soils

It is estimated that about one third of the total organic plus inorganic carbon in soils of the world exists in the form of inorganic carbonates (Doner and Lynn, 1989). Carbonates in soils can either result from pedogenic processes (secondary forms) or be inherited from the parent material (primary forms). Calcite and Mg-calcite are the most common secondary carbonates in soils. In soil profiles, these secondary carbonates accumulate in the form of glaebules or layers. The pedogenic factors related to pore waters affecting formation of secondary carbonates in soils include pH, the concentrations of inorganic and organic constituents, and the partial pressure of CO_2. Additionally, precipitation of secondary carbonates can close soil pores and change the soil water regime, and also affect the nutrient and management status of the soils. Currently, information about size and shape of carbonate glaebules in soils is collected by such time- and labor-intensive methods as mechanical separation, followed by optical microscopic mapping of thin sections (Mermut and Dasog, 1986). Secondary soil carbonates also contain such trace elements as Cd, Co, Fe, Mn, and V. However, there are no data regarding concentrations and distributions of these trace elements in carbonate glaebules.

Use of synchrotron-based XRMs and microtomography can provide needed data with simpler sample preparation. The distribution and concentrations of Ca and accessory trace elements in glaebules can be mapped rapidly with better spatial resolution. Data obtained using these new techniques will provide new insights on the genesis of secondary soil carbonates.

6.3.3 Phyllosilicates in Soils

Phyllosilicates are the principal component of soil clay fractions. Because of their high ion exchange capacities and their ability to interact with organics and soil water, phyllosilicates significantly affect a number of physicochemical properties of soils. Therefore, the role of phyllosilicates in soil genesis, and in regulating nutrient status and water movement within soil profiles has been studied extensively. Considerable advances have been made in understanding their major element chemistry, structures, and physicochemical reactivity (Dixon and Weed, 1989). However, data are sparse regarding the role of trace elements in phyllosilicates as genetic indicators, how they change chemical reactivity, and how they affect trace-nutrient status.

Soil phyllosilicates may contain, among others, a number of trace elements, including B, Co, Cr, Cu, Ga, Ge, Fe, Mn, Ni, Zn, and V. Borchardt (1989) has suggested that information about the trace element chemistry of phyllosilicates in general, and smectites in particular, can be valuable in solving problems of mineral genesis. A

study of trace elements to understand the nature of authigenic clay minerals in coal has been described briefly in Section 6.2.2.2. A systematic study of the trace-element composition of soil phyllosilicates can significantly add to knowledge of mineral genesis.

6.3.4 Trace-Element Distribution in Oxisols (Latosols and Lateritic Soils)

Oxisols include most of the soils previously designated as laterites and latosols. These highly weathered soils are generally found in tropical regions. The soils belonging to this order make up about one fifth of all soils of the tropics.

Oxisols result from intense chemical weathering characterized by desilication and subsequent accumulation of sesquioxides of iron and aluminum. Oxisol profiles that are subjected to periodic saturation develop red and gray mottled horizons called plinthites caused by mobilization and translocation of Fe. Large accumulations of plinthite can form a continuous phase in some tropical Oxisols. Such plinthite accumulations were historically referred to as laterite.

Even though Oxisols have highly leached profiles, some of the trace elements (including Cu, Cr, Ni, Co, Mn, V, and Zn) may be retained with major sesquioxide components (Nalovic and Pinta, 1970; Othman *et al.*, 1977; Ismunadji *et al.*, 1982). However, these micronutrient elements are apparently in forms unavailable to plants. A few studies have routinely focussed on measuring either the total or extractable concentrations of these elements in Oxisols.

In addition to their total concentrations, the distribution and the nature of association of these trace elements with the major oxide components of these soils must be known. Current techniques are unable to produce such data. Because of lower detection limits, better resolution, and elemental mapping capabilities, synchrotron-based XRM techniques can be used to better assess the trace element chemistry of these soils.

6.3.5 Elemental Concentrations in the Rhizosphere

The interfacial region between plant roots and ambient soil is the locus of dynamic interactions that govern the transport of various elements and water into plant roots. Both passive and metabolic processes are involved in the uptake of trace elements through the rhizosphere by the plant roots. Passive uptake occurs as a consequence

of ion diffusion along an activity gradient, whereas metabolic energy is expended by the plants in moving the ions to the root surface against an activity gradient.

Several important redox and chelation reactions occur in the rhizosphere as a part of the uptake process. For instance, Fe(III) is reduced to Fe(II) before root uptake occurs (Cheney *et al.*, 1972). Other trace elements, such as Cu, Hg, Mn, and Sn, may also be reduced before being taken up by the roots. In addition, these trace elements may be chelated by root exudates as part of the uptake process. Such chelation by root exudates may play an important role in mobilization and transport of trace elements from the rhizosphere into the bulk soil (Cataldo *et al.*, 1987). High bioaccumulation indices for B, Br, Cd, Cs, and Rb show that these are taken up easily, whereas low indices indicate that Ba, Bi, Fe, Ga, Sc, Se, Ti, and Zr are less available to plants.

The chemistry of nutrient trace elements, and of potentially toxic ones, in the rhizosphere is crucial to a better understanding of the uptake process. Trace element concentrations in the microscopic rhizosphere region cannot be determined *in situ* with current techniques. Because of their better spatial resolution and lower detection limits, the application of the synchrotron-radiation-based techniques may make it possible to resolve questions of trace-element status in the rhizosphere.

6.3.6 Trace Elements in Fossil Fuel Combustion By-Products

Large quantities of fossil fuel combustion by-products are currently being disposed of on land. Because these by-products may contain potentially deleterious constituents, extensive studies have been conducted to assess mobilization and transport of these constituents in soils and groundwater. The constituents of concern in the by-products include such trace elements as B, Cu, Cr, Cd, Mo, Ni, V, and Zn.

An important aspect of assessing the potential mobilization of these constituents is characterization of the chemical and mineralogical properties of both fresh and weathered materials. Bulk by-product materials have been extensively characterized (Mattigod *et al.*, 1990b). However, the distribution, elemental associations, and the solid phase forms of trace elements in these wastes are not known in detail. Therefore, schemes have been proposed for separating these by-products into size, density, and magnetic fractions to isolate and characterize the trace-element-enriched fractions (Mattigod and Ervin, 1983). Although studies conducted on fly ashes have shown that certain trace elements may occur in enhanced concentrations in the magnetic fractions (Mattigod *et al.*, 1990a), the solid phase forms of trace elements and elemental associations in fly ashes are not well established because of the limitations of currently available analytical techniques.

Synchrotron-based techniques can provide detailed information about the characteristics of trace elements in fly ashes and other fossil fuel combustion by-products. For instance, the distribution and concentrations of various elements on and inside trace element-enriched magnetic particles can be examined using microtomography. Such detailed data, coupled with a knowledge of critical geochemical processes, can be used to assess the mobilization potential of trace elements upon weathering.

6.3.7 Transuranic Elements in Soils

The anthropogenic transuranic elements Np, Pu, Am, and Cm are found in soils as a consequence of nuclear-energy-related activities. Depending on their origin, these elements enter the soil environments in the form of high-fired oxides, hydroxides, soluble salts, or organic complexes.

Because of their long half-lives and high radiotoxicity, considerable attention has been focussed on isotopes of two of these elements, ^{239}Pu and ^{241}Am. Studies have indicated that soils are the dominant (>99%) repository for Pu in ecosystems (Watters *et al.*, 1980). A major fraction of Pu in soils resides in the top few centimeters of the surface horizons (Francis, 1973, Little and Whicker, 1977). Biotic and abiotic factors control speciation and redistribution of these transuranic nuclides within the soil profile (Wildung and Garland, 1977).

The transuranic elements are a subset of the actinide series and occur in multiple oxidation states. In the environment, the most likely oxidation states for Np and Pu are believed to be IV, V, and VI, and for Am and Cm they are III and IV (Watters *et al.*, 1980). The redox behavior of Np and Pu is complex, and different redox species of an element can coexist in solution phase.

Based on an extensive review of available literature, Watters *et al.* (1980) concluded that because of their complex behavior, their low concentrations, and the insensitivity of analytical methods, the soil chemistry of ^{241,243}Am, ^{244}Cm, and ^{237}Np is relatively unknown. Watters *et al.* concluded that more data about their concentrations, distributions, and redox states are essential for modeling the overall environmental behavior of these transuranic elements. A number of inherent advantages make synchrotron radiation-based analytical techniques better tools to probe the behavior of these important elements in the soil environment. However, these techniques have not been applied to the problem of characterizing the transuranic elements in soils.

6.4 Importance of the Advanced Photon Source for the Synchrotron X-ray Fluorescence Microprobe

The APS will provide opportunity for order of magnitude improvements to the synchrotron XRM in two ways. First, the use of an undulator source allows much higher flux in the 10 to 40 keV range. Second, the hard x-ray wiggler (wiggler "A") provides higher flux in the 40 to 100 keV range. The NSLS bending magnets, for instance X26C, have been used to produce an XRF microprobe by the use of a simple collimator system. The obtainable flux is about $3x10^5$ photons/sec/μ^2/1% bw at 10 keV. The beam divergence is very small, so the practical limits to the beam size are set by the collimator size, which can be made <5 μm, and by the flux. A trace-element microprobe must receive about 10^{10} photons/sec on the target for reasonable detection limits with an energy dispersive detection system. With a wavelength dispersive detection system, fluxes of $>10^{11}$ photons/sec are required because collection efficiency is poorer. On X26C, therefore, beam sizes >10 μm and bandwidths >1 keV are required. In fact, beam sizes of 20 to 30 μm with white light excitation have been used with success. The white light affects the elemental sensitivity because of scattered background and the lack of tunability of the source.

The 8:1 ellipsoidal mirror to be installed on X26A should increase the flux to $6x10^8$ photons/sec/μ^2/1% bw, which is a factor of 2,000 increase. However, the raw spot produced by this mirror will be >100 μm in size. Consequently, production of a small spot requires that there be a pinhole in front of the sample. The mirror increases the horizontal beam divergence to 4 mrad. Therefore, to produce a 10 μm spot, a 5 μm pinhole must be placed within 1 mm of the sample. This is extremely difficult because of tight spacing and fluorescence from the pinhole assembly. The incident beam must be monochromatized to reduce the background. Conventional Si monochromators will reduce the flux by a factor of 1000 or more, nearly cancelling the gain in flux provided by the mirror, and ruling out the use of a WDS detector. Multilayer monochromators exist but have problems at energies above 10 keV.

The APS undulator "A" is ideally suited to an XRM in the 5 to 40 keV region. At 10 keV, it produces a flux of $1.2x10^9$ photons/sec/μ^2/1% bw and the beam is extremely well collimated. A 1 μm pinhole could be placed several centimeters from the sample with no appreciable enlargement of the spot size. The bandwidth of the undulator fundamental is about 1%, making it ideally suited to fluorescence excitation without any monochromators. Finally, a flux of 10^{11} photons/sec could be put in a 10 μm spot making it possible to use a WDS detector. The APS undulator "A" could also be coupled to a Kirkpatrick-Baez mirror (Underwood *et al.*, 1988), which would focus to a factor of 10-100 in each direction, increasing the flux by a factor of 10^2 - 10^4. This would permit the use of a high-resolution monochromator,

and thus make it possible to perform micro-EXAFS, XANES, and other experiments with a spot size as small as 1 μm.

The second way in which the APS will dramatically improve the XRF microprobe is by making it possible to work with higher energies. This will permit analysis of rare-earth elements, high-Z incompatible elements, and others, using K fluorescence to avoid the problems encountered with L-line overlap. The NSLS bending magnets produce useful radiation up to about 30 keV. The APS undulator will produce useful radiation to 20 keV with the fundamental and 40 keV with the third harmonic. For studies at 60 keV, for instance, the NSLS superconducting wiggler (X17) has a flux of $6x10^5$ photons/sec/μ^2/1% bw. This device is heavily subscribed and will only be available for XRF microprobe studies for short periods of time.

An APS type "A" wiggler produces a flux of photons that is three times greater than $2x10^6$ photons/sec/μ^2/1% bw produced by the NSLS X17 beamline. Therefore the APS type "A" wiggler would make an excellent trace-element microprobe for REE. Solid-state Ge detectors can be used to detect the fluorescence, with good resolution (1%) at these high energies. The flux at 60 keV is seven times greater than that of the existing NSLS X26 microprobe at 10 keV, and so detection limits below 1 ppm in a 10 μm spot should be achievable. With improvements in the detector system, detection limits could well be pushed below 100 ppb.

6.5 References

Bockman, R. S., M. A. Repo, R. P. Warrell, Jr., J. G. Pounds, G. Schidlovsky, B. M. Gordon, and K. W. Jones. 1990. Gallium in bone; Micron range resolutions using synchrotron x-ray microscopy. Proc. Nat. Acad. Sci. USA 87:4149-4153.

Borchardt, G. 1989. Smectites. p. 675-728. *In* J. B. Dixon and S. B. Weed (ed.) Minerals in Soil Environments, 2nd ed. Soil Sci. Soc. Amer., Madison, Wisconsin.

Campbell, A. C., M. L. Rivers, and S. R. Sutton. 1989. Trace element composition of hydrothermal plume particles by synchrotron x-ray fluorescence spectroscopy. EOS, Trans. Am. Geophys. Union 70:494.

Cataldo, D. A., C. E. Cowan, K. M. McFadden, T. R. Garland, and R. E. Wildung. 1987. Plant Rhizosphere Processes influencing Radionuclide Mobility in Soil. NUREG/CR-4976, PNL-6277, U. S. Nuclear Reg. Comm., Washington, D. C.

Chen, J. R., J. M. Back, E. C. T. Chao, J. A. Minkin, A. L. Hanson, K. W. Jones, M. L. Rivers, and S. R. Sutton. 1988. Location and Mapping of Gold Sites in unoxidized Carlin-type Ores. p. 395-398. *In* D. Sayre, M. Howells, J. Kirz, and H. Rarback (ed.) X-ray Microscopy II. Springer-Verlag, New York.

Chen, J. R., E. C. T. Chao, J. A. Minkin, J. M. Back, W. C. Bagby, M. L. Rivers, S. R. Sutton, B. M. Gordon, A. L. Hanson, and K. W. Jones. 1987. Determination of the occurrence of gold in an unoxidized Carlin-type ore sample using synchrotron radiation. Nucl. Instr. Methods B22:394-400.

Cheney, R. L., J. C. Brown, and L. O. Tiffin. 1972. Obligatory reduction of ferric chelates in iron uptake by soybeans. Plant Phys. 50:208-213.

Dixon, J. B., and S. B. Weed. 1989. Minerals in Soil Environments, 2nd ed. Soil Sci. Soc. Amer., Madison, Wisconsin.

Doner, H. E and W. C. Lynn. 1989. Carbonate, halide, sulfate, and sulfide minerals. p. 279-330. *In* J. B. Dixon and S. B. Weed (ed.) Minerals in Soil Environments, 2nd ed. Soil Sci. Soc. Amer., Madison, Wisconsin.

Francis, C. W. 1973. Plutonium mobility in soil and uptake in plants. J. Env. Qual. 2:67-70.

Gordon, B. M., A. L. Hanson, K. W. Jones, W. M. Kwiatek, G. J. Long, J. G. Pounds, G. Schidlovsky, P. Spanne, M. L. Rivers, S. R. Sutton, and J. V. Smith. 1988. An x-ray microprobe beam line for trace element analysis. p. 276-279. *In* D. Sayre, M. Howells, J. Kirz, and H. Rarback (ed.) X-ray Microscopy II. Springer-Verlag, New York, New York.

Hanson, A. L., K. W. Jones, B. M. Gordon, J. G. Pounds, W. M. Kwiatek, G. J. Long, M. L. Rivers, and S. R. Sutton. 1987. Trace element measurements using white synchrotron radiation. Nucl. Instr. Methods B24/25:400-404.

Ismunadji, M., A. Hidayat, and R. Fathan. 1982. Micronutrient problems in upland soils of Indonesia. Tropical Ag. Res. 15:289-296.

Jones, K. W., P. Z. Takacs, J. B. Hastings, J. M. Casstevens, and C. D. Pionke. 1987. Fabrication of an 8:1 ellipsoidal mirror for a synchrotron x-ray microprobe. Soc. Photooptical Eng. 749:37-44.

Jones, K. W., S. R. Sutton, M. L. Rivers, E. J. Daniels, and S. Altaner. 1989. Trace element compositions of cleat clays from anthracite coal, eastern Pennsylvania, USA. EOS, Trans. Am. Geophys. Union 70:492.

Kolker, A., S. R. Sutton, K. W. Jones, F. J. Kuellmer, and A. Araya. 1990. *In-situ* trace element microanalysis of inertinite and vitrinite macerals in New Mexico coals using synchrotron radiation. Abstract to Geological Society of America Meeting, St. Louis.

Krieger, A. S. 1988. Future directions in synchrotron-based computer microtomography. Bull. Amer. Phys. Soc. 33:1698.

Little, C. A., and F. W. Whicker. 1977. Plutonium distribution in Rocky Flats soil. Health Phys. 34:451-457.

Lu, F.-Q., J. V. Smith, S. R. Sutton, M. L. Rivers, and A. M. Davis. 1989. Synchrotron x-ray fluorescence analysis of rock-forming minerals: I. Comparison with other techniques; II. White-beam energy-dispersive procedure for feldspars. Chem. Geol. 75:123-143.

Mattigod, S. V., and J. O. Ervin. 1983. Scheme for density separation and identification of compound forms in size-density fractionated fly ash. Fuel 62:927-931.

Mattigod, S. V., D. Rai, and J. E. Amonette. 1990a. Isolation and identification of trace-element-containing solid phases. p. 3-1 to 3-10. *In* Proc. Env. Res. Conf. on Groundwater Quality and Waste Disposal. Electric Power Research Institute, Palo Alto, California.

Mattigod, S. V., D. Rai, L. E. Eary, and C. C. Ainsworth. 1990b. Geochemical factors controlling the mobilization of selected inorganic constituents from fossil fuel combustion residues. Part 1: Review of major elements. J. Env. Qual. 19:188-201.

McKenzie, R. M. 1989. Manganese oxides and hydroxides. p.439-466. *In* J. B. Dixon and S. B. Weed (ed.) Minerals in Soil Environments. 2nd ed. Soil Sci. Soc. Amer., Madison, Wisconsin.

Mermut, A. R., and G. S. Dasog. 1986. Nature and micromorphology of carbonate glaebules in some Vertisols in India. Soil Sci. Soc. Amer. J. 50:382-391.

Nalovic, L., and M. Pinta. 1970. Recherches sur les éléments traces dans les sols tropicaux: Étude de quelques sols de Madagascar. Geoderma 3:117-132.

Othman, A. B., H. Eswaran, and A. Cottenie. 1977. The total and extractable contents of five trace elements of some soils of Malaysia. MARDI Res. Bull. 5:40-49.

Rivers, M. L., and S. R. Sutton. 1989. Synchrotron x-ray fluorescence analysis of rare-earth elements. EOS, Trans. Am. Geophys. Union. 70:492.

Spanne, P., and M. L. Rivers 1987. Computerized microtomography using synchrotron radiation from the NSLS. Nucl. Instr. Methods B24/25:1063-1067.

Suen, C. J., S. R. Sutton, M. L. Rivers, K. W. Jones, and C.-L. Chou. 1989. Trace element geochemistry of coal from the Illinois and San Juan Basins using the synchrotron x-ray fluorescence microprobe. EOS, Trans. Am. Geophys. Union 70:492.

Thompson, A. C., J. W. Underwood, Y. Wu., R. D. Giauque, K. W. Jones, and M. L. Rivers. 1988. Elemental measurements with an x-ray microprobe of biological and geological samples with femtogram sensitivity. Nucl. Instrum. Methods Phys. Res. A266:318-323.

Tokashiki, Y., J. B. Dixon, and D. C. Golden. 1986. Manganese oxide analysis by combined x-ray diffraction and selective dissolution methods. Soil Sci. Soc. Am. J. 50:1079-1084.

Underwood, J. H., A. C. Thompson, Y. Wu, and R. D. Giauque. 1988. X-ray microprobe using multilayer mirrors. Nucl. Instrum. Methods Phys. Res. A266:296-302.

Watters, R. L., D. N. Edgington, T. E. Hakonson, W. C. Hanson, M. H. Smith, F. W. Whicker, and R. E. Wildung. 1980. Synthesis of the research literature. p. 1-44. *In* W. C. Hanson (ed.) Transuranic Elements in the Environment. Tech. Info. Ctr., U. S. Dept. of Energy, Washington, D. C.

White, R. N., J. V. Smith, D. A. Spears, M. L. Rivers, and S. R. Sutton. 1989. Analysis of iron sulphides from UK coal by synchrotron radiation x-ray fluorescence. Fuel 68:1480-1486.

Wildung, R. E., and T. R. Garland. 1977. The relationship of microbial processes to the fate and behavior of transuranic elements in soils, plants, and animals. PNL-2416, Battelle, Pacific Northwest Laboratories, Richland, Washington.

Appendix A

Program: Synchrotron X-ray Sources and New Opportunities in the Agricultural and Related Sciences

Monday, January 8, 1990

Synchrotron Science: A Review

8:45 - 8:50	Darrell G. Schulze (Purdue U.)	Aims of the workshop
8:50 - 9:00	David E. Moncton (Argonne National Lab.)	Welcoming remarks
9:00 - 9:15	Joseph V. Smith (U. of Chicago)	Workshop logistics
9:15 - 10:15	Gopal K. Shenoy (Argonne National Lab.)	Characteristics of synchrotron radiation sources and the design and construction schedule for the Advanced Photon Source
10:15 - 10:45	Coffee	
10:45 - 12:00	Ercan Alp (Argonne National Lab.)	X-ray absorption spectroscopy
12:15 - 1:30	Lunch in Dining Area C of Cafeteria (Bldg. 213)	Informal discussion on possible application of spectroscopy in soil chemistry and mineralogy, and in biological materials
1:45 - 3:30	Mark L. Rivers (Brookhaven National Lab.)	X-ray imaging and fluorescence analysis
3:30 - 4:00	Tea	

4:00 - 5:45	Stephen R. Sutton (Brookhaven National Lab.) Joseph V. Smith (U. of Chicago)	X-ray powder and single crystal diffraction
5:45 - 6:30	Return to hotel	
6:30 - 7:00	Reception	
7:00 - 8:00	Dinner	
8:00 - 9:00	Darrell G. Schulze and Joseph V. Smith	Planning for the future: Organization, fund raising, construction and operation of beam lines.

Tuesday, January 9, 1990

Potential Applications of Synchrotron X-ray Sources in the Agricultural Sciences
Potential Applications in Soil Mineralogy Research

8:45 - 9:15	Darrell G. Schulze (Purdue U.)	Simplifying "routine" clay mineral analysis; Identification of poorly crystallized or "amorphous" materials in soils; Applications of powder Rietveld analysis
9:15 - 9:35	Joseph W. Stucki (U. of Illinois)	Advantages of low-angle x-ray scattering in identifying collapsed layers in smectite
9:35 - 9:55	Jerry M Bigham (Ohio State U.)	Determination of the structures of poorly crystalline soil minerals
9:55 - 10:55	Joe B. Dixon (Texas A&M U.)	Potential applications to the study of Mn oxide minerals in soils
10:15 - 10:30	General Discussion	
10:30 - 11:00	Coffee	

Potential Applications in Soil Chemistry Research

11:00 - 11:05	Samuel J. Traina (Ohio State U.)	Introductory remarks
11:05 - 11:25	Clifford T. Johnston (U. of Florida)	Characterization of absorbed organic solutes: Optical versus x-ray spectroscopies
11:25 - 11:45	Sharon J. Anderson (Michigan State U.)	Properties and problems in surface speciation
11:45 - 12:05	William F. Bleam (U. of Wisconsin)	X-ray spectroscopies and the electronic structures of clays
12:05 - 12:25	Shas V. Mattigod (Battelle PNL)	Application of tomography to clay mineral systems
12:30 - 1:45	Lunch in Dining Area C of Cafeteria (Bldg. 213)	
2:00 - 5:30	Chairpersons to be selected	General discussion on possible areas of research; begin writing report
5:45 - 6:30	Drive to Art Institute of Chicago	
6:30 - 7:45	Individual viewing in the galleries	
7:45 - 8:00	Drive to restaurant with private room	
8:00 - 9:30	Dinner	
9:30	Return to hotel	

Wednesday, January 10, 1990

Workshop on Future Prospects and Planning

8:45 - 4:30	Chairpersons to be selected	Continue writing of the workshop report.

Appendix B

List of Participants

Name	Affiliation
Calvin C. Ainsworth	Battelle PNL
Ercan Alp	Argonne National Laboratory
James E. Amonette	Battelle PNL
Sharon J. Anderson	Michigan State University
Philippe Baveye	Cornell University
Paul M. Bertsch	University of Georgia
Jerry M. Bigham	Ohio State University
William F. Bleam	University of Wisconsin - Madison
Paul R. Bloom	University of Minnesota
Joe B. Dixon	Texas A&M University
Harvey Drucker	Argonne National Laboratory
James B. Harsh	Washington State University
Clifford T. Johnston	University of Florida
Shas V. Mattigod	Battelle PNL
Diane H. Rickerl	South Dakota State University
Mark L. Rivers	Brookhaven National Laboratory
Darrell G. Schulze	Purdue University
Gopal K. Shenoy	Argonne National Laboratory
Joseph V. Smith	University of Chicago
Fred E. Stafford	University of Chicago
Elizabeth Stefanski	Argonne National Laboratory
Joseph W. Stucki	University of Illinois
Stephen R. Sutton	Brookhaven National Laboratory
Michael L. Thompson	Iowa State University
Samuel J. Traina	Ohio State University

☆ U.S. GOVERNMENT PRINTING OFFICE: 1990 745-459